EXPLORING RIFAMYCIN INACTIVATION FROM THE SOIL MICROBIOME

EXPLORING RIFAMYCIN INACTIVATION FROM THE SOIL MICROBIOME

By PETER SPANOGIANNOPOULOS, B.Sc.

A thesis submitted to the school of graduate studies in partial fulfillment of the requirements for the degree of Doctor of Philosophy.

DESCRIPTIVE NOTE

DOCTOR OF PHILOSOHPY (2014) McMaster University

(Biochemistry and Biomedical Sciences) Hamilton, Ontario, Canada

TITLE: Exploring rifamycin inactivation from the soil microbiome

AUTHOR: Peter Spanogiannopoulos, B.Sc. (University of Guelph)

SUPERVISOR: Dr. Gerard D. Wright

NUMBER OF PAGES: xii, 179

ABSTRACT

Our battle against pathogens has become a challenge due to the rise in antibiotic resistance and the dwindling number of new antibiotics entering the clinic. Most antibiotics owe their origins to soil bacteria, which have been producing these natural products for millennia. The rifamycins are products of actinomycetes and semisynthetic derivatives of these have been very successful in the clinic. Rifampin (RIF) has been a cornerstone agent against tuberculosis for over 50 years. In the clinic, pathogens typically develop RIF resistance by mutation of the drug. Nonetheless, a number of diverse RIF resistance mechanisms have been described, including enzymatic inactivation.

Environmental bacteria are multidrug resistant, likely due to sharing the same niche as antibiotic producers and represent a reservoir of ancient resistance determinants. Furthermore, these resistance determinants have been linked to pathogens. Exploring the antibiotic resistome, the collection of all antibiotic resistance determinants from the global microbiota, reveals the diversity and evolution of resistance and provides insight on vulnerabilities of our current antibiotics.

Herein, I describe a diverse collection of RIF-inactivating mechanisms from soil actinomycetes. I identified heretofore unknown RIF glycosyltransferase and RIF phosphotransferase genes (*rgt* and *rph*, respectively). RGT and RPH enzymes display broad rifamycin specificity and contribute to high-level resistance. Interestingly, RIF-sensitive Gram-positive pathogens are carriers of RPH, highlighting the existence of a 'silent' resistome in clinically relevant bacteria and emphasize the importance of studying resistance from environmental bacteria. Furthermore, I identified a conserved upstream DNA motif associated with RIF-inactivating genes from actinomycetes and demonstrate its role in RIF-responsive gene regulation. Finally, I explore the use of a RIF-resistance guided approach to identify novel rifamycin producing bacteria.

This study expands the rifamycin resistome, provides evidence of vulnerabilities of our current arsenal of rifamycin antibiotics, and offers a strategy to identify new members of this family natural product family.

ACKNOWLEDGEMENTS

My past few years as a graduate student at McMaster University have truly been a tremendous experience. Firstly, I would like to thank my supervisor Dr. Gerry Wright for seeing potential in me and providing me the opportunity to fulfill my educational goals. Your creativity, enthusiasm, motivation, understanding and love for science will never be forgotten. You have provided an ideal environment for me to develop into a scientist. I must also thank Gerry for attracting the best scientists and people to join the Wright lab. During my stay in the Wright lab, I have had the pleasure of collaborating and working alongside brilliant and kindhearted trainees and employees who have positively influenced my career. I am indebted to you all and there are a few individuals whom I must particularly recognize. I thank Dr. Kalinka Koteva for alleviating my chemophobia and showing me the ropes of analytical chemistry, which has been essential in the completion of this dissertation. I must also thank Kalinka for being such a warm, caring and supportive person. Your friendship and guidance has made my stay at the Wright lab memorable. I also thank my committee members Dr. Brian Coombes and Dr. Justin Nodwell for their guidance throughout my PhD.

The research presented herein was a collaborative effort and could not have been accomplished without the contributions of Dr. Kalinka Koteva and Nick Waglechner. Furthermore, there have been a number of Wright lab members whom I must thank for taking the time to demonstrate procedures and discuss results including Dr. Georgina Cox, Dr. Vanessa D'Costa, Dr. Gianfranco De Pascale, Linda Ejim, Dr. Lindsay Kalan, Dr. Mariya Morar, Dr. Tushar Shakya, Dr. Maulik Thaker, and Dr. Grace Yim. I am particularly thankful to Grace and Georgina for reviewing this dissertation.

Finally and most importantly I thank my family for their continued love and support during my entire education. I could not have made it this far without your guidance and mentorship. I dedicate this thesis to my parents, Basil and Calliope Spanogiannopoulos and brother, George.

TABLE OF CONTENTS

LIST OF FIGURES

Chapter One

Chapter Two

Chapter Three

Chapter Four

Chapter Five

Chapter Six

LIST OF TABLES

Chapter Two

Chapter Three

Chapter Four

Chapter Five

LIST OF ABBREVIATIONS

ADP	Adenosine diphosphate
AHBA	3-amino-5-hydroxybenzoic acid
AMP	Adenosine monophosphate
ATCC	American Type Culture Collection
ATP	Adenosine triphosphate
BIAC	Broad Institute actinomycete collection
BLAST	Basic local alignment search tool
BSA	Bovine serum albumin
CAM	Chloramphenicol
CFU	Colony-forming unit
CLSI	Clinical and Laboratory Standards Institute
DMSO	Dimethylsulfoxide
DNA	Doexyribonucleic acid
DNase I	Deoxyribonuclease I
dNTP	Deoxyribonucleotide triphosphate
DTT	Dithiothreitol
EDTA	Ethylenediaminetetraacetic acid
FA	Formic acid
gDNA	Genomic deoxyribonucleic acid
GT	Glycosyltransferase
HEPES	4-(2-hydroxyethyl)-1-piperazineethanesulfonic acid
HMBC	Heteronuclear multiple bond correlation
HPLC	High-performance liquid chromatography
HRMS	High-resolution mass spectrometry
IPTG	Isopropyl β-D-1thiogalactopyranoside
KAN	Kanamycin
LB	Lysogeny broth
LC-ESI-MS	Liquid chromatography-electrospray ionization-mass spectrometry
MIC	Minimum inhibitory concentration
MRM	Multiple reaction monitoring
mRNA	Messenger ribonucleic acid
NTP	Nucleoside triphosphate

MRSA	Methicillin-resistant *Staphylococcus aureus*
MWCO	Molecular weight cutoff
Ni-NTA	Nickel-nitrilotriacetic acid
NMR	Nuclear magnetic resonance
NRRL	Northern Regional Research Laboratory
ORF	Open reading frame
PCR	Polymerase chain reaction
PK	Pharmacokinetic
PKS	Polyketide synthase
PMSF	Phenylmethylsulfonyl fluoride
qRT-PCR	Quantitative reverse transcription-polymerase chain reaction
RIF	Rifampin
RIF-G	Rifampin-glucose
RIF-P	Rifampin-phosphate
RMSD	Root-mean-square deviation
RNA	Ribonucleic acid
RNAP	RNA polymerase
RRDR	Rifampin resistance determining region
rRNA	Ribosomal ribonucleic acid
SDM	Site-directed mutagenesis
SDS-PAGE	Sodium dodecylsulfate-polyacrylamide gel electrophoresis
SIM	Streptomyces isolation media
TAPS	3-((1,3-dihydroxy-2-(hydroxymethyl)propan-2-yl)amino)propane-1-sulfonic acid
TE	Tris-EDTA
TFA	Trifluoroacetic acid
TLC	Thin layer chromatography
TMS	Tetramethylsilane
UDP	Uridine diphosphate
UV-Vis	Ultraviolet-visible
WAC	Wright Actinomycete Collection

CHAPTER ONE

INTRODUCTION

INFECTIOUS DISEASE AND ANTIBIOTICS

A Brief History of Natural Products and Disease

Ancient texts and recent research using modern techniques to study ancient DNA have provided evidence that Humankind has been engaged in battle with infectious bacterial diseases since ancient times. Pestilence was documented as early the Peloponnesian war in 431 BC, when Thucydides wrote that: "people were attacked without exciting cause, and without warning, in perfect health" (Cunha, 2004). This plague, believed to be a result of typhoid fever, killed a quarter of the Athenian army and infected a quarter of the civilian population in Southern Greece (Papagrigorakis et al., 2006). Although plagues have ravaged civilizations across the globe for as long as records have been kept, it was not until the 1800s, with seminal research by a number of European scientists including Robert Koch and Louis Pasteur, that microscopic organisms were determined to be the cause of infectious diseases. Having identified the culprits, researchers and physicians were now primed to study infectious microbes and to envision opportunities for intervention and prevention.

Prior to the knowledge of microorganisms and their relevance with infection, humans used natural products to prevent or combat disease. Natural products are defined as genetically encoded chemical compounds produced by living organisms such as animals, plants and microorganisms. Humans have appreciated the medicinal utility of these compounds for tens of thousands of years. In fact, the earliest suggestions of medicinal plant use dates back more than 60, 000 years ago by Neanderthals, as indicated by pollen deposits of medicinal plants in a grave located in the Zagros Mountains of

Kurdistan in present day Iraq (Solecki, 1975). The use of natural products for medicinal purposes is well documented in dedicated ancient texts from various civilizations. The earliest texts describing the use of natural products to treat ailments date back to 2, 600 BC from Mesopotamia (Retief and Cilliers, 2007). Ancient Egyptians and Greeks have documented the use of moulds grown on bread to treat wounds and prevent infection (Wainwright, 1989). Although unknown at the time, it was the metabolites produced by the mould that were the effective agents that prevented disease.

Today there exists a wealth of information of natural products; the dictionary of natural products contains over 260, 000 entries (www.chemnetbase.com) and is but a sample of the vast chemical diversity that exists in nature. Natural products have evolved over millennia under natural selection to interact with various biological targets including proteins, nucleic acids, and membranes. As a result of this selection, the stereochemistry of natural products is complex and exquisite. Although significant advances have been made in synthetic chemistry, natural products continue to be the medicines of choice. In fact, 50% of drugs are or have been derived from natural product sources (Berdy, 2005). Although many of these products exhibit antilife properties such as antibiotics and anticancer compounds, others have diverse bioactivities including immunosuppressant and hypolipidemic. The natural roles of many of these compounds in the environment is not entirely known.

Microbial Antagonism and Antibiotics

Antagonism between microorganisms was independently observed by many researchers, including Louis Pasteur and John Tyndall (Landsberg, 1949). These early

observations were serendipitous and occurred when a pure culture became contaminated with antibiotic producing microorganisms. Nonetheless, Pasteur anticipated the potential of harnessing this antagonism and stated if we could somehow intervene and harness this lethal interaction it could provide "perhaps the greatest hopes for therapeutics" (Kingston, 2008).

In 1928 Alexander Fleming observed a similar contamination. One of his *Staphylococcus aureus* petri dishes had become contaminated with a mould, which was later identified as *Penicillium notatum*, a common soil habitant (Fleming, 1980). He noticed that the mould was antagonizing the growth of nearby *S. aureus* colonies. Fleming envisioned harnessing this antagonism by isolating the bioactive component and using it as a therapeutic against pathogenic bacteria. Over a decade later, in collaboration with Chain and Florey, the bioactive metabolite was isolated and named penicillin, after the producing organism. Penicillin showed broad spectrum activity against Gram positive bacteria and displayed excellent bioavailability. The impact of penicillin on medicine was immense and Fleming, together with Chain and Florey were awarded the Nobel Prize in Medicine in 1945.

In 1939 René Dubos further demonstrated antagonism between soil microorganisms and pathogens. He succeeded in purifying the antagonistic metabolite, which was tyrothricin (Dubos and Hotchkiss, 1941). In this case, the producing organism was not a mould but a bacterium. Selman Waksman, Dubos' former academic supervisor, began systematically screening soil bacteria for their antagonistic properties in the 1930s. These early efforts were very fruitful and led to the discovery of many

antibiotics, including streptomycin. Streptomycin showed broad spectrum activity against both Gram negative and Gram positive bacteria and was particularly effective against tuberculosis. For his screening methodology and discoveries, Waksman was awarded the 1952 Nobel Prize in Medicine.

These natural products from microorganisms are defined as secondary metabolites since they are not directly involved in normal growth, reproduction or development of an organism. The term antibiotic, coined by Waksman, is defined as a secondary metabolite produced by a microorganism that inhibits the growth of other microorganisms in high dilutions. However, not all secondary metabolites are antibiotics and we have discovered many diverse utilities for these secondary metabolites in medicine, including anticancer and immunosuppressant therapy.

Together, Fleming and Waksman's discoveries exemplified that soil bacteria are a rich source of antibiotics. The soil environment is a highly populated and diverse niche with estimates of 10^8 -10^9 bacteria per gram of soil representing up to 10, 000 to 50, 000 different species (Roesch et al., 2007). It is generally presumed that soil is a highly competitive niche and bacteria are involved in chemical antagonism for access to the limited resources, which provides the producer an advantage. We have harnessed this potential, which has evolved over millennia, to combat infectious disease.

The pivotal discoveries by Fleming and Waksman paved the way for an era known as the Golden Age of Antibiotic Discovery (1940-1960). During this period researchers, from both industry and academia, isolated thousands of bacteria from soils obtained all over the globe in search of the next penicillin or streptomycin. From these

screens the Actinomycetes, a particular group of bacteria, were by far the most prolific producers of antibiotics and continue to be the focus of natural product discovery screening programs today. Most antibiotic scaffolds were discovered during this era, many of which are still in clinical use today. Physicians were finally provided an arsenal to manage infectious diseases. The introduction of antibiotics into the clinic is often referred to as one of the most significant contributions to modern medicine, significantly increasing the average life expectancy. In fact some experts went as far as predicting that infectious disease specialists would soon become an obsolete profession (Spellberg, 2008). However, the emergence and dissemination of antibiotic resistance would prove these experts wrong.

Antibiotic Resistance

Antibiotic resistance in pathogens is the result of mutation or gene acquisition under the selective pressure of antibiotics, which increases the tolerance of a bacterium to an antibiotic. The prospect of antibiotic resistance by bacteria was appreciated early on during the development of penicillin. Fleming acknowledged that "it is not difficult to make microbes resistant to penicillin in the laboratory by exposing them to concentrations not sufficient to kill them, and the same thing has occasionally happened in the body" (Fleming, 1945). Moreover, prior to the clinical introduction of penicillin, a report by Chain, one of the co-developers of penicillin, demonstrated that certain bacteria possessed enzymes capable of inactivating the antibiotic (Abraham and Chain, 1940). Indeed, resistance to all clinically used antibiotics emerged shortly after their introduction

into the clinic (Hopwood et al., 2007). Antibiotic resistance is an inevitable phenomenon and threatens the clinical lifespan of antibiotics.

There are three general mechanisms that bacteria utilize to avoid the inhibitory effects of antibiotics. They are alteration or protection of the drug target, reduction of drug accumulation by reduced permeability or active efflux, and enzymatic modification of the drug. These mechanisms may be specific for a particular antibiotic or broad, able to confer resistance to many unrelated antibiotics. Today, the diversity and frequency of antibiotic resistance in clinical pathogens is diminishing our available arsenal of antibiotics to combat disease. The reasons for this problem are intricate but involve an overall increase in antibiotic usage, including use as feed additives for livestock, and a lack of global regulatory rules (Laxminarayan et al., 2013). As a result, physicians are now presented with pan-resistant pathogens, such as total-drug-resistant *Mycobacterium tuberculosis* and carbapenem-resistant Enterobacteriaceae, for which there are no available antibiotics (Klopper et al., 2013; Perez and Van Duin, 2013).

Antibiotic resistance is in fact an ancient phenomenon. Soil bacteria, such as the Actinomycetes, produce and secrete antibiotics in the environment to thwart competitors. Neighboring bacteria are thus pressured to evolve mechanisms to resist the noxious effects of antibiotics. Over millennia, environmental bacteria have evolved many sophisticated antibiotic resistance mechanisms. Research in the 1970s led by Julian Davies first hypothesized that this environmental genetic reservoir may be the progenitors of antibiotic resistance determinants in pathogens when he demonstrated biochemical similarities between aminoglycoside modifying enzymes from pathogens

and environmental actinomycetes (*Streptomyces* spp.) (Benveniste and Davies, 1973). Additional studies have revealed the natural multidrug resistant phenotypes of environmental bacteria (D'Costa et al., 2006). The collection of all antibiotic resistance determinants from the global microbiota, including pathogens and environmental bacteria, has been named the antibiotic resistome. Understanding the diversity and frequency of the antibiotic resistome will facilitate our ability to anticipate and understand the evolution of antibiotic resistance. These efforts will help tease out vulnerabilities in our current arsenal of clinically used antibiotics and will provide vital information for developing resistance proof antibiotics in future drug development programs. By studying the resistome, we will be at a stage to anticipate antibiotic resistance prior to it surfacing in the clinic.

The incessant development of antibiotic resistance in pathogens drives a constant need to discover and deliver new antibiotics to the clinic. The problem is exacerbated by the reduced number of new antibiotics available to combat drug resistant strains. Since the Golden Age of Antibiotic Discovery there has been a decline in the discovery and development of new antibiotics entering the clinic. Between the introduction of penicillin into the clinic and 1970, over 20 new chemical classes of antibiotics had reached the clinic. Since then, only two new classes have been introduced (Powers, 2004; Laxminarayan et al., 2013). The reason for this decline in antibiotic development is complex, but includes the diminished returns of traditional screening discovery methods and a retreat of the pharmaceutical industry in search of more profitable drug markets (Baltz, 2006). In the past decade virtually no novel antibiotic scaffolds have

entered the clinic. The antibiotic resistance problem, in conjunction with the lack of antibiotic discovery is a dire problem, which requires immediate attention (Cooper and Shlaes, 2011).

RIFAMYCIN ANTIBIOTICS

The rifamycins belong to the ansamycin family of natural products (FIGURE 1-1 and FIGURE 1-2). Ansamycins are macrolactams that are comprised of an aromatic core derived from 3-amino-5-hydroxybenzoic acid bridged at nonadjacent positions by an aliphatic chain This family of natural products was named according to its basketlike architecture; the Latin word 'ansa' translates to handle (FIGURE 1-2). The rifamycins are broad spectrum antibiotics that selectively target prokaryotic transcription by binding and inhibiting RNA polymerase (RNAP). These antibiotics were first introduced into the clinic over 50 years ago and continue to be a cornerstone agent for the treatment of infectious disease, particularly tuberculosis.

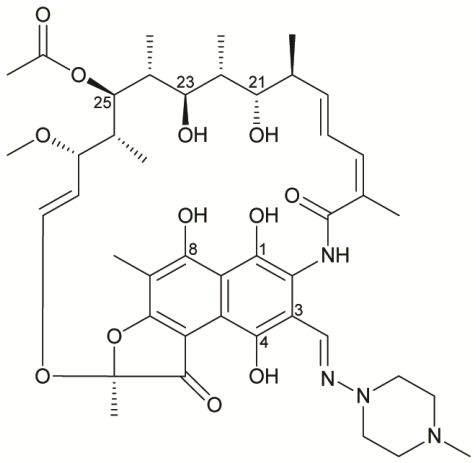

FIGURE 1-1. Structure of RIF.

The Rifamycin Antibiotic Pipeline

Rifamycin antibiotics were first described in 1959 by scientists at Lepetit Pharmaceuticals (Milan) as a mixture of metabolites produced by an actinomycete (Sensi et al., 1959). The producing microorganism, classified today as *Amycolatopsis*

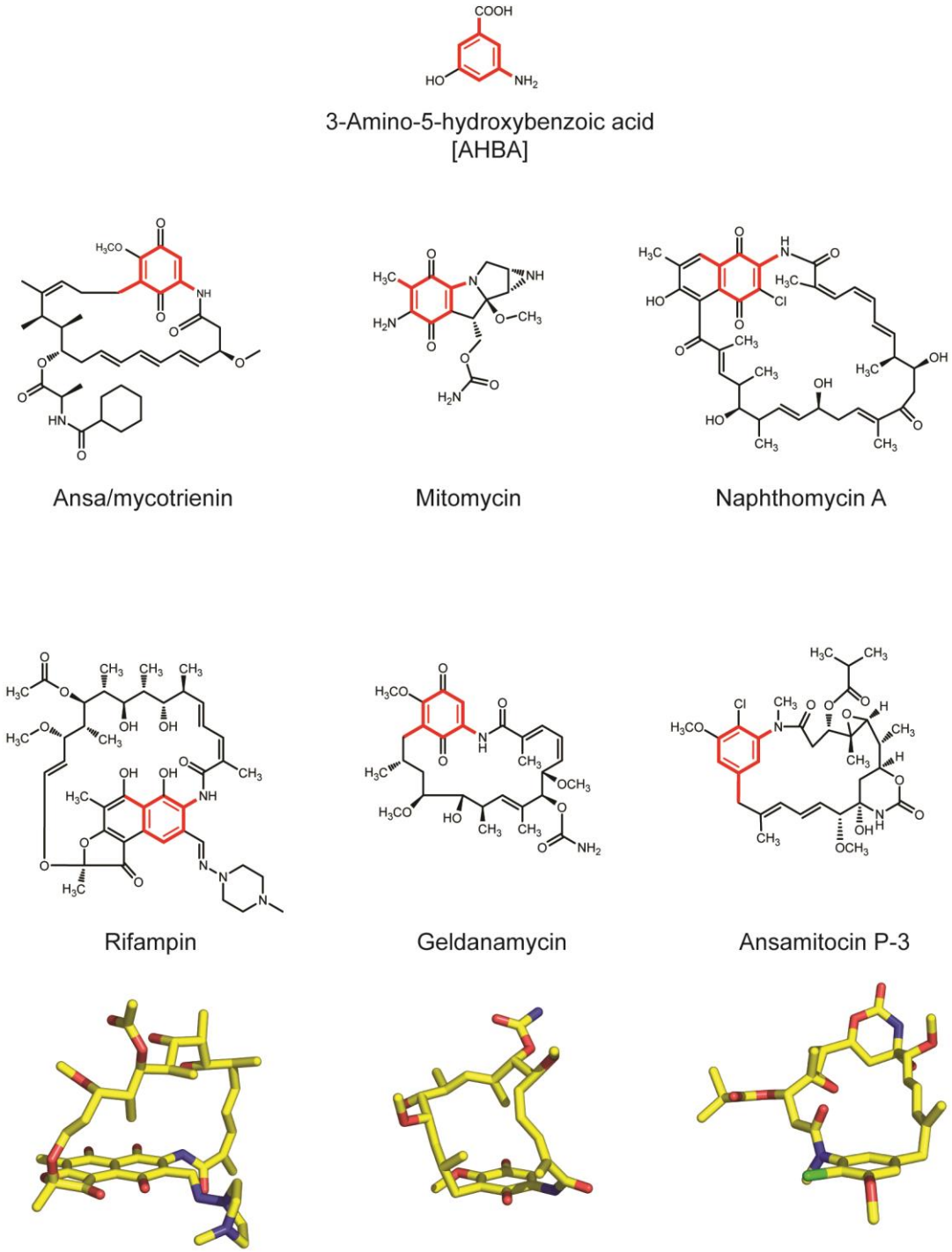

FIGURE 1-2. Structures of various ansamycin natural products. The red substructure represents the position of the AHBA moiety.

mediterranei, was isolated from a soil sample from the French Riviera. Researchers named the metabolites rifamycins after a popular French crime film at the time, *Rififi*, about a jewel heist. Rifamycin B was the first rifamycin to have its structure elucidated (FIGURE 1-3) (Brufani et al., 1964). This molecule had marginal bioactivity against Gram positive bacteria and no activity against Gram negatives. This lack of potency was attributed to the carboxylic acid (C-4 position), which impeded the molecule's ability to penetrate the bacterial cell wall (Sensi, 1983). Nonetheless, a precursor to rifamycin B, rifamycin SV, which lacks a carboxylic acid, had pronounced activity against Gram positive bacteria and was the first rifamycin approved for clinical use in 1963 (FIGURE 1-3) (Bergamini and Fowst, 1965). Rifamycin SV was poorly absorbed by the gastrointestinal (GI) tract and was therefore only administered for parenteral or topical use (Sensi, 1983). Leptit Pharmaceuticals, in collaborative efforts with scientists at Ciba-Geigy, began semisynthesis programs to generate superior rifamycin derivatives with improved bioactivity and pharmacokinetic (PK) properties. These early studies helped determine which chemical features of the antibiotic were significant for bioactivity and which tolerated chemical modifications (Wehrli, 1977; Sensi, 1983). These features were (FIGURE 1-1):

1. Positions C-1 and C-8 must contain free hydroxyl or keto groups.
2. Positions C-21 and C-23 must have free hydroxyls.
3. The *ansa* chain must be unbroken.
4. The C-3 and C-4 regions tolerate substitutions.

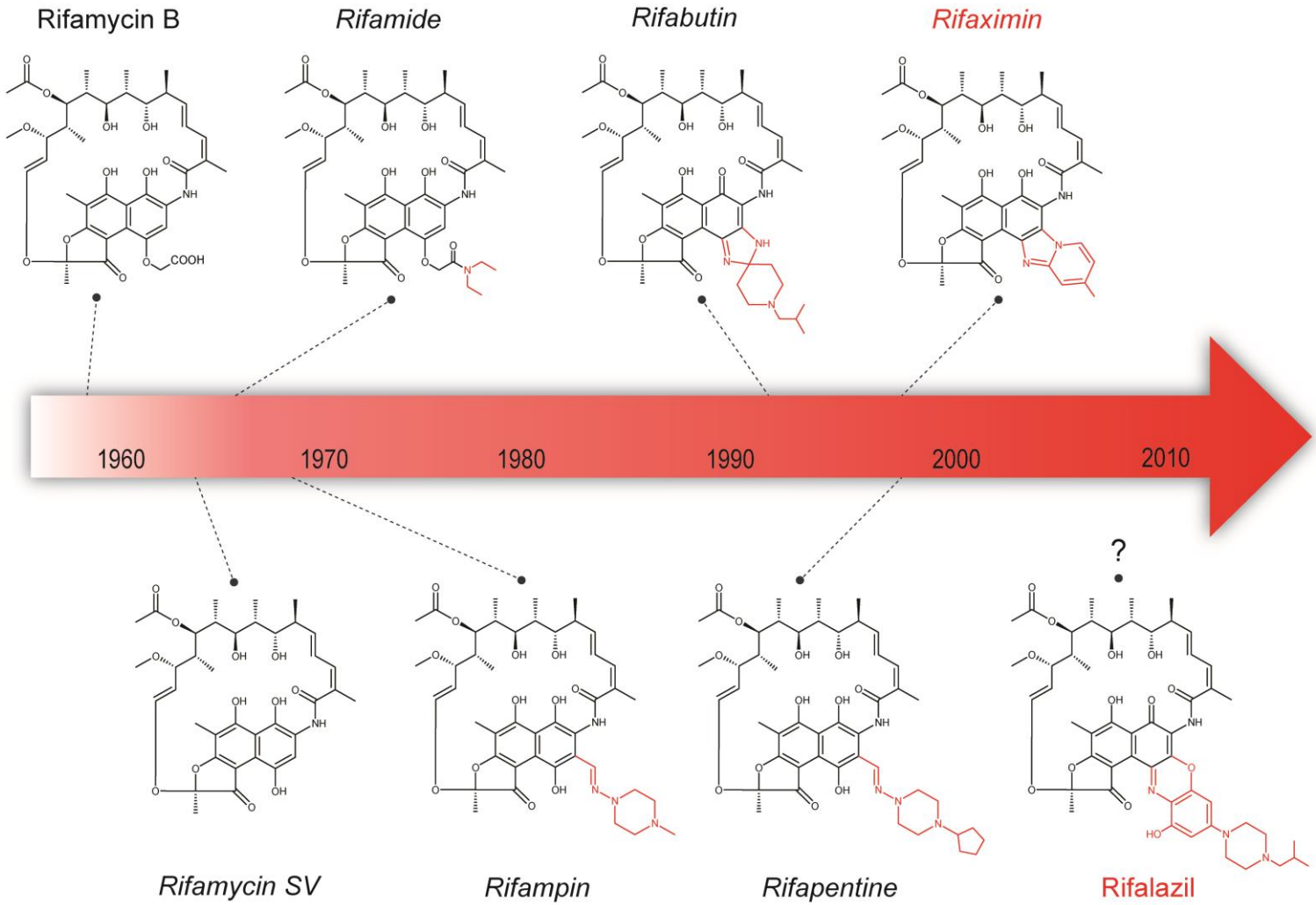

FIGURE 1-3. Rifamycin antibiotic timeline. Structures of rifamycin antibiotics and date of approval for clinical use. Italic names represent rifamycins approved for clinical use; rifamycin B was not used clinically and rifalazil has not yet been approved for clinical use. Names in red represent next generation rifamycins used for nonmycobacterial infections. Substructures highlighted in red represent synthetic modifications.

Scientists quickly established that semisynthesis at the C-3 and C-4 positions of the rifamycin scaffold offered a potential avenue for generating derivatives. The first clinically used semisynthetic rifamycin was rifamide, a diethylamide of rifamycin B, which was introduced in 1965 for the treatment of tuberculosis (FIGURE 1-3) (Pallanza et al., 1965). Fifty years later, this region continues to be the emphasis of rifamycin drug development programs. All rifamycins approved for clinical use only differ structurally at the C-3/C-4 position (FIGURE 1-3). Continued semisynthetic efforts yielded rifampin (RIF) (United States adopted name), also referred to as rifampicin, which was discovered in 1965 and approved for clinical use shortly later in 1968 (FIGURE 1-3) (Sensi, 1983). RIF has a hydrazone-linked piperazine moiety functionalized at the C-3 position. RIF shows broad spectrum activity against Gram positive bacteria and less activity against Gram negatives due to poor permeability (Wehrli and Staehelin, 1971). Most importantly, RIF is active against *Mycobacterium tuberculosis* and is one of the few antibiotics that penetrate the thick mycolic acid containing cell wall of this pathogen. RIF has remained the frontline agent against tuberculosis since its introduction into the clinic almost 50 years ago. RIF is also used for the treatment of *Haemophilus influenza* and *Streptococcus pneumoniae* infections and administered prophylactically against *H. influenza* and *Neisseria meningitidis* (Forrest and Tamura, 2010).

Although RIF has experienced great success in the clinic, this antibiotic has a number of shortcomings. Firstly, pathogens have a high propensity of developing rifamycin resistance (*vide infra*). As a result, RIF has been exclusively used in combination therapy with other antibiotics. Concerning the treatment of tuberculosis,

RIF is co-administered with isoniazid, pyrazinamide and ethambutol for at least six months (Bass et al., 1994). RIF therapy also results in a number of side effects including hepatotoxicity, inhibition of hepatic transporters, manifestation of a flu-like syndrome and induction of cytochrome P450, resulting in drug-drug interactions (Aristoff et al., 2010).

Following the introduction of RIF, semisynthesis of the rifamycin scaffold continued in efforts to generate rifamycins devoid of RIF's shortcomings. Efforts were focused on ameliorating side effects, extending the half-life and improving activity against RIF-resistant pathogenic strains. However, it would be over 20 years until the next rifamycin reached the clinic. Since RIF, a total of three semisynthetic rifamycins have been approved for clinical use (FIGURE 1-3). Rifapentine, which is structurally very similar to RIF but contains an additional cyclopentane group at the end of the C-3 piperazine moiety, was approved for clinical use in 1998 (FIGURE 1-3). Rifapentine displays an extended half-life in the body compared to RIF and thus requires oral intake twice weekly (Temple and Nahata, 1999). In addition, rifapentine is less likely to induce flu-like syndrome (Aristoff et al., 2010). Continued semisynthesis efforts yielded rifamycin derivatives with a fused ring at the C-3/C-4 position. One such molecule was rifabutin (FIGURE 1-3). Interestingly, rifabutin maintains activity against some RIF-resistant strains (Cavusoglu et al., 2004). Rifabutin also displays a longer half-life and is a lesser contributor to drug-drug interactions (Aristoff et al., 2010). Rifabutin was initially approved for clinical use in 1992 for the treatment of *Mycobacterium avium* complex (MAC) and is also used against tuberculosis.

Because of the rise in multidrug resistant pathogens and the dwindling number of new antibiotics entering the clinic, industry is returning to tried and tested antibiotic scaffolds discovered during the Golden Age of Antibiotic Discovery over 50 years ago and repurposing them to treat a broader spectrum of pathogens. RIF is experiencing an increase in use against drug-resistant pathogens, such as methicillin-resistant *Staphylococcus aureus* (MRSA) infections (Forrest and Tamura, 2010). Due to its broad spectrum activity and amenability towards semisynthesis, the rifamycin scaffold is receiving renewed interest, particularly against non-mycobacterial infections. The rifamycin derivative rifaximin has unique PK properties compared to the other clinically used rifamycins. Rifaximin is poorly absorbed and is useful against enteric pathogens (DuPont et al., 1998). This drug was initially approved for clinical use in 1998 for the treatment of traveler's diarrhea, has recently been granted orphan drug status in the United States for hepatic encephalopathy and shows promise in the treatment of irritable bowel syndrome (FIGURE 1-3) (Bass et al., 2010; Pimentel et al., 2011). Rifalazil, originally developed by Kaneka Corporation for tuberculosis, failed in phase II clinical trials (Hudson et al., 2003). Since then, the drug has been advanced by ActivBiotics Pharma and taken to Phase II clinical trials for the treatment of various pathogenic bacteria including *Chlamydia* spp. and *Clostridium difficile* and Phase III trials for the treatment of peripheral artery disease. Furthermore, a number of other rifamycin derivatives have been recently described, which are active against diverse pathogens (reviewed by Aristoff et al., 2010).

Since the introduction of the rifamycins into the clinic over 50 years ago, this scaffold continues to be the focus of many drug development programs. With the recent expansion of this drug family, the rifamycins are likely to experience an overall increase in clinical use.

Mechanism of Rifamycin Action

Early studies on RIF inhibition indicated that this family of antibiotics obstruct bacterial RNA synthesis, which represented a new bacterial target at the time of discovery (Calvori et al., 1965; Hartmann et al., 1967). Rifamycin antibiotics were potent and selective inhibitors of bacterial RNAP, with binding constants in the range of 10^{-8} M (Hartmann et al., 1967; Hartmann et al., 1968). Radioactively labeled RIF was shown to form a complex with RNAP and this interaction coincided with inhibition of RNA synthesis. RNAP isolated from RIF-resistant bacterial strains did not interact with RIF, which led to the hypothesis that RIF directly bound to RNAP (Wehrli et al., 1968). This was further supported by results demonstrating that RIF resistant RNAPs harbored single amino acid mutations (Wehrli and Staehelin, 1971). Later, it was shown that RIF inhibits the initiation phase of RNA synthesis (Sippel and Hartmann, 1968). Specifically, RIF inhibits the translocation step of RNAP during transcription, resulting in abortive di- or tri-nucleotide products (McClure and Cech, 1978). This led to the proposal of a steric occlusion model of RIF inhibition, in which RIF physically obstructs the nascent RNA chain after the first or second condensation step.

RNAP is a large multisubunit protein complex with a molecular mass of over 400 kDa consisting of 5 core subunits; $\alpha_2\beta\beta'\omega$. The crystal structure of core RNAP from

Thermus aquaticus (*Taq*) was solved in 1999 (Zhang et al., 1999). Shortly later, the structure of core *Taq* RNAP in complex with RIF was determined and was critical in understanding the mechanism of RIF inhibition and resistance (Campbell et al., 2001). RIF binds RNAP in a shallow depression deep within the RNA/DNA exit channel approximately 12 Å away from the active site Mg^{2+} ion (FIGURE 1-4). RIF is in position to clash with the elongating RNA transcript and supports the steric occlusion model of inhibition. RIF interacts with twelve amino acids all belonging to the β-subunit (encoded by the *rpoB* gene). Hydrogen bond interactions are formed between the four critical hydroxyls of RIF described above (C1, C8, C21 and C23) and six amino acids (Q393, F394, D396, H406, R409 and S411) (FIGURE 1-4 and 1-5). Numerous hydrophobic interactions are present between the naphthyl moiety of RIF and several amino acids (Q390, L391, L413, G414, E445 and I452) (FIGURE 1-4 and 1-5). The synthetic tail of RIF does not appear to be involved in any interactions with the enzyme. These twelve RIF-interacting amino acids are highly conserved across bacterial RNAPs and thus explain the broad spectrum nature of RIF (FIGURE 1-5). Additionally, this structure clarified how single amino acid substitutions either directly involved in RIF binding or surrounding the RIF binding pocket contributed to RIF resistance (FIGURE 1-5). However, this structure failed to explain how amino acid substitutions distant from the RIF binding pocket contributed to RIF resistance. The authors suggest mutations of these distant amino acids likely result in conformational alterations in the RIF binding region, resulting in decreased affinity for RIF.

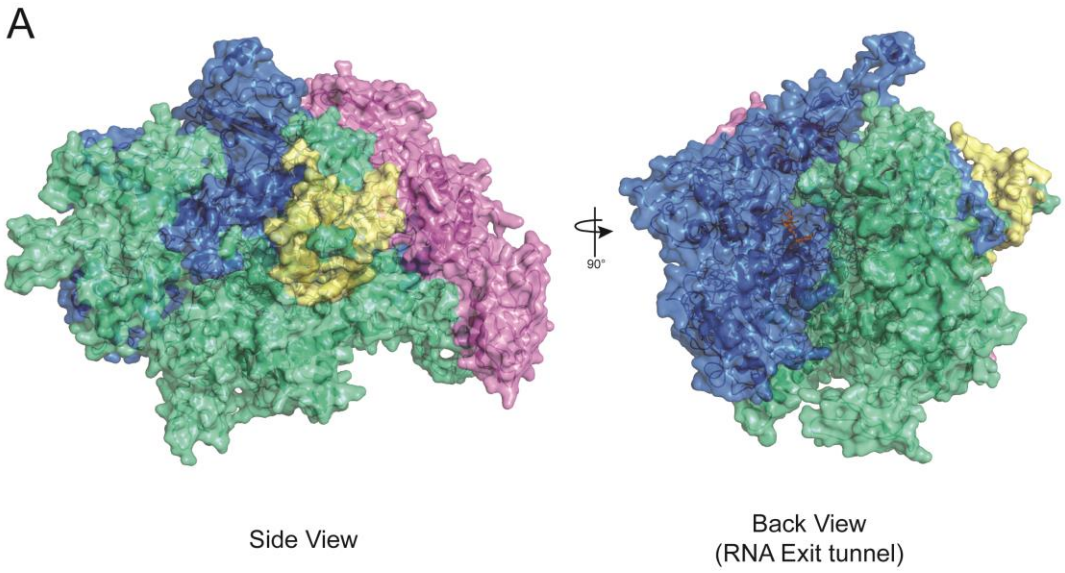

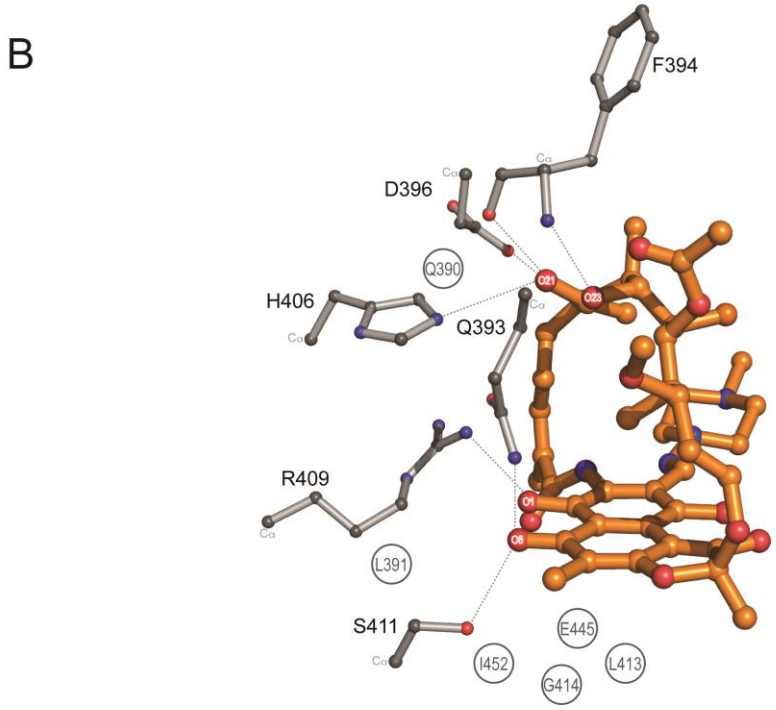

FIGURE 1-4. ***Thermus aquaticus*** **RNAP in complex with RIF.** (A) Core RNAP ($\alpha_2\beta\beta'\omega$): α subunit, pink; β subunit, blue; β' subunit, green; and ω subunit, yellow. RIF is shown in orange. (B) Amino acid residues from the β-subunit that are involved in RIF binding. Amino acid side chains represented in ball-and-stick are residues that form hydrogen bond interactions with RIF. Circled amino acids are those involved in van der Waals interactions. Red spheres are oxygen atoms and blue spheres are nitrogen atoms. Carbon atoms that belong to the β-subunit are grey, while those belonging to RIF are orange. Hydrogen bond interactions are indicated by a dashed grey line. This figure was created using PyMOL with coordinates from PDB: 1I6V. Figure was adapted from Campbell et al., 2001 and Floss and Yu, 2005.

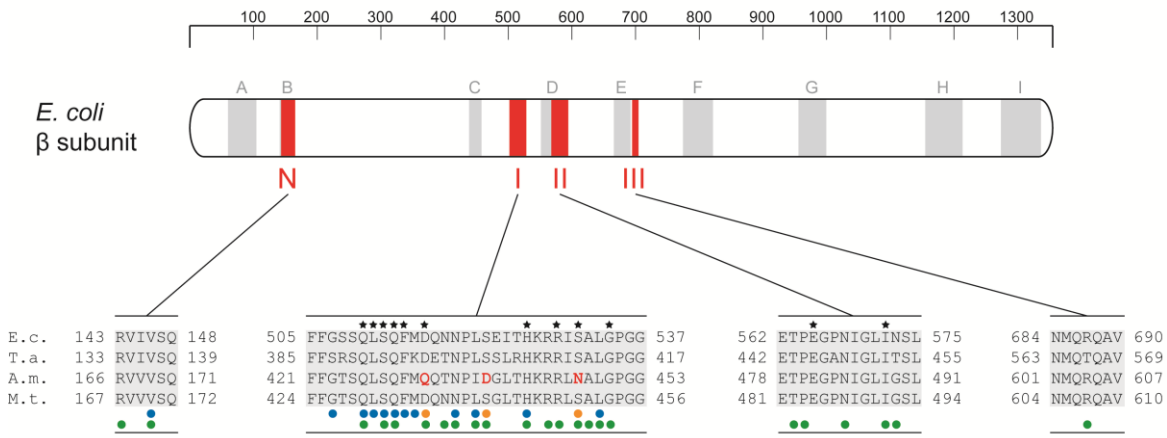

FIGURE 1-5. The β-subunit of RNAP and amino acids associated with RIF resistance. Sections highlighted in grey represent regions with high amino acid conservation across bacteria. The sections in red represent the four most common regions where RIF-resistant amino acid substitutions are located. RIF-resistant mutations are most commonly found in Region I, also referred to as the RIF resistance-determining region (RRDR). Amino acid residues labeled with a star are involved in direct interactions with RIF according to the co-structure of *T. aquaticus* RNAP and RIF (Campbell et al., 2001). Residues highlighted with an orange circle are those most frequently encountered (86% frequency) in clinical strains of RIF-resistant *M. tuberculosis* (Floss and Yu, 2005). Blue circles represent additional residues that have been associated with RIF resistance in *M. tuberculosis*. Green circles represent sites of mutation in *E. coli* that are associated with a RIF-resistance phenotype. Amino acids highlighted in red are associated with self-resistance in the rifamycin producing organism *A. mediterranei*. This figure has been adapted from Campbell et al., 2001, Floss and Yu, 2005 and Tupin et al., 2010.

In 2005 researchers solved the structure of RNAP holoenzyme (core RNAP plus σ-factor) from *Thermus thermophilus* in complex with rifapentine and rifabutin (Artsimovitch et al., 2005). This study suggested a more complex mechanism of rifamycin inhibition, based on the finding that the active site lacked the catalytic Mg^{2+} ion. They suggested an allosteric modulation model of inhibition, whereby rifamycin binding induces an allosteric signal to the active site resulting in a decrease affinity for the catalytic Mg^{2+} ion resulting in short RNAs. This study also showed that rifabutin, a

rifamycin with a C-3/C-4 tail (FIGURE 1-3), made contacts with the σ-factor and this interaction resulted in inhibition of the first phosphodiester bond of RNA synthesis. This study was challenged by researchers shortly thereafter who criticized the experimental methodology and provided biochemical evidence refuting the allosteric modulation model (Feklistov et al., 2008).

Interestingly, a number of rifamycin derivatives have been shown to retain activity against particular RIF-resistant strains. It is unclear why this is, but may involve additional interactions with RNAP outside the RIF binding pocket, such as the σ-factor (Artsimovitch et al., 2005; Aristoff et al., 2010). Additional biochemical and structural studies with both wild type and RIF-resistant RNAPs are needed to fully understand this mechanism.

Rifamycin Biosynthesis

A number of actinomycetes from soil and marine environments have been shown to produce rifamycin antibiotics. The majority of research on understanding rifamycin biosynthesis has come from *A. mediterranei*. Rifamycin is a polyketide that is synthesized by a type I modular polyketide synthase (PKS). The rifamycin biosynthetic gene cluster is composed of 43 open reading frames (ORFs) spanning over 100 kb of DNA (FIGURE 1-6) (August et al., 1998; Schupp et al., 1998). Biosynthesis is initiated by assembly of an aromatic amino acid starter unit followed by ten chain extensions using two acetate and eight propionate units (Floss and Yu, 2005). The biosynthetic gene cluster includes five type I modular PKS enzymes (*rifA-E)* responsible for chain extension and an amide synthase responsible for cyclization (*rifF*) (Kang et al., 2012).

There are also a number of enzymes involved in post-PKS modification of the rifamycin scaffold including dehydrogenases, monooxygenases and methyltransferases. The cluster also contains genes responsible for regulation and export (Floss and Yu, 2005).

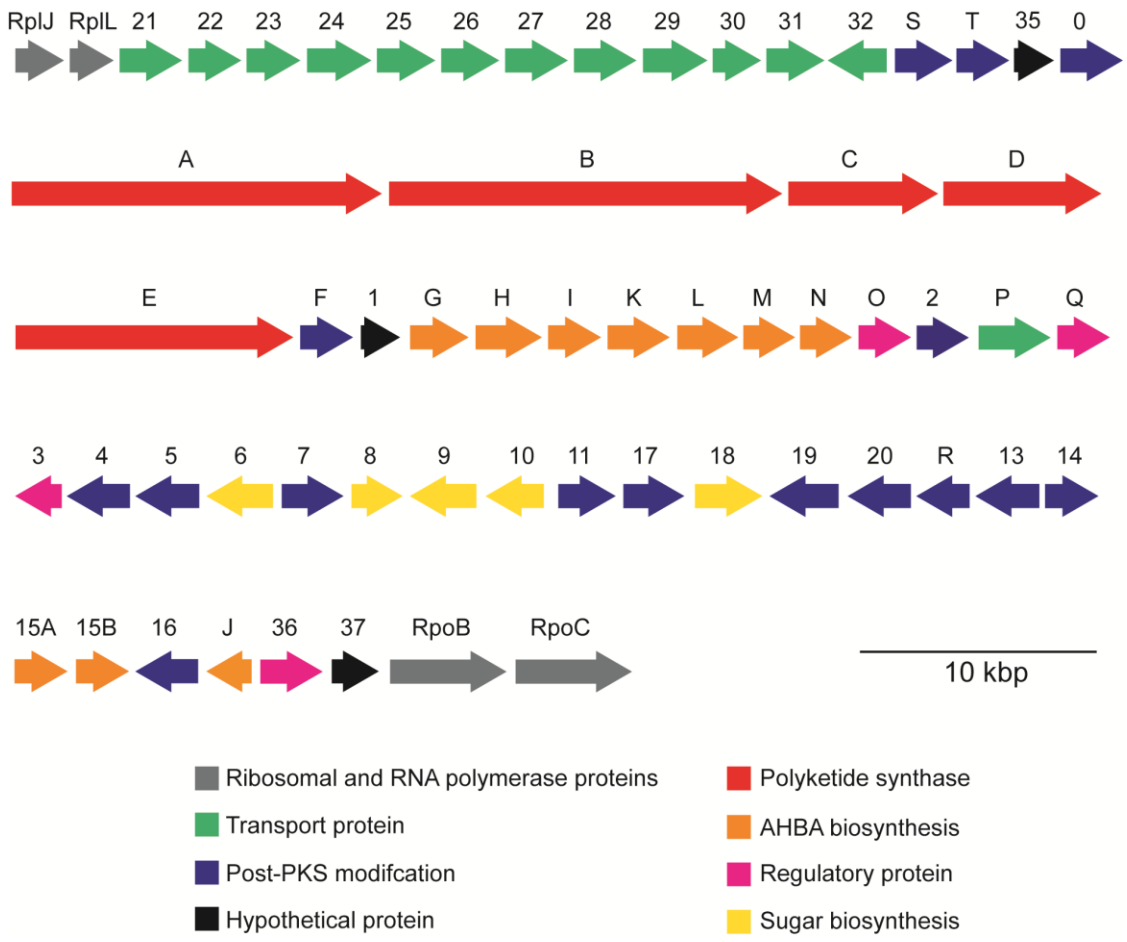

FIGURE 1-6. Genetic organization of the rifamycin biosynthetic gene cluster. Genetic cluster is from *A. mediterranei*. This figure was adapted from Floss and Yu, 2005.

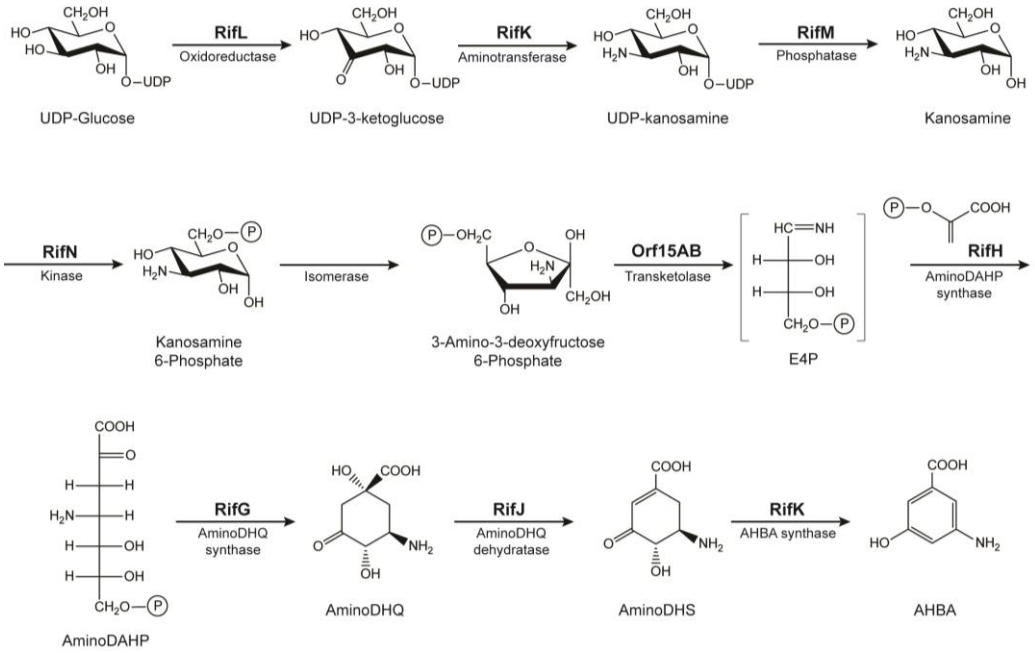

FIGURE 1-7. Proposed biosynthetic pathway of the ansamycin starter unit AHBA. E4P, erythrose 4-phosphate; AminoDAHP, 3,4-dideoxy-4-amino-D-arabino-seduheptulosonic acid 7-phosphate; AminoDHQ, 5-deoxy-5-aminodehydro-quinic acid; AminoDHS, 5-deoxy-5-aminodehydro-shikimic acid; AHBA, 3-amino-5-hydroxybenzoic acid. Figure adapted from Floss and Yu, 2005 and Floss, 2011.

The common starter unit for ansamycin biosynthesis is 3-amino-5-hydroxybenzoic acid (AHBA) (FIGURE 1-2) (Kang et al., 2012). In most cases the genes responsible for AHBA biosynthesis are localized with the entire biosynthetic gene cluster. Biosynthesis of AHBA parallels some reactions of the shikimate pathway, which is involved in the synthesis of aromatic amino acids (Floss et al., 2011). From the rifamycin biosynthetic gene cluster, 10 enzymes are believed to be required for the biosynthesis of AHBA (*rifG-N* and *orf15AB*) (FIGURE 1-6 and 1-7) (Floss et al., 2011). The AHBA synthase enzyme (RifK) is involved in two distinct reactions in the

biosynthesis of AHBA. AHBA synthase functions as an aminotransferase early in the biosynthesis of AHBA and is also involved in the final step of aromatization (FIGURE 1-7). This enzyme is highly conserved across all ansamycin biosynthetic gene clusters. It has routinely been used as a genetic probe to identify ansamycin biosynthetic gene clusters from genomic cosmid libraries or to identify potential ansamycin producers using PCR screening (August et al., 1998; He et al., 2006; Wood et al., 2007; Huitu et al., 2009; Floss et al., 2011; Wang et al., 2013).

Rifamycin Resistance

A variety of diverse RIF resistance mechanisms have been described from pathogenic and environmental strains of bacteria. Clinically, the predominant mechanism of RIF resistance is mutation of the drug target. Nonetheless, a number of pathogenic actinomycetes such as *Mycobacteria*, *Nocardia*, and *Rhodococcus* have been shown to inactivate RIF.

Alteration or Protection of the Drug Target

Mutation of the Drug Target

RIF resistance is most commonly attributed to spontaneous mutations within the *rpoB* gene, encoding the β-subunit of RNAP, resulting in single amino substitutions. Bacteria have a high propensity to develop RIF resistance at a rate 10^{-8} to 10^{-9} per bacterium per cell division and is the main reason this antibiotic is used in combination with other antibiotics (David, 1970; Gillespie, 2002). Amino acid substitutions conferring RIF resistance have been well documented in *M. tuberculosis* and *E. coli*

(Tupin et al., 2010). In *E. coli*, the majority of mutations (95%) map to the N-terminal half of the β-subunit and are generally confined to four regions: N-terminus, cluster I, cluster II and cluster III (FIGURE 1-5) (Floss and Yu, 2005). In clinical strains of *M. tuberculosis*, almost all mutations conferring RIF resistance are confined to cluster I, an 81-bp region corresponding to amino acids 432-458 also known as the RIF resistance determining-region (RRDR). In fact, three β-subunit mutations account for over 85% of clinical RIF-resistant *M. tuberculosis* isolates; these positions are S455 (41%), H440 (36%) and D430 (FIGURE 1-5) (9%) (Ramaswamy and Musser, 1998). Almost all *rpoB* mutations are associated with a fitness cost and often result in misregulation of gene expression (Reynolds, 2000; Mariam et al., 2004; Gagneux et al., 2006). With prolonged exposure, compensatory mutations in the β-subunit or other RNAP subunits (*rpoA* and *rpoC*, encoding the α-subunit and β'-subunit respectively) can ameliorate fitness costs (Reynolds, 2000; Comas et al., 2012; Casali et al., 2014). The change in gene expression associated with RIF resistance has been exploited by researchers to activate 'silent' or nonexpressed genes. For example, RIF-resistant mutants have been used to expand the substrate utilization capabilities of bacteria and induce the expression of 'silent' or poorly expressed secondary metabolites (Perkins and Nicholson, 2008; Hosaka et al., 2009; Inaoka and Ochi, 2011; Tanaka et al., 2013).

Duplication of the Drug Target

Recently, certain species from the Actinomycetales order have been shown to possess two copies of the *rpoB* gene. This occurrence was originally described in a *Nonomuraea* sp. but later extended to include other actinomycetes such as *Nocardia* spp.

and *Actinomadura* spp. (Vigliotta et al., 2005; Ishikawa et al., 2006; Tala et al., 2009). The auxiliary β-subunit (encoded by the *rpoB2* gene), was predicted to be refractory to RIF inhibition based on the primary amino acid sequence of this protein. RpoB2 contains a polymorphism at position 526 (N526H; *E. coli* numbering), which has been previously shown to contribute to RIF resistance in pathogens (Ishikawa et al., 2006; Floss and Yu, 2005). Indeed, a *rpoB2* null mutant displayed a markedly heightened sensitivity to RIF (Ishikawa et al., 2006). The *rpoB2* gene, which is not associated with the RNAP gene operon, was shown to be expressed during stationary phase, coinciding with the activation of antibiotic production. It has yet to be determined if the expression of *rpoB2* is inducible in the presence of RIF. It is hypothesized that this auxiliary *rpoB2* is involved in differential gene expression during the onset of secondary metabolite production at stationary phase (Vigliotta et al 2005).

RNAP Binding Proteins

The RbpA protein (encoded by the *rpbA* gene) is a RNAP binding protein that was shown to mediate low-level RIF resistance. *S. coelicolor* marginally upregulates *rpbA* in response to RIF and mutant strains devoid of *rbpA* display a minor increase in sensitivity to RIF (Newell et al., 2006). The *rbpA* gene is conserved across all Actinomycetes, including *M. tuberculosis*. Experiments with RpbA protein from *M. smegmatis* demonstrated the protein's ability to release RIF bound to RNAP (Dey et al., 2010; Dey et al., 2011). However, researchers from a different group have challenged this observation, and claim this behavior was not observed with RbpA from *M. tuberculosis* (Hu et al., 2012). The RbpA protein has been recently shown to directly

interact with various σ factors and is believed to influence RNAP's selectivity for particular σ factors, and thus impacting gene expression (Hu et al., 2012; Bortoluzzi et al., 2013).

Reduction of Drug Accumulation

As mentioned above, RIF and other rifamycins are not potent against Gram negative bacteria due to reduced permeability through the outer membrane (Floss and Yu, 2005). Indeed, mutant strains of Gram-negative bacteria, such as *E. coli*, lacking efflux (*acrAB-tolC* mutant) or having compromised outer membrane (*bamB* mutant) show markedly increase sensitivity to RIF (Cox et al., 2014; Aristoff et al., 2010). Gene expression studies have shown that *Mycobacterial* spp., including *M. tuberculosis*, upregulate several efflux pumps in response to RIF, contributing to low-level resistance (Siddiqi et al., 2004; Gupta et al., 2006; Jiang et al., 2008; Louw et al., 2009; Gupta et al., 2010; de Knegt et al., 2013). Similarly, examples of active efflux systems in Gram negative bacteria that pump out hydrophobic compounds, including RIF, have been described, which marginally contribute to RIF resistance (Maness and Sparling, 1973; Hagman et al., 1995; Okusu et al., 1996; Hannula and Hanninen, 2008).

Self-resistance of the Rifamycin Producer Microorganism

The rifamycin biosynthetic gene (*rif*) cluster from *A. mediterranei* does not contain any proteins dedicated to resistance. The *rif* cluster is adjacent to the genes encoding the RNAP machinery. The β-subunit sequence shows that three amino acid positions that are crucial for RIF binding are substituted in *A. mediterranei*; these are

Q432D, D438S, and N447S (Figure 1-5). In fact substitution of just one of the these residues is substantial to confer high-level RIF resistance (Floss and Yu., 2005). This triple amino acid substitution of the β-subunit is a signature of rifamycin producers and is found in other producing microorganisms (Floss and Yu, 2005). The *rif* cluster also contains efflux pumps involved in exporting the final product. The role of these pumps in rifamycin resistance has yet to be determined (Floss and Yu, 2005).

Enzymatic Inactivation of RIF

A number of actinomycetes from the suborder Corynebacterineae are pathogenic; these include members of the genera *Mycobacterium* and *Nocardia* among others. Although these bacteria typically reside in the environment, they have been reported to cause opportunistic infections, usually in immunocompromised individuals. While determining the antibiograms of these pathogenic Corynebacterineae, researchers revealed that many of these strains were resistant to RIF by inactivating the antibiotic. A total of four RIF inactivation mechanisms have been described: ADP-ribosylation, glycosylation, phosphorylation and decomposition mediated by monooxygenation. The group transfer mechanisms of resistance target one of two hydroxyls (C-21 or C-23) of RIF that make hydrogen bonding interactions with β-subunit and are imperative for binding (Figure 1-4). Therefore, the modification of one of these functional groups diminishes RIF's ability to bind and therefore inhibit its target.

ADP-ribosylation

The inactivation of RIF by *Mycobacterium smegmatis* was first described by Dabbs in 1987 (Dabbs, 1987). The inactivated RIF product was initially identified as RIF ribosylated at the C-23 hydroxyl (Dabbs et al., 1995; Morisaki et al., 1995). This mechanism was also shared by a number of species from the genus *Mycobacterium*, *Gordona* and *Tsukamurella* (Dabbs et al., 1995; Tanaka et al., 1996). The gene responsible for this phenotype, *arr* (ADP-ribosylation of RIF), was identified from *M. smegmatis* and heterologous overexpression confirmed the enzyme's ability to confer high-level RIF resistance (Quan et al., 1997; Quan et al., 1999). Inactivated RIF products generated by heterologous expression showed ADP-ribosylation at the C-23 hydroxyl of RIF (FIGURE 1-8) (Quan et al., 1999). Therefore, ribosylated-RIF, the product initially identified from *M. smegmatis*, was a degraded metabolite of ADP-ribosylated RIF (Morisaki et al., 2000). Shortly later it was revealed that the Arr enzyme was not restricted to bacteria from the Corynebacterineae suborder. An ortholog of Arr, Arr-2, was found on an integron from a clinical isolate of *Pseudomonas aeruginosa*, indicating that the *arr* gene was mobile (Tribuddharat and Fennewald, 1999). Since then, many Gram negative pathogenic bacteria have been found to carry *arr* variants on various mobile genetic elements alongside other antibiotic resistance determinants (Arlet et al., 2001; Girlich et al., 2001; Naas et al., 2001; Houang et al., 2003; da Fonseca et al., 2008; Sun et al., 2010). Interestingly, RIF is not routinely use to treat Gram negative infections, however, its association with other antibiotic resistance genes has likely contributed to its prevalence and distribution.

Recently Baysarowich et al. biochemically characterized Arr enzymes from various pathogenic and nonpathogenic bacterial genera (Baysarowich et al., 2008). Enzyme kinetic characterization and heterologous expression demonstrated that regardless of the bacterial source, all Arr enzymes conferred high-level RIF resistance. Furthermore, Arr displayed broad substrate specificity and confers resistance towards both natural product and semisynthetic rifamycins. The structure of Arr from *M. smegmatis* was also determined in complex with RIF, highlighting important molecular interactions required for substrate binding.

Glycosylation

The pathogenic actinomycete *Nocardia brasiliensis* has been shown to inactivate RIF (Yazawa et al., 1993). Analysis of the inactivated RIF product showed that glucose was added to the C-23 hydroxyl of RIF (FIGURE 1-8). Glycosylation of RIF and was reported to be restricted to bacteria from the *Nocardia* genus. (Morisaki et al., 1993; Yazawa et al., 1993; Tanaka et al., 1996). At the onset of the work described here, the gene responsible for encoding the RIF glycosyltransferase, *rgt*, has yet to be identified and protein characterized.

Phosphorylation

The phosphorylation of RIF was first described from the pathogenic actinomycete *Nocardia otitidiscaviarum*. The site of phosphorylation was the C-21 hydroxyl of RIF (FIGURE 1-8) (Morisaki et al., 1993; Yazawa et al., 1994). A number of *Bacillus* spp. were also shown to phosphorylate RIF (Dabbs et al., 1995). This finding is intriguing,

considering this genera of bacteria are highly susceptible to RIF (Dey and Chatterji, 2012). The genetic element encoding the RIF phosphotransferase, *rph*, had yet to be identified when this work began.

Decomposition

A number of bacteria from the *Nocardia*, *Mycobacterium* and *Rhodococcus* genus have been shown to decolorize RIF, abolishing activity (Dabbs, 1987; Yazawa et al., 1993; Tanaka et al., 1996). Low GC-content Gram positives such as *Bacillus* spp. have also demonstrated the ability to decolorize RIF (Dabbs et al., 1995). By screening a genomic library from the pathogen *Rhodococcus equi* for increased RIF resistance in *E. coli*, the *iri* gene (inactivation of RIF) was identified and confirmed to be responsible for decolorizing RIF (Andersen et al., 1997). The Iri protein shows similarity to monooxygenases acting upon phenolic compounds, however, a monooxygenated RIF or other modified RIF products could not be identified. An orthologous enzyme was later identified from *Nocardia farcinica* using genomics and named Rox (Hoshino et al., 2010). When Rox was expressed in *E. coli* a monooxygentated product, RIF-O, was recovered and the structure elucidated. Interestingly, the site of modification was at the synthetic tail of RIF (FIGURE 1-8). RIF-O displays significantly diminished antimicrobial activity.

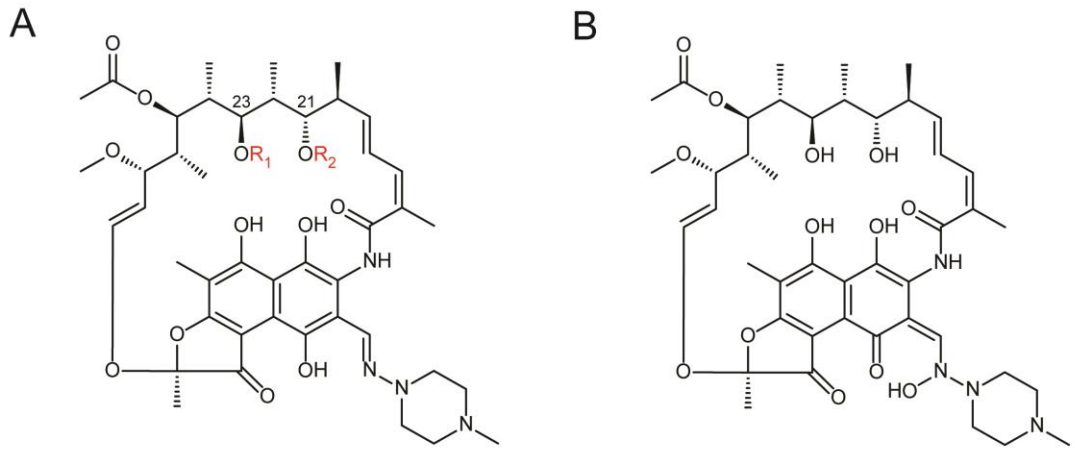

Molecule	R_1	R_2	Gene	Microorganism	Reference
RIF	H	H			
RIF-ADP-ribose	ADP-Ribose	H	*arr*	*Mycobacterium smegmatis* *Streptomyces coelicolor* *Pseudomonas aeruginosa* *Mycobacterium* spp. *Gordona* spp. *Tsukamurella* spp.	Quan et al., 1997 Baysarowich et al., 2008 Tribuddharat and Fennewald, 1999 Tanaka et al., 1996
RIF-glucose	Glucose	H	*rgt*	*Nocardia brasiliensis*	Yazawa et al., 1993
RIF-phosphate	H	PO_3H_2	*rph*	*Nocardia otitidiscaviarum* *Nocardia spp.* *Rhodococcus* spp. *Bacillus* spp.	Yazawa et al., 1994 Tanaka et al., 1996 Dabbs et al., 1995
Decomposition			*iri* *rox*	*Rhodococcus equi* *Nocardia farcinica* *Rhodococcus* spp. *Nocardia* spp. *Mycobacterium* spp. *Bacillus* spp.	Andersen et al., 1997 Hoshino et al., 2010 Dabbs, 1987 Tanaka et al., 1996 Dabbs, 1987 Dabbs et al., 1995

FIGURE 1-8. Mechanisms of RIF inactivation. Four mechanisms of RIF inactivation have been described. (A) Structure of RIF product from the group transfer mechanisms of RIF inactivation. (B) Structure of the monooxygenated RIF product, 2'-*N*-hydroxy-4-oxo-rifampin (Hoshino et al., 2010). Genes encoding RIF inactivating enzymes have been identified and characterized from microorganisms highlighted in red.

UNCOVERING THE RIFAMYCIN RESISTOME

The rifamycin family of antibiotics has been crucial in the treatment of tuberculosis and other mycobacterial-associated infections for almost 50 years. Due to the rise in antibiotic resistance along with the dwindling number of new antibiotics entering the clinic, drug development programs are returning to classic antibiotics for solutions. RIF is experiencing an increase in use for antibiotic-resistant pathogens such as MRSA. Furthermore, due to its broad spectrum activity and synthetic malleability, the rifamycin scaffold continues to be an attractive platform for drug development by pharmaceutical companies. New rifamycin derivatives, including rifaximin and rifalazil, are being developed to target a much broader array of pathologies. The main question is whether this recent expansion of the rifamycin family of antibiotics will apply pressure for the selection of more diverse rifamycin resistance determinants.

The rifamycins are products of soil bacteria that have existed for millennia. During this time frame, neighboring bacteria have evolved diverse mechanisms to resist the bactericidal effects of the rifamycins. Therefore, the soil represents a reservoir of ancient and diverse rifamycin resistance determinants. The ability of bacteria to facilitate horizontal gene transfer along with the link between antibiotic resistance genes found in pathogens and environmental bacteria, suggests that with the appropriate selection pressure, rifamycin resistance determinants will emerge into the clinic (Perry and Wright, 2013). These events would have a dramatic impact on the entire family of rifamycin antibiotics. The mobilization of rifamycin resistance genes is already underway. The *arr* gene, encoding a RIF ADP-ribosyltransferase, was originally identified from the benign

microorganism *M. smegmatis*. Today however, this gene is located on mobile genetic elements clustered with multiple antibiotic resistance genes and carried by pathogens. It is crucial to identify and characterize the rifamycin resistome; the collection of all rifamycin resistance determinants from the global microbiota. Glycosylation and phosphorylation of RIF have been previously described in the literature; however, the genes encoding these enzymes had yet to be identified when this work began. We were particularly interested in these rifamycin resistance genes because of their potential to be transferred horizontally across bacterial species.

Previous research from our group has demonstrated that soil actinomycetes are naturally multidrug-resistant (D'Costa et al., 2006). Follow up studies showed that many soil isolates were able to inactivate RIF. Using these soil isolates as a starting point, this thesis aims to:

Research Aims

1. Characterize various mechanisms of RIF inactivation from the Wright actinomycete collection (CHAPTER 2).
2. Identify the genes encoding the RIF glycosyltransferase (*rgt*) and RIF phosphotransferase (*rph*) (CHAPTER 3 and 4).
3. Characterize RGT and RPH enzymes: contribution to RIF resistance *in vivo*, prevalence and substrate specificity (CHAPTER 3 and 4).
4. Investigate a common regulatory motif associated with RIF inactivating genes from actinomycetes (CHAPTER 4).
5. Probe the ansamycin production capabilities of RIF-resistant actinomycetes (CHAPTER 5).

Identifying and characterizing the rifamycin resistome enables us to predict antibiotic resistance before it emerges into the clinic and understand the evolution of antibiotic resistance in the environment. These studies will provide pertinent information for antibiotic resistance gene surveillance initiatives and future drug development programs.

CHAPTER 2

IDENTIFICATION AND CHARACTERIZATION OF RIFAMYCIN INACTIVATING SOIL ACTINOMYCETES

CHAPTER 2 PREFACE

Parts of the research presented in this chapter have been previously published in:

> Spanogiannopoulos, P., Thaker, M., Koteva, K., Waglechner, N., and G.D. Wright. 2012. Characterization of a rifampin-inactivating glycosyltransferase from a screen of environmental actinomycetes. *Antimicrobial Agents and Chemotherapy*. 56(10): 5061-5069.
>
>

I performed all the work described in this chapter.

Acknowledgements:

I thank Prof. Michael Fischbach for providing the Broad Institute Actinomycete Collection. I appreciate assistance from Dr. Erin Westman for preliminary antibiotic resistance profiling of the Broad Institute Actinomycete Collection. I thank Dr. Kalinka Koteva for assistance with mass spectrometry.

ABSTRACT

Rifamycin antibiotics were first described over 60 years ago as natural products from the soil actinomycete *Amycolatopsis mediterranei*. Semisynthetic rifamycin derivatives have experienced great success in the clinic including rifampin (RIF), the most widely used rifamycin, which is a frontline agent against tuberculosis. The predominant mechanism of RIF resistance by pathogens is mutation of the drug target (*rpoB* gene; encodes the β-subunit of RNA polymerase). Moreover, a number of actinomycete pathogens have been shown to inactivate RIF. A recent study by D'Costa et al. examined the antibiogram of soil bacteria and demonstrated that RIF inactivation is prevalent in this environment. The aim of this study is to investigate and characterize RIF inactivation from the soil microbiota. A screen of over 500 actinomycetes identified 22 isolates with a RIF inactivating phenotype, representing over 4% of the collection. Inactivated RIF products were identified by analyzing conditioned media of isolates grown in the presence of RIF using liquid chromatography-electrospray ionization-mass spectrometry (LC-ESI-MS) and three modes of RIF inactivation were deduced: glycosylation, phosphorylation and decomposition. 16S rRNA gene analysis revealed these isolates all belonged to the *Streptomyces* or *Amycolatopsis* genus and is the first report of RIF inactivation from these genera. Furthermore, sequence analysis of the RIF resistance-determining region (RRDR) of *rpoB* revealed many isolates have a resistant RNA polymerase highlighting that environmental bacteria contain multiple mechanisms of resistance for the same antibiotic. This study reveals that soil bacteria are a reservoir of RIF inactivation determinants. The mobilization of these resistance genes into pathogens could have a deleterious impact on the efficacy of the rifamycin family of antibiotics.

INTRODUCTION

The discovery and introduction of antibiotics into the clinic is one of the greatest achievements of modern medicine. The majority of clinically used antibiotics owe their origins to environmental soil microorganisms, with bacteria from the order Actinomycetales, *Streptomyces* in particular, being the most prolific producers (Berdy, 2012). The soil environment is presumed to be a highly competitive ecosystem and it is hypothesized that antibiotic producers synthesize these lethal natural products to deter neighboring bacteria, providing a competitive advantage. The genome sequence of the model Streptomycete *Streptomyces coelicolor* revealed an astonishing genetic capacity to biosynthesize natural products, estimated at over 20 entities (Bentley et al., 2002). It has been projected that the genus *Streptomyces* may produce up to 100,000 various secondary metabolites (Watve et al., 2001; Baltz, 2006). Soil bacteria that share the same niche as antibiotic producers are pressured to evolve strategies to evade antibiotics or perish. Therefore, soil bacteria are exposed to a myriad of diverse natural product antibiotics and consequently, over millennia, have developed a variety of sophisticated antibiotic resistance mechanisms that are presented in the environment. It should come as no surprise that contemporary soil bacteria are multi-drug resistant.

The environment is therefore an ancient reservoir of antibiotics and antibiotic resistance determinants. A major concern is that these antibiotic resistance determinants may become mobile and passed on to pathogenic bacteria, which would obviously have a negative impact on the usefulness of our current clinically used antibiotics. There is now growing evidence linking antibiotic resistance genes from the environment to the clinic

(Benveniste and Davies, 1973; Marshall et al., 1997; Forsberg et al., 2012). It is a priority to explore and characterize the antibiotic resistome; the collection of all antibiotic resistance genes and their precursors in the global microbiota, from both pathogenic and nonpathogenic pathogenic bacteria (Wright, 2007). Identifying the repository of antibiotic resistance mechanisms in the environment will provide insight on the evolution of antibiotic resistance and serve as a warning of what may potentially surface in clinically relevant bacteria. With this information we can devise strategies to circumvent the selection of these determinants.

Rifamycin antibiotics were first uncovered as natural products from *Amycolatopsis mediterranei*. Semisynthetic rifamycins have experienced great success in the clinic. Rifampin (RIF), the most renowned rifamycin, continues to be a front line agent for the treatment of tuberculosis since its introduction into the clinic over 50 years ago (Aristoff et al., 2010). Furthermore, it is increasingly used as adjunctive therapy in the treatment of drug-resistant *Staphylococcus aureus* (Russell et al., 2014). The predominant mechanism of resistance to RIF in the clinic occurs through point mutations of the drug target (encoded by the *rpoB* gene) (Floss and Yu, 2005). Nonetheless, the inactivation of RIF has been previously reported as a mechanism of resistance from a number of actinomycete pathogens (Tupin et al., 2010). Four modes of RIF inactivation have been described: glycosylation, phosphorylation, ADP-ribosylation and decomposition (FIGURE 1-8).

Thus far, the emphasis of antibiotic resistance research has been centered on pathogenic bacteria. Although research on antibiotic resistance from environmental

bacteria has been conducted, these studies have generally not been comprehensive. A study by D'Costa et al. aimed to determine the antibiogram of culturable soil bacteria (D'Costa et al., 2006). This study screened a collection of almost 500 soil dwelling bacteria from the Wright Actinomycete Collection (WAC) against a panel of 21 various antibiotics. The antibiotics included in the screen encompassed natural product, semi-synthetic, and completely synthetic compounds with various modes of actions. On average each isolate was resistant to 7-8 antibiotics, confirming the multi-drug resistant phenotype of environmental bacteria. A total of 50 isolates were resistant to RIF, representing 10.4% of the collection (APPENDIX 1). Follow up studies demonstrated 21 isolates were able to inactivate RIF, representing 40.8% of the RIF-resistant isolates and 4.2% of the entire collection (APPENDIX 1). Together these findings reveal that RIF resistance and inactivation is prevalent in soil bacteria.

This study aims to identify and characterize a collection of RIF inactivating soil bacteria. We validate that RIF inactivation is prevalent in WAC isolates. In addition to the WAC, we screened a collection of actinomycetes with publically available genome sequences for RIF resistance and identified one RIF-inactivating strain. Modes of RIF inactivation were determined by identifying RIF products from conditioned media of isolates grown in the presence of RIF using LC-ESI-MS. Furthermore, isolates were characterized by sequencing of the 16S rRNA and *rpoB* genes.

MATERIALS AND METHODS

Antibiotics and Media

RIF was purchased from Sigma-Aldrich (Oakville, ON) and dissolved in DMSO. Actinomycetes were routinely grown using solid or liquid Streptomyces isolation media (SIM) (D'Costa et al., 2006).

RIF Inactivation Assay

Fresh spores were used to inoculate 5 ml of liquid SIM in culture tubes with one glass bead and incubated at 30°C with shaking at 250 rpm. RIF was added at a concentration of 20 µg/ml. At 24 hour time intervals, conditioned media samples were removed and clarified by centrifugation. A 10 µl supernatant sample was analyzed for residual RIF antimicrobial activity using the Kirby-Bauer disk diffusion assay with *Bacillus subtilis* 168 serving as the RIF-sensitive indicator microorganism on solid LB media; plates were incubated for 16 hours at 37°C (Wikler et al., 2006). Supernatants that demonstrated a complete loss of bioactivity were analyzed using high-performance liquid chromatography-electrospray ionization-mass spectrometry (LC-ESI-MS). Prior to LC-ESI-MS analysis, conditioned media samples were diluted with an equal volume of methanol and clarified by centrifugation at 15 000 × *g* for 10 min. LC-ESI-MS was performed using an Agilent 1100 Series HPLC system (Agilent Technologies Canada, Mississauga, ON) and a QTRAP LC/MS/MS System (Applied Biosystems, Carlsbad, CA). HPLC was performed using a Sunfire C18 column (5 µM, 4.6 × 50 mm) with the following method: linear gradient of 5 to 97% acetonitrile with 0.05% formic acid (FA) in water with 0.05% FA over 12 min at a flow rate of 1 ml/min.

Construction of RIF-resistant *Bacillus subtilis*

A mutant strain of *Bacillus subtilis* 168 was generated with a H482Y substitution within the β-subunit of RNAP; cluster I of the *rpoB* gene (β-526 *E. coli* numbering) (FIGURE 1-5). This mutant has been shown to have high-level RIF resistance (Nicholson and Maughan, 2002). This was accomplished using an overlapping PCR strategy followed by transformation into *B. subtilis* homologous, recombination and selection on RIF containing media. Two partial and overlapping fragments of the *B. subtilis* 168 *rpoB* gene were amplified using primers engineered with the desired mutation (CAC→TAC mutation). PCR product 1 was amplified with primers Bsub_RifR-A and Bsub_RifR-C and PCR product 2 with primers Bsub_RifR-B and Bsub_RifR-D2 (APPENDIX 2). PCR products were resolved using agarose gel electrophoresis and recovered by gel extraction. Overlapping PCR was performed using PCR products 1 and 2 and outside primers Bsub_RifR-A and Bsub_RifR-D2. The final PCR product was purified using gel electrophoresis and recovered by gel extraction. Competent *B. subtilis* cells were transformed with the final PCR product as previously described (Sadaie and Kada, 1983). Transformations were plated on LB supplemented with RIF (50 μg/ml). RIF-resistant colonies were re-streaked on LB plus RIF. Genomic DNA (gDNA) from RIF-resistant colonies was prepared and a partial fragment of the *rpoB* gene was amplified using primers BsubRifR-SeqF and BsubRifR-SeqR (APPENDIX 2). PCR products were sequenced to confirm the desired mutation.

16S rRNA and *rpoB* Gene Analysis

gDNA from each isolate was prepared by standard methods (Kieser, 2000). 16S rDNA PCR was performed using primers F27 and R1492 (Heuer et al., 1997) (APPENDIX 2). The *rpoB* gene was amplified using primers SRPOF1 and SRPOR1 (Kim et al., 2005) (APPENDIX 2). PCR products were cleaned up using agarose gel electrophoresis and gel extraction. PCR products were sequenced at the Mobix Central Facility (McMaster University, Hamilton, ON). Species relatedness was determined by analyzing the 16S rRNA gene sequences using blastn (Altschul et al., 1990).

BOX-PCR Fingerprinting Analysis

BOX-PCR was performed according to Lanoot et al. with slight modifications (Lanoot et al., 2004). PCRs were conducted using Biotools DNA polymerase (Biotools B&M Labs S.A., Madrid, Spain) with the following reaction conditions: 1× Biotools Reaction Buffer ($MgCl_2$-free), 2 mM $MgCl_2$, 200 µM dNTPs, 8% (v/v) DMSO, 1 U Biotools DNA Polymerase, 250 ng gDNA and 0.8 µM BOXAIR primer (APPENDIX 2) in a final volume of 25 µl. PCR was performed using an Eppendorf Mastercycler (Hamburg, Germany) with the following steps: initial denaturation of 95°C for 7 min, 30 cycles of 95°C for 30 sec, 53°C for 1 min and 65°C for 8 min, followed by a final extension of 65°C for 16 min. The 25 µl reaction was loaded onto a 2% (w/v) agarose gel for analysis.

RESULTS

Screening the Broad Institute Actinomycete Collection for RIF Resistance

The Broad Institute has sequenced the genomes of 20 antibiotic producing actinomycetes, referred to from here on as the Broad Institute actinomycete collection (BIAC). This initiative aims to advance genomic, bioinformatic and chemical methodologies in actinomycete biology in an effort to uncover cryptic antibiotics (The Broad Institute, 2010). The availability of annotated genome sequences provides an invaluable resource towards our efforts of identifying antibiotic resistance genes and linking genotype to a particular phenotype. We previously screened the BIAC for resistance against 27 diverse antibiotics (unpublished data). This screen confirmed that actinomycetes are naturally multi-drug resistant and reiterated the findings from D'Costa et al. (D'Costa et al., 2006). A total of four actinomycetes were resistant to RIF at 20 µg/ml (TABLE 2-1 and APPENDIX 1). These were *Streptomyces griseoflavus* Tu4000, *Streptomyces lividans* TK24, *Streptomyces viridochromogenes* DSM 40736 and *Streptomyces sviceus* ATCC 29083.

Identifying RIF Inactivating Actinomycetes

In total, 54 RIF-resistant actinomycetes were identified from the WAC and BIAC. We developed a simple assay to identify RIF inactivating bacterial isolates. The RIF inactivation assay involves growing each isolate in media supplemented with RIF and assaying conditioned media samples over time for residual RIF bioactivity using the Kirby-Bauer disk diffusion assay using RIF-sensitive *Bacillus subtilis* 168 as the indicator microorganism (FIGURE 2-1) (Wikler et al., 2006). Actinomycetes are known to

A. Biological inactivation assay

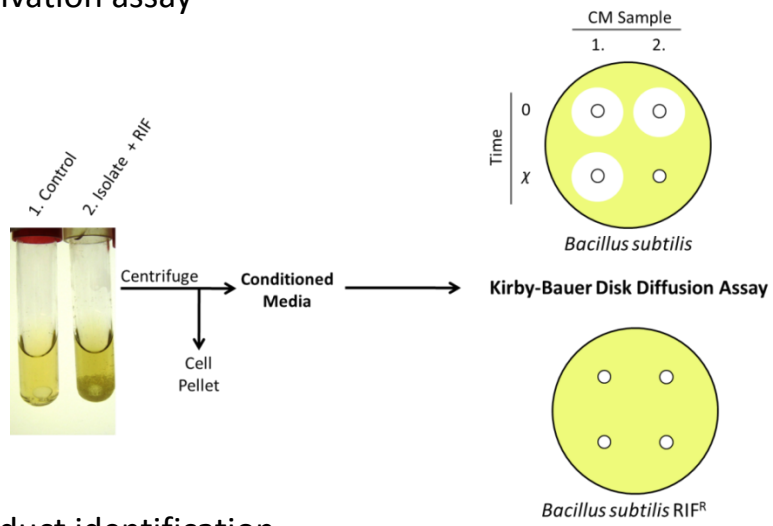

B. Inactivated product identification

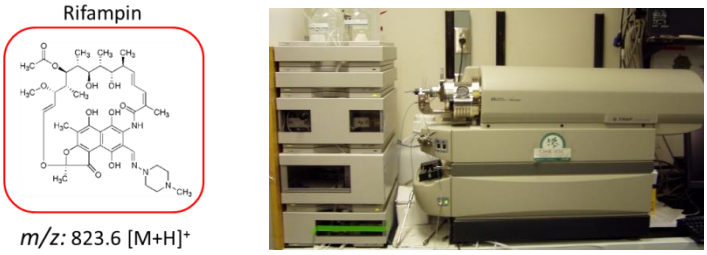

FIGURE 2-1. RIF inactivation assay outline. (A) RIF-resistant actinomycetes are grown in media supplemented with RIF (20 µg/ml). Over time, conditioned media samples are analyzed for residual RIF concentration using the Kirby-Bauer disk diffusion assay with *B. subtilis* as the indicator microorganism. As a control, conditioned media is also assayed against RIF-resistant *B. subtilis* to determine if antibiotics are produced by the actinomycete. (B) Conditioned media samples that demonstrate a loss of biological activity are analyzed using LC-MS to identify the RIF product.

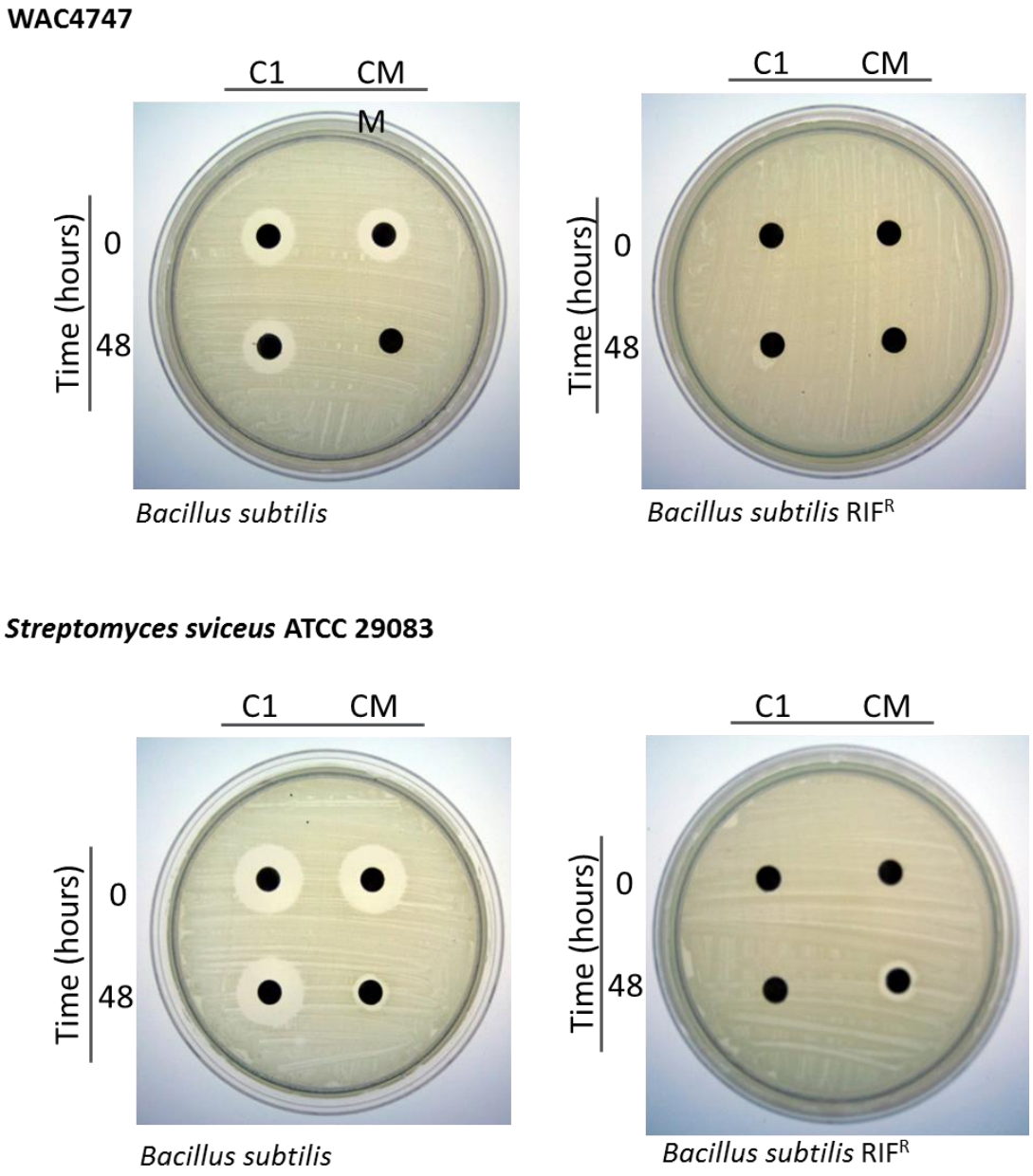

FIGURE 2-2. RIF inactivation assay. Conditioned media samples of actinomycetes grown in the presence of RIF are analyzed using the Kirby-Bauer disk diffusion assay for residual RIF activity using *B. subtilis* as the indicator microorganism. Conditioned media samples are also tested against a RIF-resistant strain of *B. subtilis* to discriminate if the actinomycetes are producing antibiotics. C1, control, media and RIF; CM, conditioned RIF-containing media.

be prolific antibiotic producers. The production of an antibiotic by an isolate may generate a false negative result using this assay; that is RIF may be completely inactivated; however, the production of an antibiotic may mask this hit. Conditioned media samples were also analyzed using a RIF-resistant mutant of *Bacillus subtilis* 168 (*rpoB* mutant) to discriminate bioactivity as a result of RIF or some other antibiotic that may be produced.

A total of 54 RIF-resistant actinomycetes were screened for RIF inactivation: 50 WAC isolates and 4 BIAC strains (APPENDIX 1). 22 actinomycetes demonstrated the ability to completely inactivate RIF, representing 41% of RIF-resistant isolates and 4.4% of the entire actinomycete collection (FIGURE 2-2 and TABLE 2-1). This finding highlights that RIF inactivation is prevalent in environmental actinomycetes.

TABLE 2-1. Number of RIF-resistant and RIF-inactivating actinomycetes.

Actinomycete Collection	Total Number of Isolates/Species	Number RIF-resistant	Number RIF-inactivating
Wright Actinomycete Collection (WAC)	481	50	21
Broad Institute Actinomycete Collection (BIAC)	20	4	1
Total	501	54	22

Actinomycetes Inactivate RIF Using Various Mechanisms

Conditioned media samples that demonstrated a loss of RIF bioactivity were next analyzed using liquid chromatography-electrospray ionization-mass spectrometry (LC-ESI-MS) to identify inactivated RIF products. From all conditioned media samples, two different modified antibiotic peaks were identified with each resulting in a shift in retention time while maintaining a UV-visible light (UV-Vis) absorption spectrum similar to that seen with RIF (TABLE 2-2). Mass spectrometry of the modified RIF products confirmed an increase in the mass-to-charge ratio (*m/z*) consistent with the glycosylation and phosphorylation of RIF (TABLE 2-2) (Morisaki et al., 1993; Yazawa et al., 1993; Yazawa et al., 1994). Additionally, a number of isolates appeared to decompose RIF where no identifiable peak could be detected; a result similar to what has been originally reported from *Rhodococcus equi* (Andersen et al., 1997). Interestingly, ADP-ribosylated RIF was not identified from any samples. Therefore, soil-dwelling actinomycetes utilize a variety of mechanisms to inactivate RIF.

TABLE 2-2. Inactivated RIF products identified by LC-ESI-MS.

Retention Time (minutes)	Observed *m/z* $[M+H]^+$	Mass Difference	Mode of Inactivation	Number of Isolates
6.63 (RIF)	823.2			
5.90	985.5	162.3	Glycosylation	11
7.46	900.8	77.6	Phosphorylation	5
-	-	-	Decomposition	6

Characterization of RIF-inactivating Soil Actinomycetes

Subsequently, the species diversity associated with our RIF inactivating bacterial isolates was explored. The 16S rDNA housekeeping gene is routinely used as a marker for bacterial phylogeny and taxonomy (Janda and Abbott, 2007). A fragment of the 16S rDNA gene of each isolate was amplified by PCR using primers optimized for actinomycetes (Heuer et al., 1997). Amplified products were sequenced and then analyzed using blastn to determine 16S rDNA relatedness (Altschul et al., 1990). All isolates most closely resembled species from the genus *Streptomyces* with the exception of a single *Amycolatopsis* species (TABLE 2-3). This is the first report of RIF inactivation from these genera.

Interestingly, a number of RIF-inactivating isolates possessed identical 16S rDNA sequences. These strains not only shared a common mechanism of inactivation but were all isolated from the same geographic soil sample (APPENDIX 1). This suggested that some of our RIF-inactivating isolates may be clones. We turned to a PCR fingerprinting technique called BOX-PCR to dereplicate RIF inactivating isolates (Lanoot et al., 2004). This method utilizes a single oligonucleotide primer that is complimentary to interspersed repeated DNA sequences. PCR with this single primer generates a fingerprint of PCR products specific for each bacterial species. Isolates that generate identical PCR fingerprints are considered clones. Following BOX-PCR analysis, nine RIF-inactivating isolates were confirmed to be clones. WAC4839 was selected as a representative from this cluster (FIGURE 2-3). This analysis confirmed we have successfully identified 14 unique RIF-inactivating species (TABLE 2-3).

A previous study by Kim et al. demonstrated that a proportion of *Streptomyces* spp. are naturally RIF resistant due to an amino acid substitution in the β-subunit of RNA polymerase (Kim et al., 2005). The β-subunit of RNAP and the RIF resistance determining region (RRDR) in particular is highly conserved across bacteria (Floss and Yu, 2005). Kim et al. showed that a number of *Streptomyces* spp. possess an asparagine at position 531 (N531; *E. coli* numbering) of the β-subunit instead of the conserved serine (S531). Mutation of β-subunit S531 is well-known to be associated with RIF resistance and is in fact one of the most common mutations found from RIF-resistant pathogens (FIGURE 1-5) (Ramaswamy and Musser, 1998). We were interested in determining if our RIF-inactivating isolates contained the RIF-resistant N531 polymorphism. Actually, previous reports have shown that actinomycetes may contain multiple mechanisms of RIF resistance (Ishikawa et al., 2006; Hoshino et al., 2010). Using PCR, we amplified and sequenced the RRDR of *rpoB* from each isolate. Most of the *rpoB* genes corresponded to the RIF-sensitive S531 type β-subunit. However, four isolates possessed a RIF-resistant N531 type β-subunit (TABLE 2-3). These results highlight that some actinomycetes possess multiple mechanisms of RIF resistance.

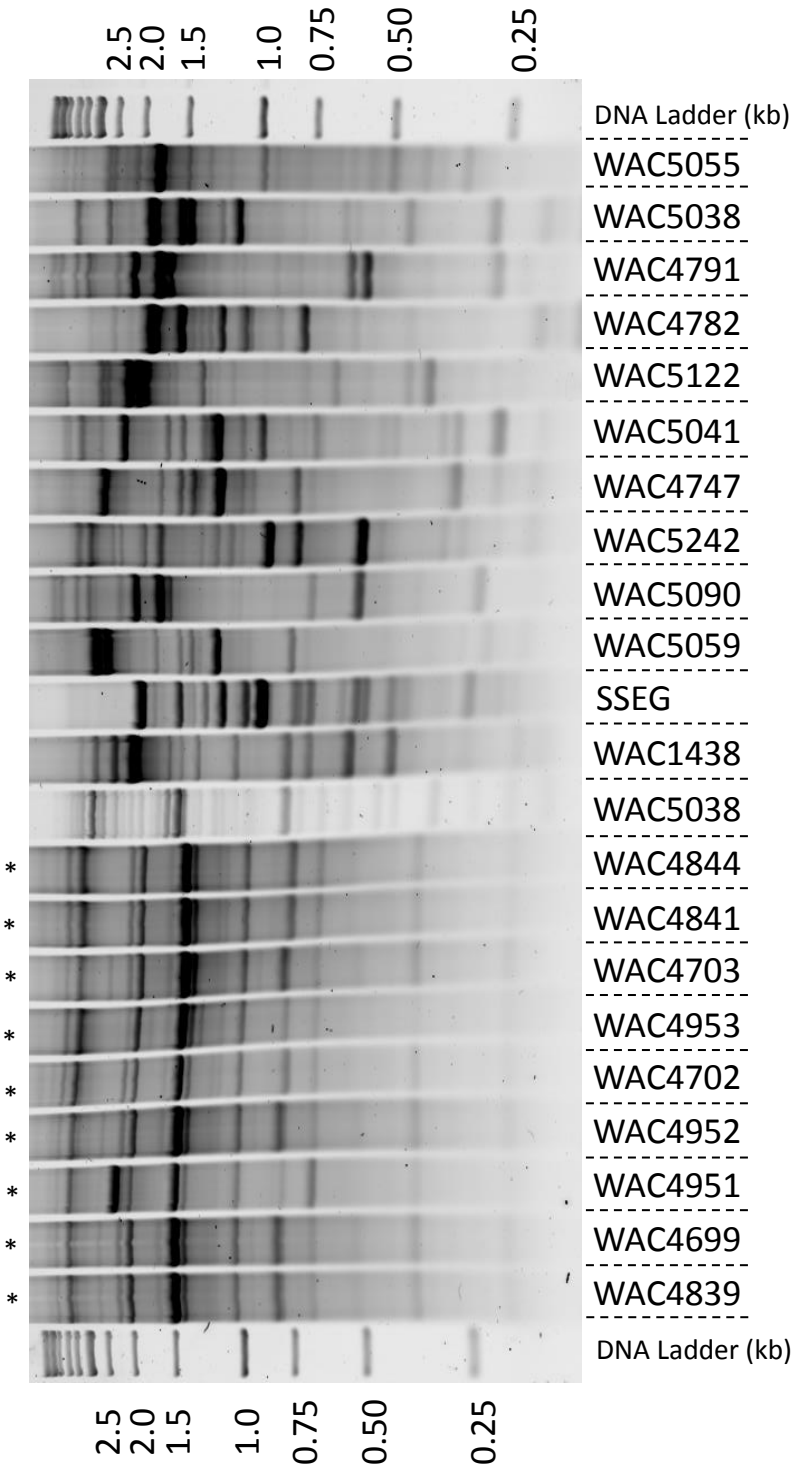

FIGURE 2-3. Dereplication of the 22 RIF-inactivating actinomycetes. BOX-PCR analysis of 22 actinomycete isolates. Isolates that generate identical PCR product fingerprints are considered clones and are highlighted with an asterisk.

TABLE 2-3. Summary of RIF-inactivating actinomycete isolates.

Isolate/ Strain	16S rDNA Relatedness	RpoB Type[1]	RIF Product *m/z* $[M+H]^+$	Mode of Inactivation
WAC1438	*Streptomyces speibonae*	N	986.1	Glycosylation
WAC4839	*Streptomyces olivoverticillatus*	N	985.1	Glycosylation
WAC5038	*Streptomyces pseudogriseolus*	N	985.2	Glycosylation
SSEG	*Streptomyces sviceus* ATCC 29083	S	901.1	Phosphorylation
WAC4747	*Streptomyces viridochromogenes*	S	900.7	Phosphorylation
WAC5059	*Streptomyces viridochromogenes*	S	900.8	Phosphorylation
WAC5090	*Streptomyces chartreusis*	S	900.7	Phosphorylation
WAC5242	*Streptomyces flavovariabilis*	S	900.8	Phosphorylation
WAC4782	*Streptomyces flavovariabilis*	S	-	Decomposition
WAC4791	*Streptomyces chartreusis*	S	-	Decomposition
WAC5055	*Streptomyces omiyaensis*	S	-	Decomposition
WAC5041	*Amycolatopsis echinogonensis*	S	-	Decomposition
WAC5122	*Streptomyces castaneus*	S	-	Decomposition
WAC5188	*Streptomyces umbrinus*	N	-	Decomposition

[1] Refers to position 531 of β-subunit RNAP (*E. coli* numbering). S (serine) is associated with RIF-sensitivity; N (asparagine) confers RIF-resistance (Kim et al., 2005).

DISCUSSION

The various modes of RIF inactivation were first described in the mid-1990s as mechanisms of resistance from opportunistic pathogens. These bacteria belonged to the Corynebacterineae suborder, which normally reside in soil environments. Excluding the *arr* gene, these resistance mechanisms have not yet become clinically relevant and therefore very little research has followed.

In this study we have demonstrated that environmental bacteria utilize an assortment of mechanisms to inactivate RIF. We have identified a subset of actinomycetes that inactivate RIF by glycosylation, phosphorylation and decomposition (TABLE 2-3). Interestingly, inactivation of RIF by ADP-ribosylation was not observed. Although these modes of inactivation have been previously recognized in other bacteria, this is the first report identifying environmental *Streptomyces* and *Amycolatopsis* spp. as a reservoir of these genetic elements. This indicates RIF inactivation is more widespread than previously reported.

A number of isolates appeared to decompose RIF to a degree where no product could be identified. This mechanism of inactivation has been previously reported from *Rhodococcus* and *Nocardia* spp. (Andersen et al., 1996; Hoshino et al., 2010). Decomposition of RIF likely involves the disassembly of the aromatic naphthalene core resulting in loss of RIF's characteristic absorbance profile. Follow up studies of RIF decomposition using radioactively labeled RIF could provide more structural details about the products generated from this mechanism of inactivation.

We have revealed that a number of RIF-inactivating actinomycetes also possess a RIF-resistant RNAP β-subunit. This finding highlights that, in addition to the multidrug phenotypes of environmental bacteria, they also possess multiple modes of resistance towards the same antibiotic. We have demonstrated that environmental actinomycetes are a reservoir of diverse RIF-inactivating determinants. To date, these resistance mechanisms have not become clinically relevant. However, the recent expansion of the rifamycin family of antibiotics may apply pressure for the selection of a more diverse set of RIF resistance determinants, which may include RIF inactivating genes. Furthermore, the mobilization of these genes through plasmids or transposons would have catastrophic consequences on the efficacy of the entire family of rifamycin antibiotics. It is therefore a priority to identify and characterize RIF inactivating genes for antibiotic resistance surveillance programs and drug development initiatives, which could lead to the production of strategically designed resistance-proof rifamycin antibiotics.

The genes encoding the RIF glycosyltransferase and phosphotransferase have yet to be identified and enzymes characterized. Our future efforts aim to identify and characterize these two RIF resistance determinants.

CHAPTER THREE

IDENTIFICATION AND CHARACTERIZATION OF A RIFAMYCIN-INACTIVATING GLYCOSYLTRANSFERASE FROM WAC1438

CHAPTER THREE PREFACE

Portions of the research presented in this chapter have been previously published in:

> Spanogiannopoulos, P., Thaker, M., Koteva, K., Waglechner, N., and G.D. Wright. 2012. Characterization of a rifampin-inactivating glycosyltransferase from a screen of environmental actinomycetes. *Antimicrobial Agents and Chemotherapy*. 56(10): 5061-5069.
>
>

I performed the majority of work described here. Nick Waglechner is credited with assembly of the WAC1438 genome and Dr. Kalinka Koteva is recognized for the physiochemical analysis of rifampin-glucose. We also thank Dr. Maulik Thaker for assistance with *Streptomyces* genetics.

Acknowledgements:

I thank Christine King for assistance with sequencing of the WAC1438 genome. I am grateful to Prof. Tomohiro Tamura of the National Institute of Advanced Industrial Science and Technology (AIST) Japan for the gifts of *Rhodococcus erythropolis* L-88 and pTIP-QC1. I thank Prof. Michael Fischbach for providing *Streptomyces albus* J1074 and Dr. Inga Kireeva for assistance with high-resolution mass spectrometry.

ABSTRACT

Soil bacteria represent an ancient and diverse repository of antibiotics and antibiotic resistance determinants. Identifying and characterizing the soil resistome will provide an early warning of what we may eventually encounter in pathogenic bacteria. Rifampin (RIF), introduced into the clinic 50 years ago, has remained a frontline agent for the treatment of tuberculosis and other mycobacterial diseases. Most pathogens develop resistance to RIF by mutation of the drug target, the β-subunit of RNA polymerase (encoded by *rpoB*). Nonetheless, a diverse set of RIF inactivating mechanisms have been identified from both pathogenic and environmental bacteria. One such mechanism, originally identified from the pathogenic actinomycete *Nocardia brasiliensis*, involves glycosylation of RIF. We recently identified RIF glycosylation from a collection of soil actinomycetes, which included WAC1438. We assembled a draft genome sequence of WAC1438 and identified the associated RIF glycosyltransferase open reading frame, *rgt1438*. The role of the *rgt1438* gene in RIF inactivation was confirmed by its disruption from the bacterial chromosome of WAC1438, resulting in the loss of ability to modify RIF and a 4-fold decrease in the RIF minimum inhibitory concentration (MIC). Heterologous overexpression of *rgt1438* using the RIF-sensitive host *Streptomyces albus* J1074 resulted in a 64-fold increase in RIF resistance. Using an *in vitro* assay with purified recombinant enzyme, Rgt1438 inactivated a variety of natural product and semi-synthetic rifamycin antibiotics with comparable steady-state kinetic constants. Our results identify *rgt1438* as a RIF resistance determinant capable of conferring high-level and broad rifamycin resistance.

INTRODUCTION

The group transfer mode of antibiotic resistance is one of the most diverse mechanisms of resistance (Wright, 2005). This mode requires highly specialized and selective enzymes, which modify antibiotics in a manner that attenuates their ability to bind their target. Glycosyltransferases (GTs) are enzymes that catalyze the transfer of an activated sugar substrate, usually a nucleotide diphosphate sugar (e.g. UDP-glucose), to an acceptor substrate (Lairson et al., 2008). Thus far, glycosylation as a mechanism of resistance has not emerged in the clinic and has only been sparsely reported in environmental bacteria. The first antibiotic resistance GT identified was the *mtg* gene product of *Streptomyces lividans*, responsible for the glycosylation of erythromycin using UDP-glucose. Additionally, our group reported that bacteria from both soil and cave environments utilize glycosylation as a mechanism of resistance towards the third-generation semisynthetic macrolide antibiotic telithromycin (D'Costa et al., 2006; Bhullar et al., 2012), however the genetic determinant responsible for this phenotype has yet to be identified.

Glycosylation is a common and vital mechanism in natural product chemical diversity. Many natural product antibiotics rely on sugar residues for biological activity (e.g. erythromycin and vancomycin). Natural product GTs genes are often co-located within biosynthetic gene clusters and act late in assembly. Furthermore, glycosylation has been reported as a mechanism of self-resistance by antibiotic producing bacteria, as is the case of the macrolide producers *Streptomyces antibioticus* (oleandomycin) and *Streptomyces venezuelae* (methymycin/neomethymycin) (Vilches et al., 1992; Zhao et al.,

2003; Bolam et al., 2007). In these examples the inactive glycosylated product is assembled intracellularly and then excreted by specialized transporters. Specific β-glucosidases on the exterior of the cell catalyze the removal of sugar moieties, activating the biological activity of the natural product.

The inactivation of RIF by glycosylation was first described by Yazawa et al. as a mechanism of resistance by the pathogenic actinomycete *Nocardia brasiliensis* (Yazawa et al., 1993). The site of glycosylation was determined to be the hydroxyl at the C-23 position of RIF (FIGURE 1-8). An unpublished gene from *N. brasiliensis*, *rgt*, encoding the RIF GT enzyme has been identified and submitted to GenBank (AF394943.1).

We have previously identified three *Streptomyces* soil isolates that inactivate RIF by glycosylation (TABLE 2-3). In this chapter we describe the identification and characterization of a RIF GT from WAC1438. Using gene inactivation and heterologous expression, we validate the *rgt1438* gene is responsible for the glycosylation of RIF. Furthermore, *in vitro* assays using purified Rgt1438 enzyme demonstrate its ability to modify a broad spectrum of rifamycin antibiotics.

MATERIALS AND METHODS

Bacterial Strains and Reagents

Escherichia coli TOP10 (Invitrogen, Carlsbad, CA) was routinely used as the cloning host. *E. coli* ET12567/pUZ8002 was used as the donor strain for conjugal transfer for both WAC1438 and *Streptomyces albus* J1074. *Rhodococcus erythropolis* L-88 and plasmid pTIP-QC1 were used for overexpression of *rgt1438* (Nakashima and Tamura, 2004; Mitani et al., 2005). UDP-glucose, RIF, rifamycin SV, rifabutin, and rifaximin were purchased from Sigma (St. Louis, MO). Rifamycin B was obtained from Ryan Scientific (Mount Pleasant, SC).

RIF Inactivation Assay

Fresh spores were used to inoculate 5 ml of Streptomyces isolation media (SIM) in culture tubes with one glass. Following incubation for 3 days at 30°C with aeration, RIF was added at a concentration of 20 μg/ml and a sample was taken for the zero time point. At specified time intervals, conditioned media was removed and analyzed for residual RIF bioactivity using the Kirby-Bauer disk diffusion assay with *Bacillus subtilis* 168 as the RIF-sensitive indicator microorganism; plates were incubated for 16 hours at 37°C (Wikler et al., 2006). Samples were also analyzed by LC-ESI-MS with an Agilent 1100 Series LC system (Mississauga, ON) and a QTRAP LC/MS/MS System (Applied Biosystems/MDS Sciex, Foster City, CA). An equal volume of methanol was added to each conditioned media sample followed by clarification by centrifugation at 15 000 rpm for 10 min. A 10 μl sample was analyzed by HPLC or LC-ESI-MS using the method described below.

WAC1438 Genome Sequencing and Annotation

WAC1438 genomic DNA (gDNA) was sequenced using the Roche 454 platform. gDNA was sheared into approximately 800 bp fragments using a Covaris S220 ultrasonicator (Woburn, MA) and libraries were prepared following the XL Rapid Library Preparation Method manual (454 Life Sciences, Branford, CT). Emulsion PCR and sequencing were carried out according to the manufacturer's instructions for the FLX instrument. DNA was sequenced in two separate runs and the reads were assembled using MIRA version 3.4.0 using the 'denovo, genome, accurate, 454' quick switch parameters using six passes (Chevreux, 1999). The resulting assembly consisted of 270 contigs totaling 8 201 776 bp with an N50 statistic of 72 334 bp.

Inactivation of the *rgt1438* Gene from WAC1438

The *rgt1438* gene from WAC1438 was disrupted by insertional inactivation using a suicide vector. A partial internal gene fragment of *rgt1438* (~550 bp) was amplified by PCR using primer rgtPartF and rgtPartR (APPENDIX 2). The PCR product was cloned into pSUIC (pSET152 digested with *Eco* RI and *Hind* III; lacks *attP* and *int* (ΦC31) and thus functions as a suicide vector when introduced into *Streptomyces* spp). The resulting construct was named pSUIC-*rgt1438part*. pSUIC-*rgt1438part* was introduced into *E. coli* ET12567/pUZ8002 by transformation for conjugal transfer to WAC1438. Conjugations were performed as previously described (Kieser, 2000). Transconjugants were selected by growth on apramycin at 25 µg/ml and confirmed by PCR and amplicon sequencing. The mutant strain was named WAC1438 *rgt1438*::pSUIC.

Construction of pIJ8600K-*rgt1438* for Complementation and Heterologous Expression

The *rgt1438* gene was amplified by PCR using primers rgtF-pIJK and rgtR-pIJK (APPENDIX 2). The resulting PCR product was directionally cloned using *Nde* I and *Bam* HI into pIJ8600K (pIJ8600 derivative (Kieser, 2000) with a kanamycin (KAN) resistance cassette obtained from pCR4blunt-TOPO (Invitrogen, Carlsbad, CA) in replacement of the apramycin resistance cassette) constructing plasmid pIJ8600K-*rgt1438*. This construct was introduced into *E. coli* ET12567/pUZ8002 by transformation, and then conjugally transferred to WAC1438 *rgt1438*::pSUIC. Transconjugants were selected on media supplemented with KAN at 25 μg/ml. The resulting strain was named WAC1438 *rgt1438*::pSUIC + pIJ8600K-*rgt1438*. pIJ8600K-*rgt1438* was also introduced to *Streptomyces albus* J1074 generating strain *S. albus* J1074 + pIJ8600K-*rgt1438*.

RIF Minimal Inhibitory Concentration Determinations

RIF minimal inhibitory concentration **(**MIC) determinations were performed as previously described protocol, with minor modifications (Kim et al., 2005). Spores were used to inoculate a 5 ml starter culture of SIM with one glass bead. Starter cultures were incubated at 30°C, with aeration, for 3 days. Bacteria were harvested by centrifugation and washed three times with a 0.85% saline solution. The cell pellet was resuspended in 5 ml of 0.85% saline solution and briefly dispersed by sonication. 100 μl of the resulting bacterial suspension was used to inoculate SIM agar supplemented with RIF ranging from concentrations of 0.25–512 μg/ml. The average titer of bacteria was 10^7 colony-

forming units (CFU)/ml. Plates were incubated at 30°C for 3 days. The RIF MIC was determined as the lowest concentration of drug that failed to yield any bacterial colonies.

Overexpression and Purification of Recombinant Rgt1438 Protein using *Rhodococcus erythropolis* L-88

A 1.3 kb DNA fragment containing *rgt1438* was amplified by PCR from gDNA of WAC1438 using the primers rgtF and rgtR (APPENDIX 2). Using the restriction sites incorporated into the primers, the *rgt1438* was directionally cloned into the pTIP-QC1 vector using *Nde* I and *Hind* III, introducing an N-terminal His-tag (Nakashima and Tamura, 2004). The pTIP-QC1-*rgt1438* construct was introduced into *Rhodococcus erythropolis* L-88 cells by electroporation as previously described (Desomer et al., 1990; Shao et al., 1995; Mitani et al., 2005). Transformants were selected on LB containing 30 µg/ml chloramphenicol (CAM). Following one week of incubation at 30°C, a single colony was used to inoculate a starter culture of 25 ml LB containing 30 µg/ml CAM and incubated for 48 hours at 30°C with shaking at 250 rpm. The 25 ml starter culture was used to inoculate 1 L of LB and grown to an optical density at 600 nm of 0.5 at 30°C with shaking at 250 rpm. Expression of *rgt1438* was induced by the addition of 1 µg/ml thiostrepton followed by incubation for an additional 16 hours. Cells were harvested by centrifugation at 5,000 × *g* for 15 min, washed with 0.85% saline solution, and stored at -20°C. In preparation for lysis, the cell pellet was thawed and resuspended in 20 ml of buffer A [50 mM TAPS (pH 8.4), 250 mM NaCl, 5 mM imidazole] supplemented with lysozyme at a final concentration of 1 mg/ml and incubated on ice for 1 hour. Phenylmethylsulfonyl fluoride (PMSF) (1 mM final concentration) and pancreatic bovine

DNase I (1 µg/ml final concentration) were added to the cell suspension and processed using a Constant Systems continuous flow cell disruptor (Daventry, United Kingdom). The sample was clarified by centrifugation at 50 000 × *g* for 30 min and the resulting supernatant was applied onto a 5-ml Ni-nitrilotriacetic acid (Ni-NTA) column (Qiagen, Valencia, CA) pre-equilibrated with buffer A. The column was washed with 5 column volumes of buffer A. Bound protein was eluted with a stepwise gradient of buffer B [50 mM TAPS (pH 8.4), 250 mM NaCl, 500 mM imidazole] over 25 column volumes. Protein fractions were analyzed using sodium dodecylsulfate-polyacrylamide gel electrophoresis (SDS-PAGE) and fractions containing protein corresponding to the correct molecular weight of Rgt1438 were pooled and dialyzed in 3 L of buffer C [50 mM TAPS (pH 8.4)] overnight at 4°C. This protein fraction was then applied to a 1 ml Mono Q 5/50 GL column (GE Healthcare, Fairfield, CT) pre-equilibrated with buffer C at a flow rate of 0.5 ml/min. Proteins were eluted from this column using a linear gradient of 0-100% buffer D [50 mM TAPS (pH 8.4), 500 mM NaCl] over 50 column volumes. Protein fractions were analyzed using SDS-PAGE and fractions containing Rgt1438 were pooled, concentrated and stored at -20°C with 10% (w/v) glycerol. Protein concentration was determined using the Bio-Rad Bradford protein assay (Hercules, CA).

in vitro RIF Glycosylation Assay and Steady-State Kinetics

Enzymatic activity assays of Rgt1438 consisted of rifamycin antibiotic and UDP-glucose substrates incubated with 50 mM TAPS (pH 8.4), 10 mM $MgCl_2$, 1 mM dithiothreitol (DTT), 1 mg/ml bovine serum albumin (BSA) and Rgt1438. Reactions were performed at room temperature and at specific time intervals aliquots were

quenched with an equal volume of ice-cold methanol with 0.05% trifluoroacetic acid (TFA). For analysis using thin layer chromatography (TLC), RIF and UDP-glucose were added at 1 mM and 10 mM respectively and the reactions were initiated with the addition of Rgt1438 at 1 µM. At specified time intervals, a 10 µl aliquot of the reaction was quenched with 10 µl of methanol and 5 µl was applied to a silica gel TLC plate (Macherey-Nagel, Düren, Germany). TLC plates were resolved using a 4:1 chloroform:methanol solvent system (Yazawa et al., 1993). Steady-state kinetics was performed using 2.5 nM of enzyme and reactions were initiated with the addition of 50 µl UDP-glucose in a final reaction volume of 250 µl. To determine rifamycin K_m values, the UDP-glucose concentration was held constant at 1 mM and the rifamycin concentrations were varied from 1 to 100 µM. For the K_m determination of UDP-glucose, the rifampin concentration was held constant at 100 µM and the UDP-glucose concentration was varied from 5 to 400 µM. Progress curves were generated by analyzing 50 µl aliquots taken at several time points. Quenched reactions were stored on ice for 10 min. and clarified by centrifugation at 4°C. Samples were then analyzed by analytical HPLC using a Waters e2695 system (Milford, MA) with a XSelect CSH C18 5 µm column (4.6 × 100 mm) using a linear gradient of 25-97.5% of acetonitrile in water with 0.05% TFA over 11 min at a flow rate of 1 ml/min. Product peaks were integrated using Waters Empower 3 Software to determine the quantity of product generated. Initial rates were calculated using the linear portion of progress curves. Reactions were performed in triplicate. Initial rates were analyzed by non-linear least-squares fitting (equation 1):

$$v = V_{max}\, S/(K_m + S) \quad (1)$$

Production and Purification of RIF-Glucose

A large scale reaction to generate RIF-glucose (RIF-G) consisted of 50 mM TAPS (pH 8.4), 1 mM RIF, 10 mM UDP-glucose, 10 mM $MgCl_2$, 2 mM DTT and 5 µM of RGT1438 in a total volume of 10 ml. The reaction proceeded at room temperature and progress was monitored using TLC as described above. The crude reaction was lyophilized and resuspended in DMSO. The RIF-G product was purified using a Waters Sep-Pak C18 cartridge pre-equilibrated with dH_2O. Following the removal of water soluble components, RIF-G was eluted with 50% of acetonitrile in water and lyophilized. The final product was resuspended in DMSO and purity was assessed using LC-ESI-MS.

Physiochemical Analysis of Glycosylated RIF Products

High resolution mass spectra (HRMS) of glycosylated rifamycin products were obtained using a ThermoFisher LTQ-XL-Orbitrap Hybrid Mass Spectrometer (Bremen, Germany), equipped with an electrospray interface operated in positive and negative ion mode. The RIF-G product was identified by comparison of 1-D NMR spectral data with data previously reported in the literature (Yazawa et al., 1993), 2-D NMR analysis and HRMS analysis. The NMR spectra were measured on a Bruker AVIII 700 MHz instrument in DMSO-d_6 (Cambridge Isotope Laboratories Inc., Andover, MA). Chemical shifts are reported in ppm relative to tetramethylsilane (TMS) using the residual solvent signals at 2.50 and 39.50 ppm as internal references for the ^{1}H and ^{13}C spectra, respectively. The presence of the D-glucose moiety was confirmed by NMR by the

signals at δ_C 103.0 (C-1'), 73.8 (C-2'), 76.6 (C-3'), 70.1 (C-4'), 76.8 (C-5') and 63.1 (C-6') (APPENDIX 3). The site of glycosylation was determined by heteronuclear multiple bond correlation (HMBC) experiment, which showed the couplings between H-23 (δ_H 3.33) and C-1', and the comparison of ^{1}H and ^{13}C- NMR spectra of RIF and RIF-G. The signals for H-23 and C-23 have shifted downfield with 0.5 and 10.6 ppm, respectively (APPENDIX 3). The coupling constant of the anomeric proton at 4.19 ppm (J=7.4 Hz) was consistent with the β configuration of the glucose moiety, as previously reported (Yazawa et al., 1993). No other significant differences were observed. The structure was confirmed to be 23-(O-[β-D-glucopyranosyl]) rifampin.

RESULTS

Identification of *rgt1438* from WAC1438

The glycosylation of RIF has been previously reported as a resistance mechanism from the pathogenic actinomycete *Nocardia brasiliensis* (Yazawa et al., 1993). We identified a total of three *Streptomyces* isolates that inactivated RIF by glycosylation and selected one of these, WAC1438, for further characterization (TABLE 2-3). To identify the gene associated with the RIF GT, we prepared a draft genome sequence of WAC1438. Using the unpublished *rgt* sequence from *N. brasiliensis* as a reference (GenBank AF394943.1), we identified an ORF, *rgt1438*, located on a 43 kb contig, which showed 72% nucleotide and 69% protein identity to the *N. brasiliensis* element (FIGURE 3-1).

A blastp analysis of Rgt1438 searching the non-redundant protein sequences database revealed a similarity to the inverting GT-B superfamily of GTs (Altschul et al., 1997). The GT-B family of GTs share a similar overall architecture, which is composed of two structurally homologous β/α/β Rossmann-like domains that are separated by a short interdomain linker peptide (Lairson et al., 2008). The N-terminal domain is responsible for binding the acceptor substrate and the C-terminal binds the donor substrate. GTs are further subdivided into families based on protein fold and the reactions they catalyze (Coutinho et al., 2003). Rgt1438 most closely resembles proteins from the GT1 family. This family includes GTs that modify diverse organic substrates including cofactors, steroids, peptides and antibiotics. Due to the therapeutic importance of these substrates, the GT1 family of GTs has been extensively characterized structurally

and mechanistically. Rgt1438 shows the strongest similarity with GTs involved in the tailoring of glycopeptide antibiotics (TABLE 3-1). The N-terminal domain, responsible for acceptor binding, contains a stretch of amino acids called the hypervariable region, due to its high degree of variability, and has been demonstrated to impart substrate specificity (Mulichak et al., 2001).

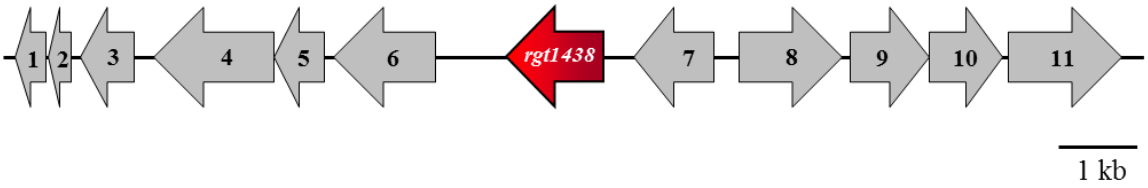

Open Reading Frame	Annotation
1	Lactoylglutathione lyase
2	ArsR transcriptional regulator
3	Hydrolase
4	FAD-dependent oxidoreductase
5	PadR transcriptional regulator
6	Mg/Mn-dependent protein phosphatase
rgt1438	**Rifampin glycosyltransferase**
7	LacI family transcriptional regulator
8	Extracellular sugar binding protein
9	Sugar transport permease
10	Sugar ABC transporter
11	Putative β-glucosidase

FIGURE 3-1. The *rgt1438* gene from WAC1438. Genetic organization of *rgt1438* and surrounding open reading frames from the WAC1438 genome.

We performed a global protein alignment of Rgt1438 with GtfD (PDB 1IIR) from the vancomycin glycopeptide biosynthetic gene cluster to identify conserved and variable regions using ESPrit 3.0 (http://espript.ibcp.fr/ESPript/cgi-bin/ESPript.cgi) (FIGURE 3-2) (Gouet et al., 2003). This alignment clearly shows these two enzymes share strong identity. Conserved features include the interdomain linker (IDL) (Rgt1438 positions 222-229) and the putative catalytic aspartate (Asp13) (FIGURE 3-2) (Mulichak et al., 2004). Furthermore, the alignment reveals the N-terminal domain has two stretches of amino acids with low identity, corresponding to the hypervariable region (Rgt1438 positions 57-85 and 123-165) (Mulichak et al., 2001). These stretches of amino acids are presumed to be the region responsible for binding rifamycin. To visualize the hypervariable region of Rgt1438 we generated a structural model using I-TASSER (http://zhanglab.ccmb.med.umich.edu/I-TASSER) (Roy et al., 2010). The Rgt1438 model has high confidence (C-score 1.61) and structural alignment of GtfD and Rgt1438 reveals an almost identical architecture (template modeling score (TM-score) of 0.861 and a root-mean-square deviation (RMSD) of 2.16) (FIGURE 3-3). The position of the hypervariable region of the Rgt1438 model is highlighted and the amino acid residues belonging to this region are likely to be involved in binding RIF. Overall, these findings suggest that Rgt1438 is very similar to the GTs involved in natural product biosynthesis.

TABLE 3-1. Glycosyltransferases that share high protein identity with Rgt1438.

Glycosyl-transferase	Description	PDB/ Accession No.	Percent Identity
GtfB	Catalyzes the transfer of glucose from UDP-glucose to the 4-hydroxyphenylglycine of the glycopeptide antibiotic chloroeremomycin	1IIR	56.7
GtfA	Catalyzes the transfer of 4-epivancosamine from TDP-4-epivancosamine to the β-OH -tyrosine of chloroeremomycin	1PN3	53.9
GtfD	Catalyzes the transfer of epivancosamine from TDP-4-epivancosamine to the glucose moiety of vancomycin	1RRV	53.6
SorF	Catalyzes the transfer of glucose from UDP-glucose to sorangicin A	ADN68481.1	42.8

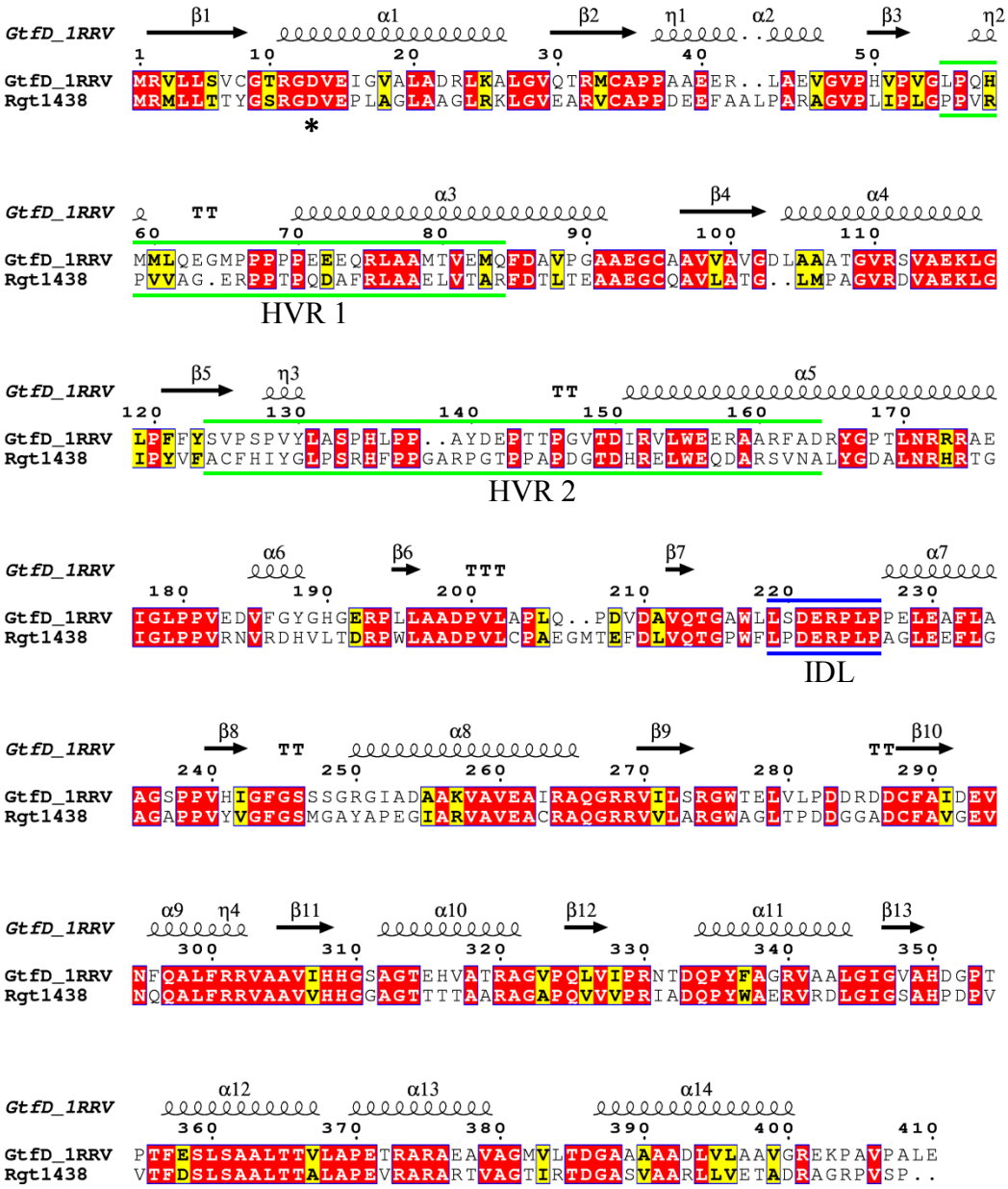

FIGURE 3-2. Rgt1438 and GtfD protein alignment. A global protein alignment of Rgt1438 and GtfD (PDB 1RRV) was performed using ClustalW (http://www.ebi.ac.uk/Tools/msa/clustalw2) (Larkin et al., 2007). Secondary structure was incorporated into the alignment using ESPript 3.0 (http://espript.ibcp.fr/ESPript/cgi-bin/ESPript.cgi) (Gouet et al., 2003) from the crystal structure of GtfD (Mulichak et al., 2004). The hypervariable region (HVR) is highlighted with green bars and the interdomain linker (IDL) with blue bars. The putative catalytic aspartate residue is indicated using an asterisk.

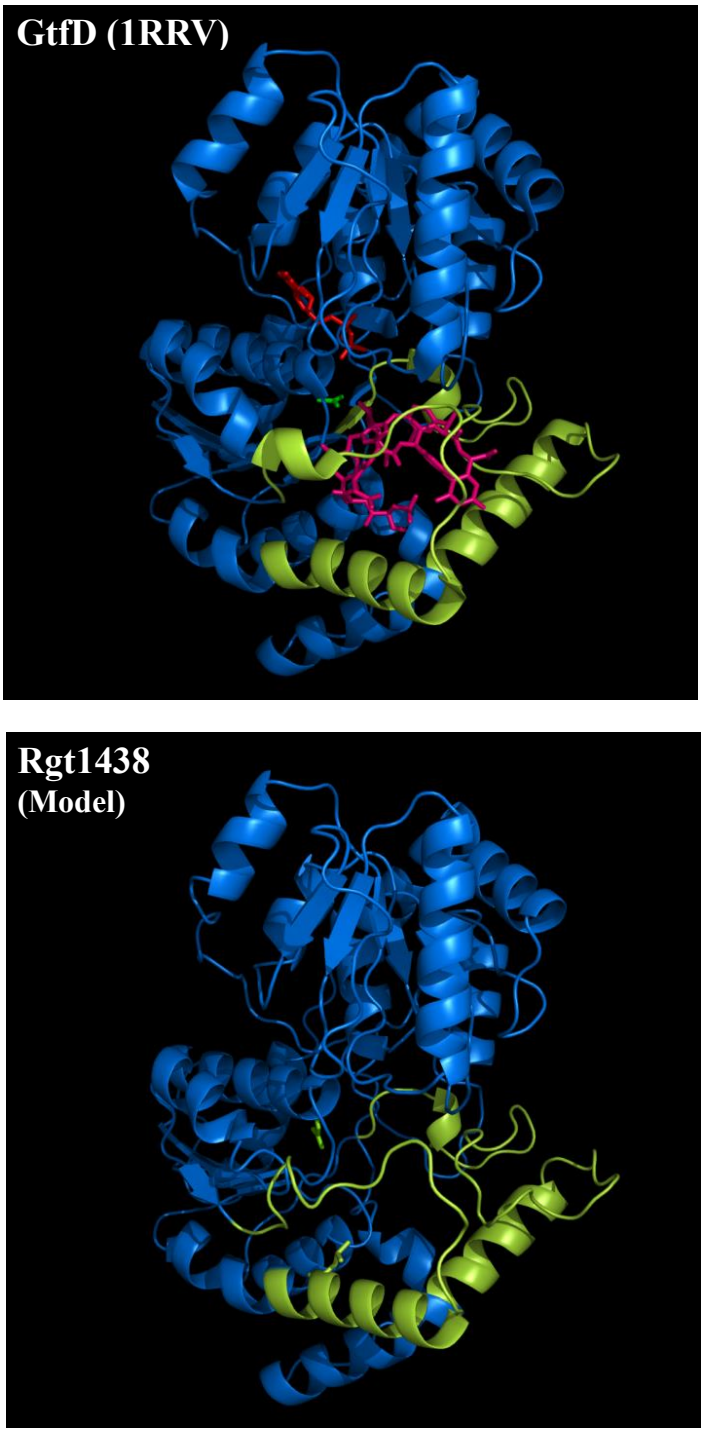

FIGURE 3-3. Structural comparison of the Rgt1438 model with GtfD. A model of Rgt1438 was created using I-TASSER (http://zhanglab.ccmb.med.umich.edu/I-TASSER) (Roy et al., 2010). The TDP nucleotide is shown in red and the vancomycin pseudoaglycone (DVV) is shown in pink. The hypervariable region is highlighted in yellow and the putative catalytic aspartate residue is shown in green. Figure was prepared using PyMOL.

The *rgt1438* Gene is Responsible for the Glycosylation of RIF

To confirm the *rgt1438* gene does indeed encode the RIF GT we constructed a mutant strain of WAC1438 with a disrupted *rgt1438* gene (WAC1438 *rgt1438*::pSUIC) and examined its ability to inactivate RIF. In this experiment, strains were grown in the presence of RIF and conditioned media samples were analyzed for residual RIF concentration using the Kirby-Bauer disk diffusion assay and high-performance liquid chromatography (HPLC). As shown in FIGURE 3-4, WAC1438 is capable of completely inactivating RIF within 24 hours. In comparison, mutant strain WAC1438 *rgt1438*::pSUIC has lost the ability to inactivate RIF. We then complemented this mutant with an intact *rgt1438* gene on an inducible integrating plasmid creating strain WAC1438 *rgt1438*::pSUIC + pIJ8600K-*rgt1438*. Under non-inducing conditions, this strain appears to inactivate a fraction of RIF, demonstrated by a slightly smaller zone of inhibition compared to the control (FIGURE 3-4), most likely attributed to leaky expression from the *ptipA* promoter (Vierling et al., 2001). Upon addition of the inducer, this strain completely inactivates RIF comparable to the wild type (FIGURE 3-4), corroborating a role of *rgt1438* with drug modification. Modification of RIF was confirmed by analyzing conditioned media samples using HPLC (FIGURE 3-4).

The *rgt1438* Gene Confers RIF Resistance

WAC1438 exhibits a RIF MIC of 64 μg/ml (TABLE 3-2). WAC1438 *rgt1438*::pSUIC on the other hand demonstrated a four-fold higher sensitivity to RIF (MIC of 16 μg/ml) (TABLE 3-2). This increase in sensitivity was reversed when the

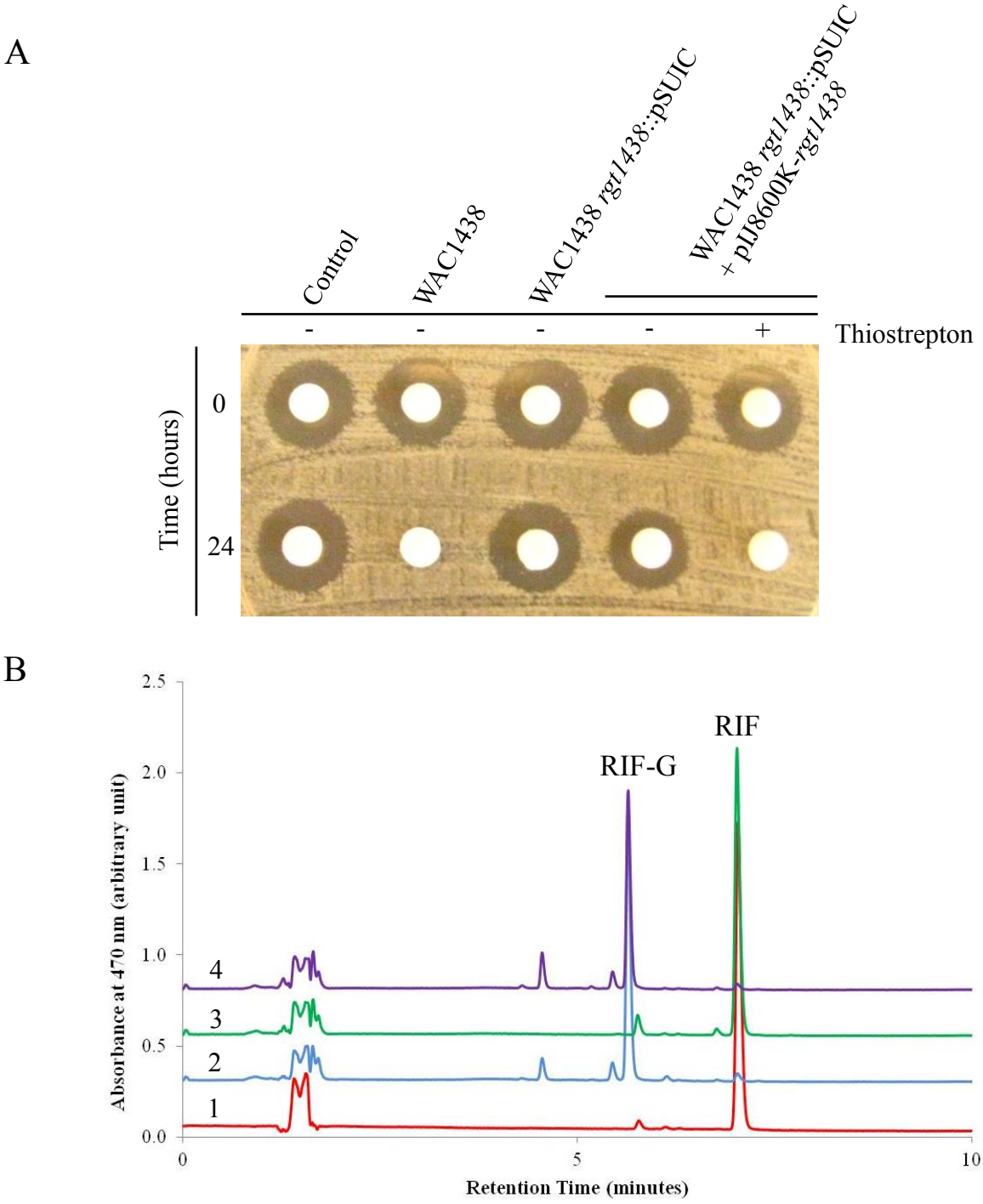

FIGURE 3-4. The *rgt1438* gene product is responsible for the inactivation of RIF. (A) WAC1438 strains were grown for 3 days in liquid SIM, at which point RIF was added (20 µg/ml) and represented the time point 0 h. Cultures were grown for 24 h and conditioned media samples were applied onto filter paper disks overlaid on a lawn of RIF-sensitive *Bacillus subtilis*. A control sample consisted of media (SIM) plus RIF. The inducer thiostrepton was added at a concentration of 1 µg/ml. (B) Conditioned media samples were also analyzed by HPLC to confirm the modification of RIF. 1, Control (SIM plus RIF); 2, WAC1438; WAC1438 *rgt1438*::pSUIC; WAC1438 *rgt1438*::pSUIC + *rgt1438*-pIJ8600K.

mutant was complemented with *rgt1438* (strain WAC1438 *rgt1438*::pSUIC + pIJ8600K-*rgt1438*) (TABLE 3-2). Interestingly, mutant WAC1438 *rgt1438*::pSUIC displayed a relatively high RIF MIC, suggesting this microorganism has an additional mechanism of RIF resistance. Recently, Kim et al. explored the natural RIF resistance phenotype of *Streptomyces* spp. (Kim et al., 2005). They attributed resistance to a single amino acid polymorphism at position 531 within the β-subunit of RNAP (*E. coli* numbering). An asparagine substitution at position 531 (N531) correlates with a higher RIF MIC level (≥ 16 μg/ml) compared to the RIF sensitive allele (FIGURE 1-5). This finding is consistent with biochemical and crystallographic studies that implicate S531 in hydrogen bond interactions with RIF (FIGURE 1-4) (Campbell et al., 2001; Gill and Garcia, 2011). Additionally, this amino acid position has been linked to natural RIF resistance from various bacterial genera (Gaurivaud et al., 1996; Alekshun et al., 1997; Stamm et al., 2001). Investigation of the draft genome sequence of WAC1438 identified a single candidate *rpoB* gene predicted to encode a β-subunit with the N531 substitution, thereby accounting for the high RIF MIC in the mutant. We conclude that WAC1438 possesses multiple mechanisms of RIF resistance.

To further validate the role of Rgt1438 as an antibiotic resistance determinant, we introduced the associated gene into *Streptomyces albus* J1074, which has previously been shown to be RIF sensitive (Sanchez-Hidalgo et al., 2010). *S. albus* J1074 contains a RIF sensitive (S531) β-subunit and displays a RIF MIC of 2 μg/ml. *S. albus* pIJ8600K-*rgt1438* on the other hand showed a 32-64-fold increase in RIF MIC (TABLE 3-2). This result confirms the ability of *rgt1438* to confer high-level RIF resistance.

TABLE 3-2. RIF MIC determinations.

Strain	Inducer[1]	RIF MIC (μg/ml)
WAC1438	-	64
WAC1438 *rgt1438*::pSUIC	-	16
WAC1438 *rgt1438*::pSUIC + *rgt1438*-pIJ8600K	-	64
	+	64
Streptomyces albus J1074	-	2
Streptomyces albus J1074 *rgt1438*-pIJ8600K	-	64
	+	128

[1]Thiostrepton was supplemented at 1 μg/ml

Steady-State Kinetic Analysis of the Rgt1438 enzyme

Efforts to overexpress Rgt1438 in *E. coli* failed despite numerous attempts. We therefore turned to protein expression in the actinomycete *Rhodococcus erythropolis* L-88, which we have previously found useful in generating soluble and active protein expressed from high-GC content genes (Nakashima and Tamura, 2004; Mitani et al., 2005; Shakya et al., 2011). Using this system, soluble and active N-terminal His_6-tagged Rgt1438 was successfully overexpressed and purified to high homogeneity using a two-column chromatographic protocol (FIGURE 3-5). Rgt1438 was assayed using UDP-glucose and resolved by TLC, which showed complete turnover of RIF within 60 minutes using 1 μM of enzyme (FIGURE 3-5). The glycosylated RIF product, RIF-G, was then purified and analyzed by high-resolution mass-spectrometry and nuclear magnetic resonance (NMR) spectroscopy, which verified the regiospecificity of glucose transfer

and identified the RIF-G product as 23-(O-[β-D-glucopyranosyl])rifampin (APPENDIX 3). This structure is consistent with the inactivated RIF-G product previously described from *N. brasiliensis* (Yazawa et al., 1993).

We developed a quantitative HPLC method to assess the steady state kinetic properties of Rgt1438 (FIGURE 3-6). The enzyme demonstrated normal rectangular hyperbolic saturation with both RIF and UDP-glucose as variable substrates with K_m values of 3.74 μM and 24.1 μM respectively and a k_{cat} of 0.20 per second per enzyme molecule (TABLE 3-3). We next investigated the substrate specificity of Rgt1438 with a number of semi-synthetic rifamycin antibiotics and the natural products rifamycin B and SV. All the rifamycins tested served as substrates for Rgt1438 (FIGURE 3-7). Additionally, Rgt1438 displayed comparable kinetic constants towards all rifamycins (TABLE 3-3). The various glycosylated products were confirmed using high-resolution mass spectrometry (HRMS) (TABLE 3-4). A number of non-rifamycin antibiotics (glycopeptides, macrolides, etc.) were also evaluated as substrates for Rgt1438, however, no detectable products could be identified.

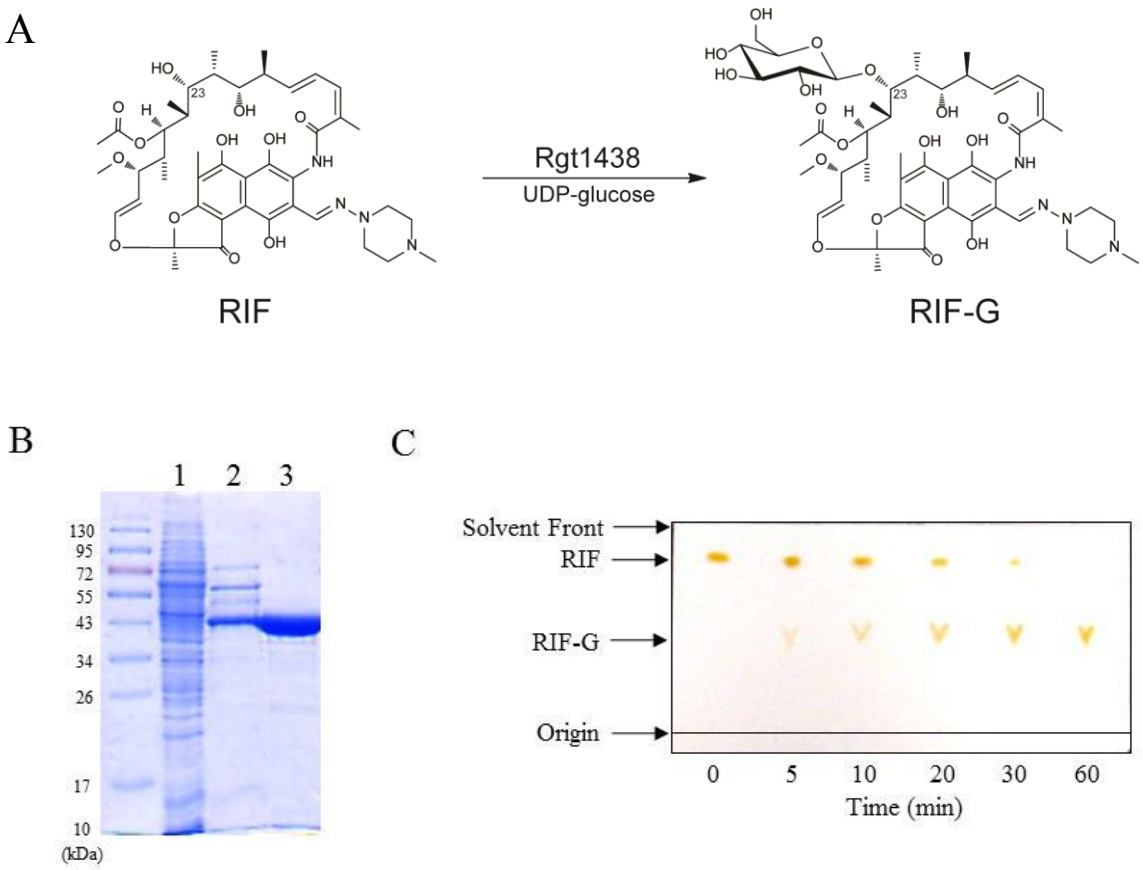

FIGURE 3-5. Purification and *in vitro* TLC assay of recombinant Rgt1438. (A) The Rgt1438 enzyme glycosylates RIF at the C-23 hydroxyl using UDP-glucose as a co-substrate. (B) SDS-PAGE analysis of purified Rgt1438. 1, Crude soluble protein fraction; 2, Ni-NTA chromatography purified; 3, MonoQ chromatography purified. (C) Rgt1438 TLC assay. At specified time intervals, aliquots of the reaction were quenched with an equal volume of methanol and product formation was assessed by TLC.

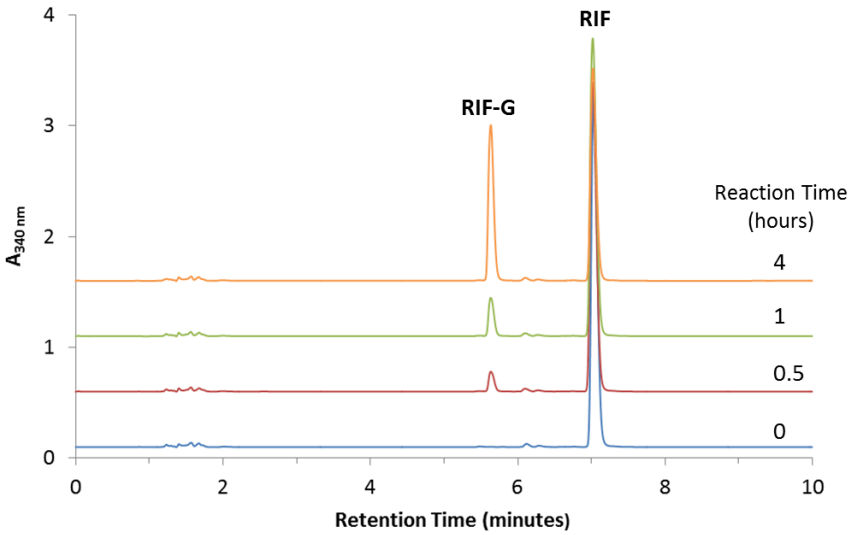

FIGURE 3-7. Rgt1438 HPLC assay. Rgt1438 enzyme was assayed using RIF and UDP-glucose substrates. Reactions were quenched by the addition of ice-cold methanol with 0.05% TFA, clarified by centrifugation and then analyzed by HPLC. The glycosylated RIF product (RIF-G) resulted in a shift in retention time.

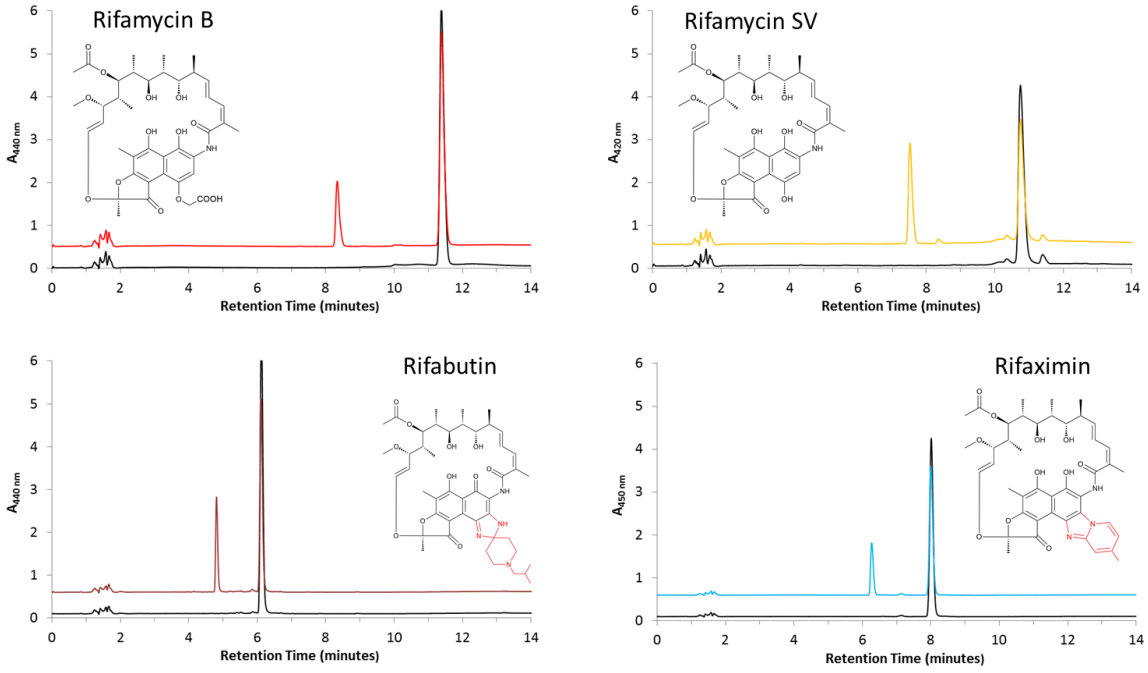

FIGURE 3-8. Rgt1438 inactivates various rifamycin antibiotics. Black HPLC trace is a control lacking Rgt1438 enzyme. The glycosylated RIF products result in a shift in retention time, shown in the color trace.

TABLE 3-3. Steady-state kinetic characterization of Rgt1438.

Substrate	K_m (μM)	k_{cat} (s^{-1})	k_{cat} / K_m (s^{-1} M^{-1})
Rifampin	3.74 ± 0.04	0.20 ± 0.07	5.35×10^4
Rifamycin B	6.41 ± 1.02	1.12 ± 0.05	1.75×10^5
Rifamycin SV	1.43 ± 0.50	0.15 ± 0.01	1.07×10^5
Rifabutin	1.42 ± 0.39	0.15 ± 0.01	1.06×10^5
Rifaximin	6.09 ± 0.14	0.16 ± 0.01	2.68×10^4
UDP-glucose	24.1 ± 2.06	-	8.30×10^3

TABLE 3-4. HRMS analysis of glycosylated rifamycin antibiotic products.

Antibiotic	Glycosylated Product				
	Exact Mass (Da)	Expected *m/z* (Da)		Observed *m/z* (Da)	
		$[M+H]^+$	$[M+H]^-$	$[M+H]^+$	$[M+H]^-$
Rifampin	984.4580	985.4659	983.4509	985.4696	ND[1]
Rifamycin B	917.3681	918.3760	916.3602	ND	916.3638
Rifamycin SV	857.3470	858.3549	856.3391	ND	856.3436
Rifabutin	1 008.4943	1 009.5022	1 007.4864	1 009.5054	ND
Rifaximin	947.4052	948.4134	946.3973	948.4166	ND

[1] ND, not determined

DISCUSSION

Our group has previously reported that soil bacteria utilize a variety of mechanisms to inactivate rifamycins, including glycosylation (CHAPTER 2) (Spanogiannopoulos et al., 2012). Herein, we confirm the *rgt1438* gene from WAC1438 is responsible for the glycosylation of RIF. Furthermore, using heterologous overexpression and *in vitro* enzyme assays, we confirm the Rgt1438 enzyme is capable of modifying both natural and semisynthetic rifamycin antibiotics.

We previously reported that some environmental Streptomyces isolates that inactivate RIF also possess a RIF-resistant β-subunit of RNAP (CHAPTER 2). This study further confirmed this observation, where a mutant strain of WAC1438 devoid of a functional *rgt1438* gene maintained a RIF-resistant phenotype. *Nocardia farcinica* has been shown to be resistant to RIF as a consequence of possessing an alternative RIF-resistant β-subunit (target duplication with resistance-associated site mutation) as well as possessing the Rox enzyme, which catalyzes the decomposition of RIF (Ishikawa et al., 2006; Hoshino et al., 2010). This finding suggests that in addition to the multidrug resistance phenotypes of environmental bacteria, they may also possess multiple modes of resistance to a single antibiotic.

With the continued development of new rifamycin antibiotics along with their use to now combat a much broader range of bacterial infections, the rifamycin family of antibiotics will likely experience an increase in clinical application. This will further exert selective pressure for a more diverse panel of RIF resistance determinants, such as those that already exist in environmental bacteria. Identifying and characterizing the RIF

resistome will provide crucial insight for future drug development programs, involving the strategic design of molecules that are recalcitrant to modification by resistance enzymes such as Rgt1438.

CHAPTER FOUR

THE DISCOVERY OF A CONSERVED RIFAMYCIN RESPONSIVE REGULATORY ELEMENT LEADS TO THE IDENTIFICATION OF A RIFAMYCIN INACTIVATING PHOSPHOTRANSFERASE

CHAPTER FOUR PREFACE

The majority of the research presented in this chapter has been previously published in:

> Spanogiannopoulos, P., Waglechner, N., Koteva, K., and G.D. Wright. 2014. A rifamycin inactivating phosphotransferase family shared by environmental and pathogenic bacteria. *Proceedings of the National Academy of Sciences of the United States of America*. 111(19): 7102-7107.

I performed the majority of work described here. Nick Waglechner is credited with assembly of the WAC4747 genome and phylogenetic analysis. Dr. Kalinka Koteva is recognized for the physiochemical analysis of the rifampin-phosphate product and assistance with mass spectrometry.

Acknowledgements:

I thank Christine King for assistance with the sequencing of the WAC4747 genome. I thank Prof. Michael Fischbach for providing *Streptomyces sviceus* ATCC 29083. I am grateful to Prof. Lori Burrows for the gift of *Listeria monocytogenes* str. 4b. F2365. I thank Dr. Andrew McArthur for assistance with the phylogenetic analysis of the RPH protein family.

ABSTRACT

Environmental bacteria are multidrug resistant and represent a reservoir of ancient antibiotic resistance determinants, which have been linked to genes found in pathogens. Exploring the environmental antibiotic resistome, therefore, reveals the diversity and evolution of antibiotic resistance and also provides insight into the vulnerability of clinically used antibiotics. In this study we describe the identification of a highly conserved regulatory motif, the RAE, which is found upstream of genes encoding rifampin (RIF) inactivating enzymes from a diverse collection of actinomycetes. Using gene expression assays, we confirmed that the RAE is involved in RIF-responsive gene regulation. By using the RAE as a probe for new RIF-associated genes in several actinomycete genomes, we identified a heretofore unknown RIF resistance gene, *rph*. The RPH enzyme is a RIF-inactivating phosphotransferase and represents a new protein family in antibiotic resistance. RPH orthologs are widespread in bacterial genera and found in RIF resistant and paradoxically in sensitive bacteria including the opportunistic pathogens *Bacillus cereus* and *Listeria monocytogenes*. Heterologous expression and *in vitro* enzyme assays with purified RPHs from diverse bacterial genera demonstrate that these enzymes are capable of conferring high level resistance towards a variety of clinically used rifamycin antibiotics. This work identifies a new antibiotic resistance protein family and reinforces the fact that the study of resistance in environmental microorganisms can serve to identify resistance elements with relevance to pathogens.

INTRODUCTION

The antibiotic phosphotransferase family of enzymes is one of the largest groups of antibiotic inactivating enzymes. These enzymes are NTP-dependent *O*-phosphotransferases that modify antibiotics and attenuate their ability to bind their biological targets (Wright, 2005). The largest and best studied is the aminoglycoside phosphotransferase group (APH), with over two dozen APHs identified (Morar and Wright, 2010). Biochemical and structural similarities suggest that APHs are related to eukaryotic protein kinase (ePK) even though they share little identity at the amino acid level (Hon et al., 1997). Genes encoding APHs are often located within mobile genetic elements, such as plasmids and transposons, and are well distributed across diverse bacterial pathogens, and is a contributing factor to why aminoglycosides are not routinely used in the clinic today (Shi et al., 2013). A group of enzymes that show similarly to APHs and phosphorylate macrolide antibiotics have been also identified (MPHs) (Taniguchi et al., 1999). MPHs have been found in pathogenic bacteria, however, to date they are not nearly as widespread as APHs (Phuc Nguyen et al., 2009).

Antibiotic phosphorylation is also a strategy used by antibiotic producers as a mechanism of self-resistance. The producer of the antibacterial peptide tuberactinomycin synthesizes an inactive phosphorylated final product, facilitated by the VPH enzyme (Skinner and Cundliffe, 1980). VPH shows similarity to the APH/MPH protein family. Similarly, the producer of chloramphenicol (CAM), *Streptomyces griseus*, possesses CPT, an enzyme that inactivates CAM by phosphorylation (Mosher et al., 1995). Structural studies of CPT have shown that this enzyme does not belong to the APH/MPH

protein family, but rather shares features common with the monophosphate kinase family, which shows relatedness to shikimate kinase (Izard and Ellis, 2000).

The phosphorylation of RIF was first described in the mid-1990s as mechanism of resistance from the pathogenic actinomycete *Nocardia otitidiscaviarum* (FIGURE 4-1) (Yazawa et al., 1994). This strain was shown to modify the C-21 hydroxyl position of RIF. Despite the fact that RIF phosphorylation has been known for 20 years, the gene encoding the RIF phosphotransferase (*rph*) has yet to be identified. Our group is interested in identifying the RPH enzyme to determine its prevalence and potential as a resistance determinant.

Herein we describe the discovery of a conserved *cis* nucleotide element associated upstream of various genes encoding RIF-inactivating enzymes from actinomycetes. By exploiting this conservation, we successfully identified the heretofore unrecognized *rph* gene. Through a combination of phylogenetics, heterologous protein expression, and *in vitro* enzyme assays we establish that RPH orthologs are prevalent in both environmental and pathogenic bacteria, conferring high-level and broad resistance against clinically used rifamycin antibiotics. This effort highlights the power of screening non-coding regions of genome data in the discovery of new resistance elements and identifies an unexpected silent resistome from pathogens.

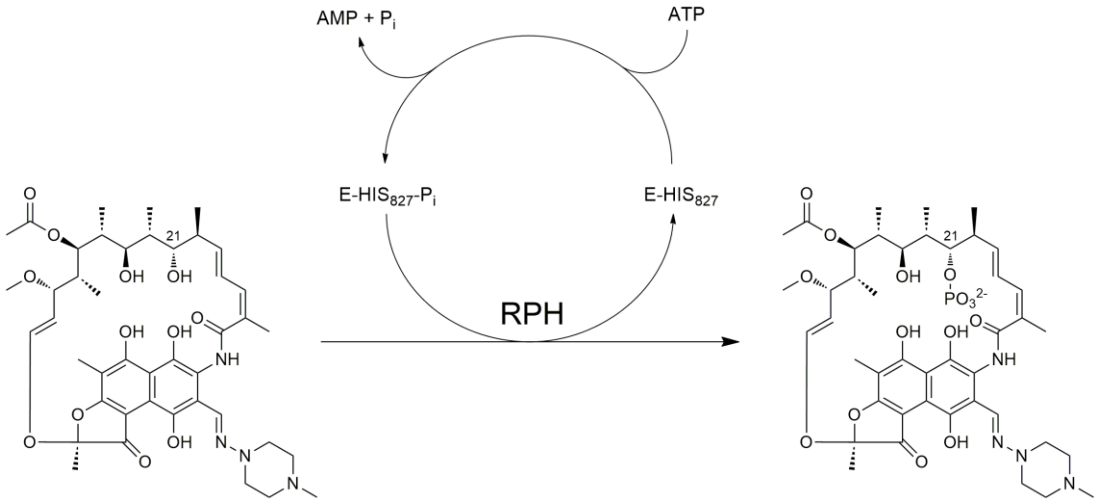

FIGURE 4-1. The phosphorylation of RIF catalyzed by RPH. RPH phosphorylates RIF at the C-21 hydroxyl.

MATERIALS AND METHOFS

Search and Alignment of the RAE

Nucleotide sequence alignments were performed using ClustalW (Larkin et al., 2007) using the 250 bp sequences upstream of the start codons for each of the previously identified RIF inactivating enzymes; *arr-ms* from *Mycobacterium smegmatis* str. MC2 155 (CP001663.1), *rox* from *Nocardia farcinica* (AP006618.1), *iri* from *Rhodococcus equi* (U56415.1), and *rgt1438* from WAC1438 (JX028276.1).

The RAE sequence (GGGGCTTGCGGCAAGGCCC) was used to query the non-redundant and whole-genome shotgun databases of GenBank with BLAST using modified parameters for short queries (Altschul et al., 1997). When the local alignments did not include the entire nucleotide element, the sequence alignment for each hit was expanded to include the entire length of the RAE. The accession number of each hit was used to retrieve the database entry for each sequence and expanded to include 1.5 kb upstream and downstream of the RAE and each record was scanned to identify protein features. If the RAE occurred inside a coding sequence or if there were no protein features upstream or downstream of the RAE, the hit was dropped from further consideration. The accepted RAEs were used to create a sequence logo using WebLogo (http://weblogo.berkeley.edu) (Crooks et al., 2004). To explore the relationship of the RAE with surrounding proteins, the amino acid sequences corresponding to the coding sequences surrounding each putative RAE were retrieved. The sequences were pooled and loosely clustered at 30% identity using USEARCH (Edgar, 2010).

WAC4747 Genome Sequencing and Assembly

WAC4747 genomic DNA (gDNA) was sequenced using the Roche 454 platform. DNA was sheared into approximately 800-bp fragments using a Covaris S220 ultrasonicator (Woburn, MA), and library preparation, emulsion PCR and sequencing were carried out according to the manufacturer's instructions for the FLX instrument. Reads were assembled using MIRA version 3.4.0, using the "de novo," "genome," "accurate," and "454" quick-switch parameters for six passes (Chevreux, 1999). The resulting assembly consisted of 4184 contigs totaling 6 867 703 bp with an N50 statistic of 2 522 bp.

Gene Inactivation from WAC4747 and *Streptomyces sviceus* ATCC 29083

Gene disruptions were accomplished by insertional inactivation as previously described (Spanogiannopoulos et al., 2012). A partial fragment (~1000 bp) of the *rph4747* gene from WAC4747 was amplified by PCR using primers rph4747-part-F and rph4747-part-R and cloned into pSUIC (a suicide version of pSET152 (Kieser, 2000) that lacks *attP* and *int*). The *rph-Ss* gene from *S. sviceus* ATCC 29083 was amplified using primers rph-Ss-part-F and rph-Ss-part-R and cloned as described above. The helicase gene from WAC4747 was amplified using primers hel4747-part-F and hel4747-part-R. Conjugations were performed according to standard protocol (Kieser, 2000). A list of oligonucleotide primers can be found in APPENDIX 2.

RIF Inactivation Assay

Fresh spores were used to inoculate 5 ml of SIM media (D'Costa et al., 2006). Cultures were grown for 4 days at 30ºC with shaking at 250 rpm. 0.5 ml of culture was then used to inoculate 4.5 ml of fresh SIM containing RIF at 20 µg/ml and represented the zero time point. At 48 hours, conditioned media was analyzed for residual RIF activity using the Kirby-Bauer disk diffusion assay using *Bacillus subtilis* as the RIF-sensitive indicator microorganism (Wikler et al., 2006). Additionally, supernatant samples were mixed with an equal volume of methanol, clarified by centrifugation and analyzed using a Waters e2695 HPLC system (Milford, MA) equipped with an XSelect CSH C18 5-µM column (4.6 × 100 mm) with the following method: linear gradient of 37 to 55% acetonitrile in water with 0.05% TFA at 1 ml/min over 12 minutes.

Kanamycin Resistance Reporter Assay

The kanamycin (KAN) resistance reporter constructs were generated using an overlapping PCR strategy. An approximately 250 bp region of DNA located directly upstream of the *rph4747* gene was amplified by PCR using primers P4747-F and P4747/neo-R. Primers P4747/neo-F and neo-R were used to amplify the KAN resistance cassette from pCR4Blunt-TOPO (Invitrogen, Carlsbad, CA). The 5' ends of primers P4747/neo-R and P4747/neo-F contained overhangs allowing the fusion of the two PCR products into one product using overlapping PCR. After 15 cycles of the overlapping PCR program, outer primers P4747-F and neo-R were added to the reaction for amplification; the 5'ends of these primers included restriction endonuclease sites for downstream cloning. The final PCR product was resolved on a 1% (w/v) agarose gel and

purified using PureLink Quick Gel Extraction kit (Invitrogen, Carlsbad, CA) and directionally cloned into pSET152. This plasmid was moved into WAC4747 by conjugation as previously described (Kieser, 2000) and the resulting strain was named WAC4747-P_{RAE}/*neo*-pSET152. The P_{RAE}/*neo*-pSET152 construct was also introduced into WAC1438, *Streptomyces sviceus* ATCC 29083, *Streptomyces coelicolor* A3(2) and *Streptomyces albus* J1074. The $P_{RAE\text{-}\Delta IR}$/*neo*-pSET152 construct was made by amplifying two fragments of the WAC4747 promoter on either side of the RAE; the 5' end was amplified with primers P4747/neo-F and P4747-D-R and the 3' end was amplified with primers P4747-D-F and P4747/neo-R. The 5'ends of primers P4747-D-R and P4747-D-F introduced identical overhangs in each PCR product, which replaced the RAE sequence with a random sequence of 19 nucleotides. Overlapping PCR was used to fuse the two promoter PCR fragments. The mutated promoter was then fused with the KAN resistance cassette using overlapping PCR as described above.

RIF-resistant mutants of the WAC4747-P_{RAE}/*neo*-pSET152 reporter construct were generated by plating fresh spores on Bennett's agar media (Kieser, 2000) supplemented with 250 µg/ml RIF. RIF-resistant colonies were picked and re-streaked on RIF-containing media. The *rpoB* gene was amplified by PCR using primers SRPOF1 and SRPOR1 (Kim et al., 2005) and sequenced to confirm the site of mutation. The mutations corresponded to either H526Y or S531F substitutions of the β-subunit of RNA polymerase (*E. coli* numbering) (FIGURE 1-5). Amino acid substitutions at these positions are recognized to confer RIF resistance (Floss and Yu, 2005).

Reporter assays were performed by plating approximately 10^6 spores on Bennett's agar media supplemented with KAN at a concentration of 5 µg/ml. Subinhibitory concentrations of various antibiotics were applied onto paper disks and plates were incubated for 3-4 days at 30°C. A list of oligonucleotide primers can be found in APPENDIX 2.

Gene Expression Analysis of *rph4747*

The transcriptional expression of the *rph4747* gene from WAC4747 was analyzed by quantitative reverse transcription-PCR (qRT-PCR). Fresh spores of WAC4747 were used to inoculate a 5 ml starter culture of liquid Bennett's media and this culture was grown for 4 days at 30°C with shaking at 250 rpm. A 0.5 ml aliquot of the WAC4747 starter culture was used to inoculate 50 ml of fresh Bennett's media and then incubated until mid-log phase (36 hours). This represented the zero time point. RIF or DMSO (vehicle control) was added to the culture and grown for an additional 1 or 2 hours. 4 ml of culture was harvested and frozen at -80°C until processing. RNA was extracted with the Fermentas GeneJET RNA purification kit according to the manufacturer's protocol for bacteria with some modifications. Cell pellets were resuspended in 250 µl of 10 mM (TE) buffer pH 8.0 plus lysozyme at 5 mg/ml and incubated at 30°C for 5 min. 650 µl of Lysis Buffer, glass beads and 500 µl of phenol:chloroform (50:50) were added to each sample and vortex for 5 min followed by centrifugation at 20 000 × *g* for 10 min. The supernatant was removed, mixed with an equal volume of chloroform and centrifuged at 20 000 × *g* for 10 minutes. The supernatant was removed, 350 µl of 100% ethanol was added and this solution was applied onto a GeneJET RNA purification column. The

column was washed and eluted as described by the manufacturer. Contaminating gDNA was removed by treating RNA samples with Fermentas RNase-free DNase I. The resulting RNA was used for cDNA synthesis using the SuperScript VILO cDNA synthesis kit (Invitrogen, Carlsbad, CA). qRT-PCRs were performed using Phusion DNA polymerase (Invitrogen, Carlsbad, CA) with 1 × SYBR Green I (Invitrogen, Carlsbad, CA) using a Bio-Rad C1000 Thermocycler with the following program: 98°C for 3 min, 45 cycles of 98°C for 10 sec, 70°C for 30 sec, and 72°C for 6 sec, followed by 72°C for 10 min. The *rph4747* gene was amplified with primers rph4747q-F and rph4747q-F. 16S rRNA was used as an internal reference and was amplified using primers 16Sq-F and 16Sq-R. The Livak method was used for comparing gene induction in the presence of RIF versus DMSO. qRT-PCRs were performed in triplicate from 3 independent biological replicates. A list of oligonucleotide primers can be found in APPENDIX 2.

Phylogenetic Analysis of the RPH Protein Family

The domains of RPH were identified using the NCBI Conserved Domain Database (Marchler-Bauer et al., 2013). 1644 proteins sharing the same domain architecture (PRK06241) were retrieved using the Conserved Domain Architecture Retrieval Tool (CDART) (Geer et al., 2002). This domain architecture consists of CDD216434, "Pyruvate phosphate dikinase, PEP/pyruvate binding domain" at the N-terminus and CDD201201 "PEP-utilizing enzyme, mobile domain: pfam00391" at the C-terminus with a variable length of sequence separating the two domains. To further reduce the number of sequences for analysis, this set was filtered for proteins with a

minimum of 350 residues separating the two domains, leaving 1066 proteins. This list was further reduced by selecting proteins with a BLAST hit having a minimum Expect value of 1.0 e^{-10} to a protein on the list of investigated sequences. This procedure resulted in a final list of 670 proteins.

To remove redundant protein sequences the dataset was clustered with a minimum identity of 70% using USEARCH, resulting in 208 clusters (Edgar, 2010). These centroid sequences were aligned using MUSCLE v3.8.1 (Edgar, 2004). A phylogenetic tree was estimated using RAxML v8.0.2 using a GTR amino acid model with gamma rate parameters and a proportion of invariant sites for 1000 rapid bootstrap replicates (Stamatakis, 2014). A subset of those clusters including the RPH4747 sequence formed a clade with 100% bootstrap support. This led us to select a set of 49 clusters, representing 350 individual sequences. We constructed an improved alignment using these 351 sequences and performed another phylogenetic analysis as described above.

Cloning of Various *rph* Genes

The *rph-Ss* gene was amplified by PCR from gDNA of *Streptomyces sviceus* ATCC 29083 using primers rph-Ss-F and rph-Ss-R and subsequently cloned into pET28b (Novagen, Billerica, MA) yielding the construct pET28b-*rph-Ss*. The *rph-Ss* gene was also amplified by PCR using primers rph-Ss-SUMO-F and rph-Ss-R and cloned into pE-SUMO (LifeSensors, Malvern PA) for protein overexpression as a SUMO protein fusion construct. The *rph4747* gene from WAC4747 was amplified using primers rph4747-F and rph4747-R and cloned into pET22b generating construct pET22b-*rph4747*. The *rph-*

Bc gene from *Bacillus cereus* ATCC 14579 was amplified using primers rph-Bc-F and rph-Bc-R and cloned into pET19Tb (pET19b with a TEV cleavage site in place of the enterokinase site) resulting in construct pET19Tb-*rph-Bc*. The *rph-Lm* gene from *Listeria monocytogenes* str. 4b F2365 was amplified with primers rph-Lm-F and rph-Lm-R and cloned into pET19Tb creating the construct pET19Tb-*rph-Lm*. A complete list of oligonucleotide primer sequences can be found in APPENDIX 2.

Site-directed Mutagenesis

Site-specific mutation of the *rph-Bc* gene was performed using Phusion High-Fidelity DNA polymerase using primers rph-Bc-SDM-F and rph-Bc-SDM-R (APPENDIX 2). The site-directed mutagenesis (SDM) reaction consisted of 1×HF Phusion DNA Polymerase buffer, 25 ng of pET19Tb-*rph-Bc* (template), 0.25 µM of each primer, 200 µM dNTP mix and 1 U Phusion DNA polymerase. The SDM reaction was performed using a Thermo Scientific PCR machine with the following method: initial denaturation, 30 seconds at 98ºC; denaturation, 98ºC for 10 seconds; primer annealing, 55ºC for 30 seconds; DNA synthesis, 72ºC for 4 minutes; and 30 seconds; the denaturation, primer annealing and DNA synthesis steps were repeated for 16 cycles. *Dpn* I was added to the SDM reaction and incubated for 2 hours at 37ºC. 1 µl of this reaction was introduced into *E. coli* TOP10 by transformation and positive transformants were selected on LB supplemented with ampicillin. Plasmids were purified and sequenced to confirm the site-specific mutation. The resulting construct was named pET19Tb-*rph-Bc*-H287A and was introduced into *E. coli* Rosetta(DE3)pLysS by transformation for RIF MIC determination and protein overexpression.

RIF MIC Determinations

Minimum inhibitory concentration (MIC) assays were performed according to the CLSI standard broth microdilution protocol (CLSI, 2012). Isopropyl β-D-1-thiogalactopyranoside (IPTG) was used at a final concentration of 100 µM. MICs were performed using *E. coli* Rosetta(DE3)pLysS as the host.

RPH Overexpression and Purification

RPH proteins were overexpressed using the auto-induction protocol described by Studier (Studier, 2005) using *E. coli* Rosetta(DE3) pLysS. A few colonies from a fresh overnight plate were used to inoculate 0.5 L of 2×ZYM-5052 media (Studier, 2005). Cultures were incubated at 25ºC with shaking at 200 rpm for 40 hours. Subsequently, cells were harvested by centrifugation, washed with 0.85% saline, pelleted and stored at -20ºC. Cell pellets were thawed and resuspended in 30 ml of Buffer A (50 mM HEPES pH 7.5, 300 mM NaCl, 10 mM imidazole) supplemented with 1 mM phenylmethylsulfonyl fluoride (PMSF) and 1 µg/ml DNase and lysed using a Constant Systems continuous-flow cell-disruptor (Daventry, United Kingdom). The cell lysate was clarified by centrifugation at 25,000 × *g* for 30 minutes and the soluble protein fraction was applied onto a 5 ml nickel-nitrilotriacetic acid (Ni-NTA) column (Qiagen, Venlo, Netherlands). The column was then washed with 5 column volumes of Buffer B (50 mM HEPES pH 7.5, 300 mM NaCl, 20 mM imidazole). RPH protein was eluted from the column by applying 5 column volumes of Buffer C (50 mM HEPES pH 7.5, 300 mM NaCl, 300 mM imidazole). Elution fractions were analyzed by SDS-PAGE and fractions containing RPH were pooled and dialyzed against 3.0 L of dialysis buffer (50

mM HEPES pH 7.5, 300 mM NaCl, 1 mM DTT) for 3 hours at 4ºC. RPH-Ss-SUMO fusion protein was digested with SUMO protease while recombinant His-tagged RPH-Bc and RPH-Lm were digested with TEV protease. Protease treatments were carried out at 10ºC for 16 hours. The resulting protein solution was applied onto a Ni-NTA column and RPH protein was collected in the flow-through. RPH proteins were further purified using gel-filtration chromatography with a HiLoad 26/60 Superdex 200 prep grade column (GE Healthcare, Fairfield, CT) using Buffer D (50 mM HEPES pH 7.5, 300 mM NaCl). Protein fractions were analyzed using SDS-PAGE and fractions containing purified RPH were pooled, concentrated and stored at -20ºC with 15% (w/v) glycerol.

Kinetic Characterization of RPH

A RPH enzymatic reaction consisted of RPH reaction buffer (50 mM HEPES pH 7.5, 5 mM $MgCl_2$, and 40 mM NH_4Cl_2), RIF, ATP, BSA (1 mg/ml) and RPH enzyme. Reactions were carried out at room temperature and initiated with the addition of ATP. Thin layer chromatography (TLC) assays were performed in a total volume of 1 ml with 0.5 mg of RPH, 1 mM RIF and 10 mM ATP. Reaction aliquots were quenched with an equal volume of methanol and 5 µl was analyzed using silica TLC with methanol:chloroform (50:50) (Yazawa et al., 1994).

Steady-state kinetic characterization of RPH enzymes was performed using liquid chromatography electrospray ionization mass spectrometry (LC-ESI-MS) and multiple reaction monitoring (MRM). A QTRAP LC/MS/MS System (Applied Biosystems, Carlsbad, CA) mass spectrophotometer equipped with electrospray ion source was used for quantitation of RIF-P and an internal standard (IS). The IS was C21-C23 acetonide-

RIF, which is not a substrate of RPH and was synthesized as previously described (Kump and Bickel, 1973). The collision energy was set at 35 eV, RIF-P was detected in MRM mode with the following transitions: 902.9→399.1 (declustering potential (DP) 58.00 eV). The IS was detected using the 861.1→397.1 transition (DP 32 eV). Chromatography separation was achieved using an Agilent 1100 HPLC system equipped with a Waters C18 Sunfire 5 µm column (4.6 x 50 mm) using the following method: linear gradient of 45 to 100% acetonitrile in water with 0.05% formic acid (FA) for 3 minutes at a flow rate of 1 ml/min. A standard curve was generated using RIF-P at various concentrations ranging from 5 to 500 nM normalized to the IS and the correlation coefficient (R^2) was > 0.99. The K_m of ATP was determined using the following conditions: 10-250 µM ATP, 5 µM RIF, a final enzyme concentration of 0.5 nM and samples were analyzed for RIF-P formation at 10, 20 and 30 minutes. The K_m of RIF was determined as follows: 500 µM ATP, 0.0625-2.5 µM RIF, a final enzyme concentration of 0.05 nM and samples were analyzed for RIF-P formation every 20, 40 and 60 minutes. All reactions were performed in triplicate. Reactions were terminated by mixing a 50 µl aliquot with an equal volume of stopping solution (ice-cold methanol plus IS). Samples were clarified by centrifugation (15,000 × *g* for 10 minutes) and a 50 µl sample was analyzed for RIF-P product using LC-ESI-MS/MRM. Product and IS peaks were integrated using the Agilent Analyst software. The quantity of RIF-P produced was calculated using the standard curve. Initial rates of reaction were analyzed by nonlinear least squares fitting of the following equation (1):

$$v = V_{max} S / (K_m + S) \quad (1)$$

Enzyme assays measuring inorganic phosphate were performed with the EnzChek Phosphate Assay Kit according to the manufacturer's guidelines (Molecular Probes, Eugene, OR). RPH-Bc and RPH-Bc-H287A were assayed using an HPLC assay. Reaction conditions included enzymes at a final concentration of 0.01 µM and saturating concentrations of substrates; RIF at 10 µM and ATP at 250 µM. At specified time intervals, reaction aliquots were quenched with ice-cold methanol and analyzed by HPLC using the previously described method above.

Production, Purification and Physiochemical Analysis of RIF-P

A large scale reaction consisted of 1 × RPH reaction buffer, 20 mg of RIF, 5 mM ATP, and 0.75 mg/ml RPH-Ss in a final volume of 20 ml. The reaction was incubated at room temperature for 20 hours. An equal volume of acetonitrile was added to the reaction, the precipitate was clarified by centrifugation and the resulting solution was lyophilized. The product was resuspended in a minimal volume of DMSO and water (50:50) and purified using semi-preparative HPLC using a Waters e2695 system (Milford, MA) equipped with an XSelect CSH C18 5 µM column (10 × 100 mm) with the following method: linear gradient of 15 to 100% acetonitrile in water with 0.05% TFA over 12 minutes at 3 ml/min. The purity of the final product was assessed using LC-MS. The structure of RIF-P was confirmed by 1-D and 2-D NMR experiments on a Bruker AVIII 700 MHz instrument equipped with a cryoprobe in deuterated DMSO. Chemical shifts are reported in parts per million relative to tetramethyl silane using the residual solvent signal as an internal signal. High resolution mass spectra (HRMS) were obtained using a ThermoFisher-XL-Orbitrap Hybrid mass spectrometer equipped with

electrospray interface operated in positive and negative ion mode. For unequivocal determination of the regiospecificity of RPH, the NMR spectra of RIF and RIF-P were completely assigned by a combination of 1-D and 2-D NMR techniques. Although the overall appearance of the ^{1}H spectra was similar to that of RIF, there were some distinct chemical shift changes. For example, one of the multiplets at 3.76 ppm was deshielded to 4.36 ppm of the spectra. This chemical shift was assigned to H-21 (APPENDIX 4). The other available site for phosphorylation is at the C-23 hydroxyl. The multiplet assigned to H-23 at 2.80 ppm appeared essentially the same chemical shift and multiplicity as the corresponding signal in RIF and was therefore eliminated as a site for modification. In the ^{13}C spectra, the coupling resonance assigned to C-21 was split by a ^{31}P spin coupling of 6.5 Hz. This observation provided an additional confirmation of phosphorylation at position C-21. The combined results from all NMR experiments undoubtedly indicated that the site of modification is the hydroxyl group at position C-21, confirming 21-(O-phosphoryl)rifampin

.

RESULTS

Initial Attempts to Identify the *rph* Gene

Our group has identified a collection of RIF-phosphorylating soil actinomycetes (TABLE 2-3). Our first attempt to identify the gene responsible for this phenotype involved a functional genomic screen. A genomic cosmid library of WAC4747 was created and the resulting *Escherichia coli* library was screened for a RIF-resistance phenotype. Although this approach has been successful in the identification of antibiotic resistance determinants, we failed to identify any RIF-resistant clones. Next, we turned to a genomics approach. In this approach we scanned the genome of *Streptomyces sviceus* ATCC 29083 for genes encoding proteins resembling the two antibiotic phosphotransferase protein families, APH/MPH and CPT, and identified 13 candidate *rph* genes (TABLE 4-1). Each gene was cloned and heterologously expressed in *E. coli*. Unfortunately, none of the genes conferred RIF resistance. Finally, we attempted to isolate the RPH enzyme from. *S. sviceus* ATCC 29083 by using activity-guided protein purification using γ-^{32}P-ATP as the phosphoryl donor, which would have been followed by protein mass spectrometry. This approach was also unsuccessful.

A Conserved Nucleotide Element is Associated with RIF Inactivating Genes

A diverse collection of RIF inactivating mechanisms have been described from various pathogenic and nonpathogenic actinomycetes (FIGURE 1-8). We reported the identification and characterization of a RIF-inactivating glycosyltransferase (*rgt1438*) from a screen of soil actinomycetes (Spanogiannopoulos et al., 2012) (CHAPTER 3).

TABLE 4-1. List of putative *rph* genes from *S. sviceus* identified by genomics.

Putative *rph* gene	Locus	Gene annotation
*prk*1	SSEG_08349.1	Aminoglycoside phosphotransferase
*prk*2	SSEG_06982.1	Aminoglycoside phosphotransferase
*prk*3	SSEG_01252.1	Aminoglycoside phosphotransferase
*prk*4	SSEG_09729.1	Aminoglycoside phosphotransferase
*prk*5	SSEG_07974.1	Aminoglycoside phosphotransferase
*prk*6	SSEG_05705.1	Aminoglycoside phosphotransferase
*prk*7	SSEG_08746.1	Aminoglycoside phosphotransferase
*prk*8	SSEG_03089.1	Phosphotransferase
*prk*9	SSEG_06518.1	Phosphotransferase
*prk*10	SSEG_07644.1	Conserved hypothetical protein/Kinase
*prk*11	SSEG_00965.1	Serine/threonine protein kinase
*prk*12	SSEG_06057.1	Serine/threonine protein kinase
*prk*13	SSEG_10719.1	Aminoglycoside phosphotransferase

Examination of the intergenic DNA sequence upstream of *rgt1438* identified a 19 base-pair (bp) inverted repeat (IR) motif; 9-bp repeats separated by a single nucleotide spacer (FIGURE 4-2). We hypothesized that this element could be involved in gene regulation. The conservation of this putative RIF-associated element (RAE) was examined by scanning the upstream intergenic regions from various characterized genes encoding RIF-inactivating enzymes (FIGURE 1-8) (Andersen et al., 1997; Quan et al., 1997; Hoshino et al., 2010; Spanogiannopoulos et al., 2012). This collection included three mechanisms of RIF inactivation (glycosylation, ADP-ribosylation, and monooxygenation) from four divergent genera of actinomycetes (*Streptomyces*, *Mycobacteria*, *Rhodococcus*, and *Nocardia*) (FIGURE 4-2). The RAE was conserved upstream of all these genes with near perfect nucleotide identity (FIGURE 4-2). A blastn search of the RAE was conducted focused on intergenic regions of the nucleotide collection (nr) and whole-genome shotgun contigs (wgs) from NCBI (Altschul et al.,

1997). The RAE was found over 400 times and was predominantly associated with actinobacterial genomes. The RAE was not associated with rifamycin-producing bacteria. A sequence logo with this RAE collection demonstrates the remarkable conservation of this element (FIGURE 4-2). To determine if there is a correlation between the RAE and specific genes, we compiled a list of available divergent ORFs flanking each RAE and loosely binned orthologous proteins. The RAE was strongly associated with ORFs resembling previously characterized RIF-inactivating enzymes (FIGURE 4-2). The RAE is observed accompanying ORFs encoding Arr (RIF ADP-ribosyltransferase), RIF monooxygenase or RGT (RIF glycosyltransferase) enzymes at a frequency of 0.33. Furthermore, the RAE is strongly associated with a number of uncharacterized ORFs; the RAE is found upstream of ORFs annotated as PEP synthases and 2 distinct helicases (FIGURE 4-3). This survey revealed that the RAE is highly conserved across many actinobacterial genomes and has coevolved with a repertoire of genes including RIF-inactivating genes and several other genes, which are presumably expressed in response to RIF.

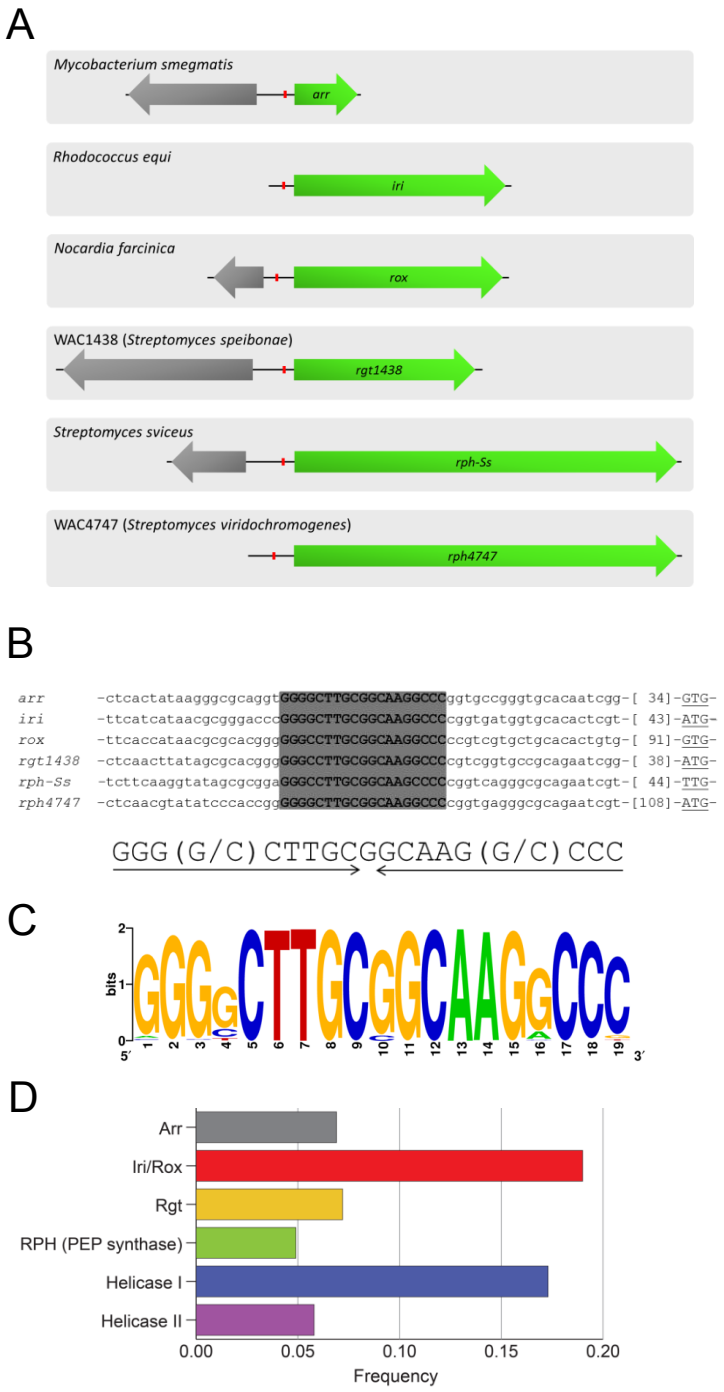

FIGURE 4-2. A conserved motif is associated with various RIF-inactivating enzymes. (A) The RAE, rifamycin-associated *cis* element, is conserved upstream of all previously characterized RIF inactivating genes; *arr*, RIF ADP-ribosyltransferase; *iri* and *rox*, RIF monooxygenase; *rgt1438*, RIF glycosyltransferase; and *rph-Ss* and *rph4747*, RIF phosphotransferase. The red line indicates the position of the RAE. (B) An alignment of the RAE identified a conserved 19 nucleotide inverted repeat boxed in gray. (C) Sequence logo from over 400 RAEs found in the nucleotide collection (nr) and whole-genome shotgun contig (wgs) databases. Sequence logos were generated using WebLogo (http://weblogo.berkeley.edu) (Crooks et al., 2004). (D) RAE gene associations.

The *rph* Gene is Responsible for Phosphorylating RIF

A number of actinomycetes capable of inactivating RIF by phosphorylation have been described, however, the gene responsible for this phenotype, *rph*, has yet to be identified (FIGURE 1-8) (Yazawa et al., 1994; Spanogiannopoulos et al., 2012). The strong correlation of the RAE with genes encoding RIF-inactivating enzymes led us to apply this link to identify the *rph* gene. In a previous phenotypic screen we identified a collection of RIF-phosphorylating soil actinomycetes and thus we selected one of these strains, WAC4747, for further investigation (TABLE 2-3) (Spanogiannopoulos et al., 2012). The draft genome of WAC4747 (most closely resembling *Streptomyces viridochromogenes* based on 16S rRNA analysis) was determined. Additionally, *Streptomyces sviceus* ATCC 29083, annotated genome is publically available, was also identified as a RIF-phosphorylating strain (TABLE 2-3). Putative *rph* genes were identified by probing the genome sequences of WAC4747 and *S. sviceus* for the RAE and examining associated downstream genes. The RAE was not found to be flanking any genes resembling known antibiotic phosphotransferases (APH/MPH and CPT family) (Morar and Wright, 2010). The RAE was found on 2 contigs within the WAC4747 genome: on a 3 kb contig upstream of an (ORF) encoding a putative phosphoenolpyruvate (PEP) synthase (ORF1) and on an 8.5 kb contig upstream of a putative helicase (ORF2) (TABLE 4-2). Similarly, the RAE was found upstream of predicted PEP synthase and helicase ORFs within the *S. sviceus* genome, in addition to a candidate RIF monooxygenase (TABLE 4-2). PEP synthase and helicase proteins have not been previously associated with antibiotic resistance. Helicases harness the energy of

ATP hydrolysis for separation of nucleotide strands while PEP synthases catalyze the conversion of ATP and pyruvate to PEP, AMP and P_i (Cooper and Kornberg, 1967; Singleton et al., 2007). Orthologous genes of ORF1 and ORF2 are conserved in other actinomycete genomes and are co-localized with the RAE (FIGURE 4-2).

TABLE 4-2. RAEs from WAC4747 and *S. sviceus* genomes and associated genes.

Actinomycete	RAE Sequence	Associated ORF	Accession Number
WAC4747	GGGGCTTGCGGCAAGGCCC	RPH	KJ151292
	GGGCCTTGCGGCAAGGCCC	DNA/RNA helicase	KJ151292
Streptomyces sviceus ATCC 29803	GGGCCTTGCGGCAAGCCCC	RPH	EDY61575
	GGGCCTTGCGGCAAGATCC	RIF monooxygenase	EDY55462
	GGGGCTTGCGGCAAGGCCC	DNA/RNA helicase	EDY53511

We individually disrupted ORF1 and ORF2 from WAC4747 and evaluated the ability of the mutant strains to phosphorylate RIF. Analysis of conditioned media from WAC4747 grown in the presence of RIF showed complete inactivation of RIF within 48 hours (FIGURE 4-3). In contrast, a mutant strain of WAC4747 with a disrupted ORF1 (putative PEP synthase) failed to inactivate RIF (FIGURE 4-3). Disruption of ORF2 (putative helicase) in WAC4747 had no effect on RIF inactivation. This suggests that ORF1 (named *rph4747*) encodes the RPH enzyme. Inactivation of the orthologous putative PEP synthase gene from *S. sviceus* (*rph-Ss*) generated identical results (FIGURE

4-3). Mutant strains of WAC4747 and *S. sviceus* with a disrupted *rph* gene displayed a modest 2-fold decrease in RIF MICs in comparison to the wild type strains (TABLE 4-3). This suggests, similar to other actinomycetes, WAC4747 and *S. sviceus* harbor multiple RIF resistance mechanisms (CHAPTER 3) (Hoshino et al., 2010; Spanogiannopoulos et al., 2012).

We assessed the ability of the *rph* gene to contribute to RIF resistance by expression in a heterologous host. Introduction of *rph4747* or *rph-Ss* into RIF-sensitive *Escherichia coli* conferred a 64-fold increase in RIF MIC compared to the control (TABLE 4-4). *E. coli* expressing *rph* displayed high level resistance up to or over 512 µg/ml towards a panel of natural product and clinically used semi-synthetic rifamycin antibiotics (TABLE 4-4). This highlights *rph*'s ability to confer broad high-level resistance towards the rifamycin family antibiotics.

TABLE 4-3. RIF MIC determination of *Streptomyces* strains.

Strain	**RIF MIC** (µg/ml)
WAC4747	64
WAC4747 pSET152	64
WAC4747 *rph4747*::pSUIC	32
Streptomyces sviceus ATCC 29083	64
Streptomyces sviceus ATCC 29083 pSET152	64
Streptomyces sviceus ATCC 29083 *rph-Ss*::pSUIC	32

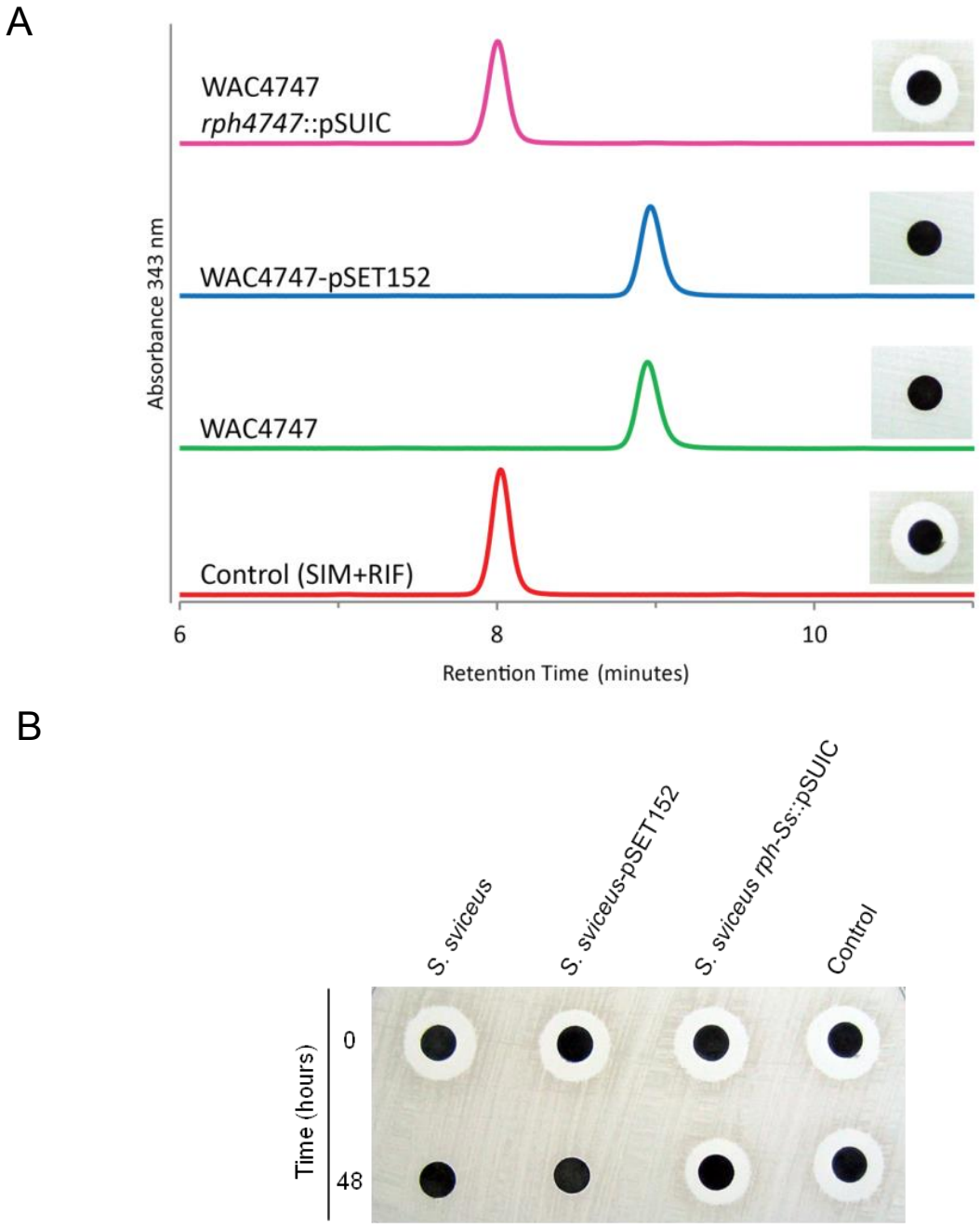

FIGURE 4-3. The *rph* gene is responsible for inactivating RIF by phosphorylation. Strains of WAC4747 were grown in the presence of RIF for 48 hours and conditioned media was analyzed for residual RIF activity using a RIF-sensitive indicator organism (*B. subtilis*). Samples were additionally analyzed using HPLC analysis. (A) WAC4747 and the control, WAC4747-pSET152 (empty vector), completely inactivate RIF within 48 hours. The *rph4747* mutant strain, WAC4747 *rph4747*::pSUIC, does not inactivate RIF and is comparable to the control of media and drug (SIM+RIF). Chromatograms are displayed at an absorbance of 343 nm. (B) Inactivation of the *rph-Ss* gene from *S. sviceus* ATCC 29803 generates identical results.

TABLE 4-4. Rifamycin MIC of *rph* genes heterologously expressed in *E. coli*.

Construct[1]	IPTG	MIC (µg/ml)			
		RIF	Rifamycin SV	Rifabutin	Rifaximin
pET22b	-	8	64	8	16
	+	8	64	8	16
pET22b-*rph4747*	-	512	512	512	64
	+	>512	>512	512	512
pET28b	-	8	64	8	16
	+	8	64	8	16
pET28b-*rph-Ss*	-	512	>512	512	512
	+	>512	>512	512	512
pET19Tb	-	8	64	8	8
	+	8	64	8	8
pET19Tb-*rph-Bc*	-	128	256	64	64
	+	>512	>512	512	512
pET19Tb-*rph-Lm*	-	128	128	32	32
	+	>512	>512	512	512
pET19Tb-*rph-Bc*-H827A	-	8			
	+	8			

[1] *E. coli* Rosetta(DE3)pLysS host

The RAE Responds to RIF

Due to the strong association of the RAE and genes encoding RIF inactivating enzymes, we hypothesized that this DNA motif is involved in gene expression in response to RIF. Changes in transcript levels of *rph4747* expression were monitored using qRT-PCR with growth of WAC4747 in the presence or absence of RIF. In the presence of RIF, the *rph4747* transcript was upregulated 63 and 91-fold after 1 and 2 hours of growth respectively, in comparison to the control, DMSO (FIGURE 4-4). This finding confirms genes paired with the RAE are up regulated in response to RIF.

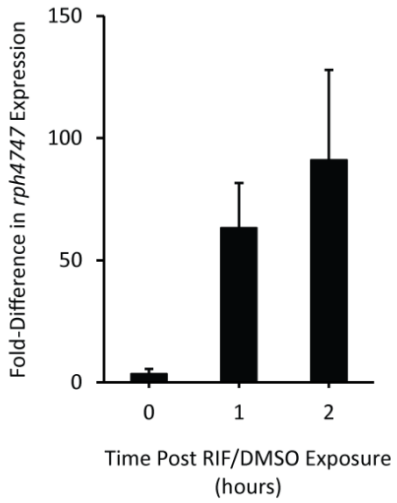

FIGURE 4-4. The *rph4747* gene is upregulated in response to RIF. qRT-PCR analysis of *rph4747* transcripts. WAC4747 was grown in the presence of RIF or DMSO. Data is presented as fold-difference in *rph4747* transcripts from three independent biological replicates and error bars represent standard deviations.

To validate the role of the RAE in RIF specific gene regulation we constructed a kanamycin (KAN) resistance reporter assay. The reporter was constructed by fusing the intergenic DNA upstream of the *rph4747* gene ahead of a promoter-less KAN resistance cassette followed by integration into the genome of WAC4747, creating the strain WAC4747-P_{RAE}/*neo*-pSET152. This strain was not KAN resistant; demonstrating that gene expression downstream of the RAE is tightly regulated. On the other hand,

exposure to subinhibitory concentrations of rifamycin antibiotics (RIF and the parent natural product rifamycin SV) induced growth on KAN containing media, confirming the RAE is involved in rifamycin-responsive gene regulation (FIGURE 4-5). A number of diverse antibiotics, from natural and synthetic origins, inhibiting various biological targets failed to induce KAN resistance, confirming gene regulation from the RAE is rifamycin specific (FIGURE 4-5). Additionally, a reporter construct was made where the RAE was replaced with a random sequence of nucleotides. This construct failed to respond to RIF (FIGURE 4-5) and established that the RAE nucleotide sequence is critical for gene expression.

In some instances, antibiotic resistance gene expression is dependent on the antibiotic successfully binding and inhibiting its target (Narayanan and Dubnau, 1985; Allen et al., 2009). We generated RIF-resistant *rpoB* mutants of WAC4747-P_{RAE}/*neo*-pSET152 to determine if inhibition of RNAP is a prerequisite for RAE-mediated gene induction. This mutant strain gained KAN resistance in response to RIF (FIGURE 4-5), indicating that gene expression mediated by the RAE is independent of RNAP inhibition.

The reporter construct was also introduced into a number of other *Streptomyces* to determine the universality of RAE-mediated gene expression. We included the following *Streptomyces* spp.: WAC1438 and *S. sviceus*, RIF-inactivating strains with RAE; *Streptomyces coelicolor*, RIF-resistant RNAP; and *Streptomyces albus*, RIF-sensitive. Upon the addition of sub-inhibitory concentrations of RIF, all strains gained KAN resistance (FIGURE 4-5). This finding suggests the mechanism of gene induction mediated by the RAE is universal across *Streptomyces* species.

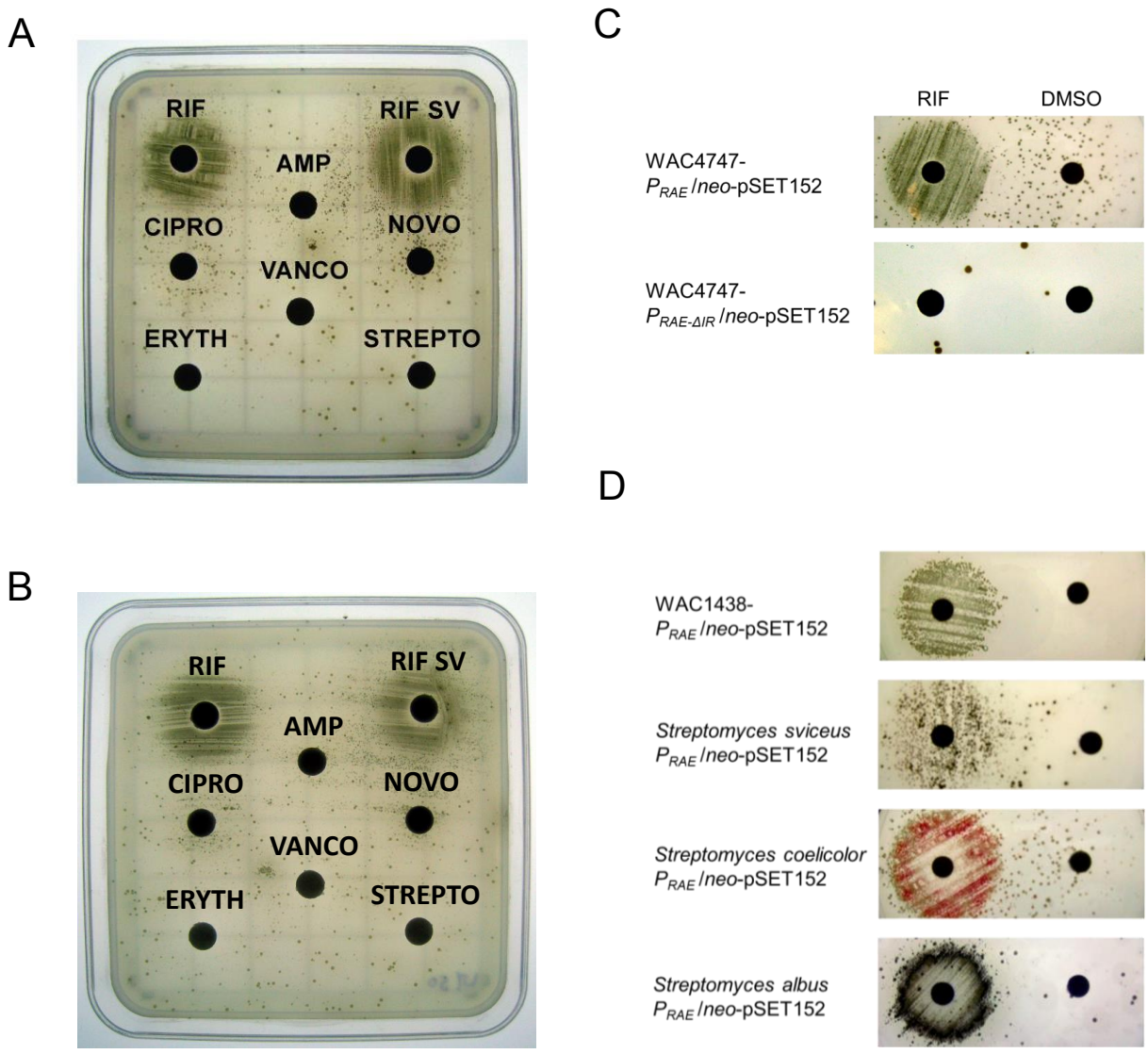

FIGURE 4-6. The RAE is involved in gene regulation in response to RIF. A WAC4747 KAN resistance reporter assay. (A) The RAE from WAC4747 was fused to a promoterless KAN resistance cassette and integrated in the genome of WAC4747. Growth on KAN-containing media was only achieved in the presence of RIF and RIF SV. Subinhibitory concentrations of antibiotics were used: RIF, rifampin, 2.5 µg; RIF SV, rifamycin SV, 5 µg; AMP, ampicillin, 5 µg; CIPRO, ciprofloxacin, 0.5 µg; NOVO, novobiocin, 0.05 µg; VANCO, vancomycin, 0.05 µg; ERYTH, erythromycin, 0.125 µg; STREPTO, streptomycin, 0.05 µg. (B) A RIF-resistant mutant (*rpoB* mutation) of the reporter strain in (A) gains KAN resistance in response to RIF and RIF SV. (C) A reporter strain lacking the RAE (WAC4747-$P_{RAE\text{-}\Delta IR}$/*neo*-pSET152) cannot grow on KAN-containing media in the presence of RIF. (D) The KAN resistance reporter construct was introduced into a variety of *Streptomyces* spp. All strains gained KAN resistance in the presence of RIF.

Diversity of the RPH Protein Family

A blastp analysis of the RPH enzyme reveals it is related to enzymes annotated as PEP synthases (EC 2.7.9.2). The mechanism of PEP synthase proceeds via a phosphoenzyme intermediate whereby the β-phosphate of ATP is transferred to a histidine residue, which in turn is transferred to pyruvate (Narindrasorasak and Bridger, 1977). PEP synthase is composed of three domains; the N-terminal domain is responsible for nucleotide binding, the C-terminal domain binds pyruvate and the central segment contains the catalytic domain (HIS domain).

A global alignment of RPH4747 and PEP synthase from *E. coli* indicates low overall amino acid similarity, but relatively high similarity near the N-terminus. A search of the Conserved Domain Database (CDD) (Marchler-Bauer et al., 2013) with RPH demonstrated the N-terminus consists of an ATP-binding domain, similar to PEP synthase. In contrast to PEP synthase, the HIS domain of RPH is located at the C-terminus (FIGURE 4-6). The central region of RPH4747 shows no similarity to any previously characterized proteins. Therefore, RPH4747 shares some similarities with PEP synthase but the overall domain architectures of these two enzymes differ. A search of the RPH using the Conserved Domain Architecture Retrieval Tool (CDART) (Geer et al., 2002) demonstrated this domain architecture is found in over 1600 proteins and is primarily restricted to bacterial genomes. Although the majority of these enzymes are annotated as PEP synthases (or PEP binding proteins), there is no biochemical evidence confirming this activity and therefore represent an unexplored protein family.

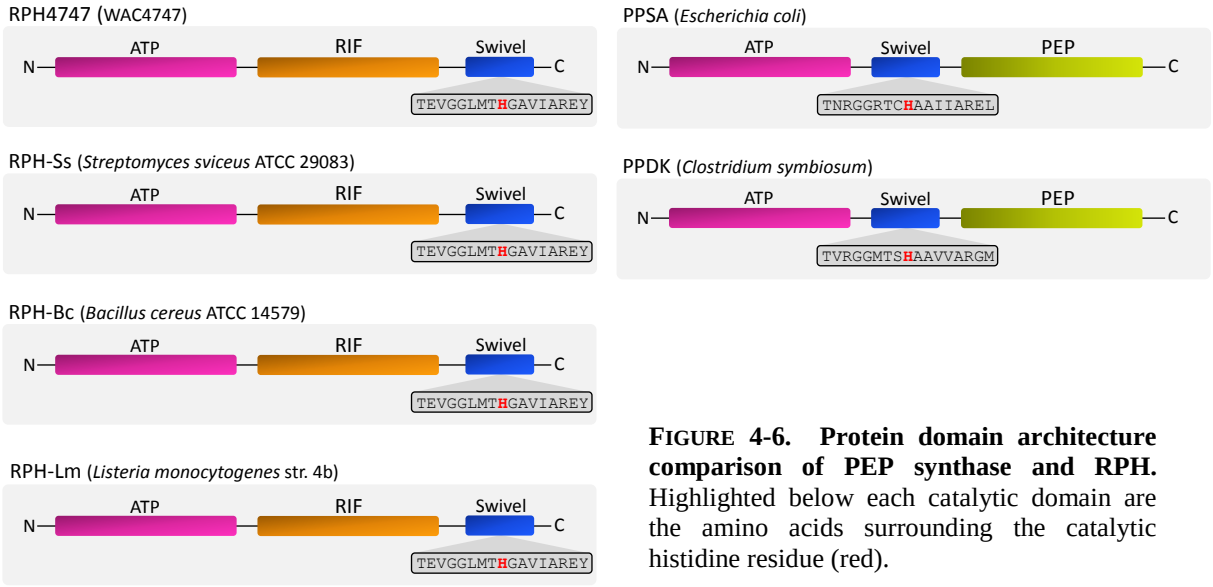

FIGURE 4-6. Protein domain architecture comparison of PEP synthase and RPH. Highlighted below each catalytic domain are the amino acids surrounding the catalytic histidine residue (red).

We used I-TASSER to generate a structural model of RPH4747 (http://zhanglab.ccmb.med.umich.edu/I-TASSER) (Roy et al., 2010). A comparison of this model with the structure of PEP synthase from *Neisseria meningitidis* (PDB: 2OLS) revealed a high level of structural similarity between the ATP-binding domains located at the N-terminus ofboth enzymes (FIGURE 4-7). The remaining domains of the enzymes show very little or no structural similarities. In the PEP synthase structure, the catalytic HIS domain is sandwiched between the ATP and PEP-binding domains. In contrast, the RPH4747 model positions the HIS domain at a region of the enzyme distant from the ATP-binding domain. Since the RPH protein is quite unique compared to proteins in the PDB, we cannot rely on this model for the 3D positioning of the domains.

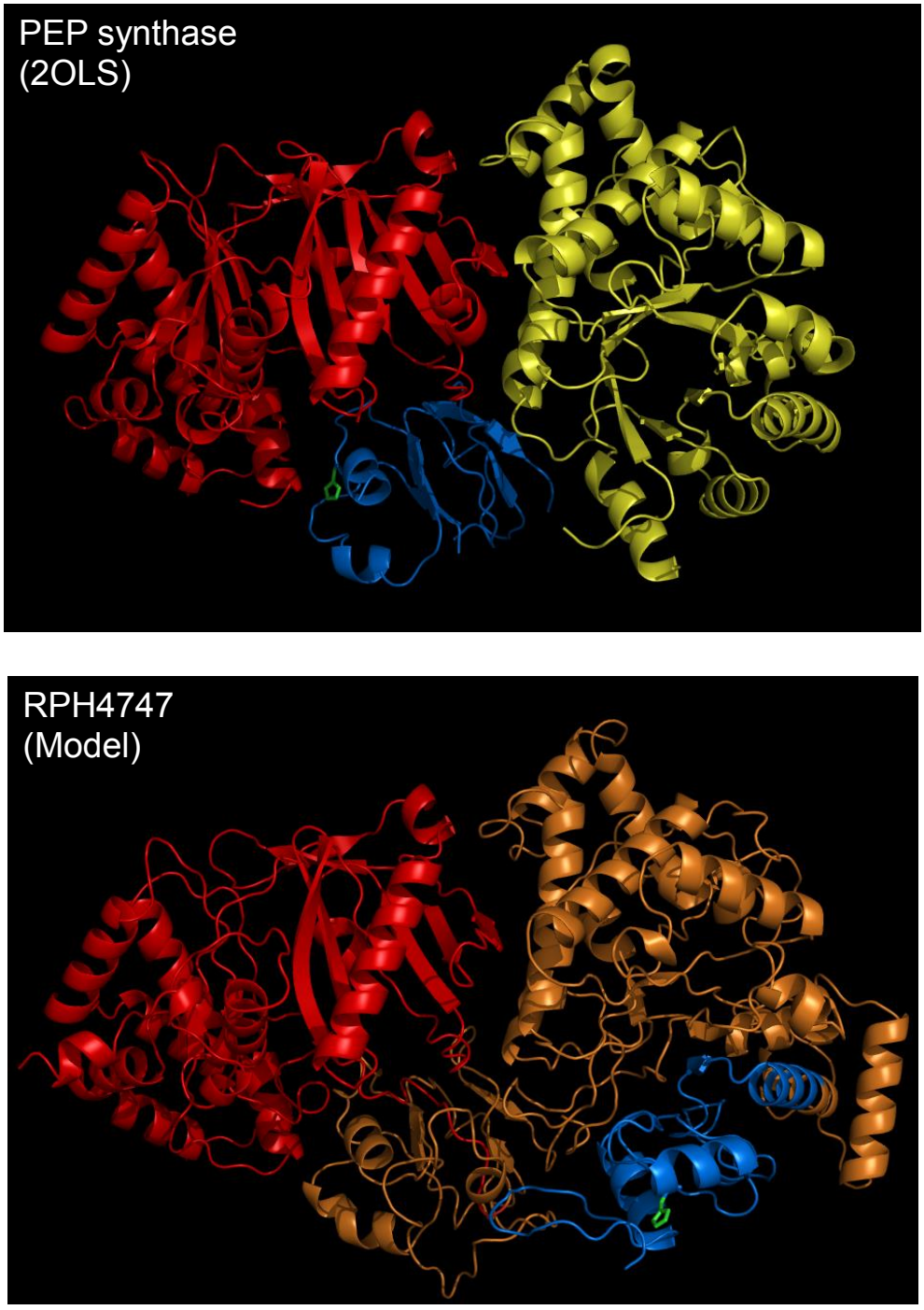

FIGURE 4-7. Structural comparison of PEP synthase and the RPH4747 model. PEP synthase is from *Neisseria meningitidis* (PDB: 2OLS). RPH4747 structure model was generated using I-TASSER (http://zhanglab.ccmb.med.umich.edu/I-TASSER) (Roy et al., 2010). Protein domains are highlighted in color: ATP-binding domain, red; catalytic-HIS domain, blue; PEP-binding domain, yellow; and the RIF-binding domain, orange.

We performed a phylogenetic analysis of the RPH protein family to explore the relationship of the sequences in this family. The RPH cladogram is shown in FIGURE 4-8. We can identify several clades with high bootstrap support that correspond to well defined taxonomic groups even if resolution within and between these groups remains unclear. RPH proteins are widely distributed, predominately in Gram positive bacteria. Although many RPH orthologs are found within Actinobacteria, the majority are associated with Bacilli and Clostridia species. We examined the intergenic DNA sequence upstream of these RPH ORFs and discovered that the majority of ORFs from the Actinobacteria are associated with the RAE (FIGURE 4-8). This is consistent with our previous survey of the RAE and associated ORFs. (FIGURE 4-2). The RAE was not associated with any other RPHs outside Actinobacteria. It is therefore uncertain whether the enzymes from non-Actinobacterial species possess RPH activity.

A previous biochemical screen by Dabbs et al. showed that a number of bacteria from the genus *Bacillus* inactivated RIF by phosphorylation (Dabbs et al., 1995). This report was intriguing considering *Bacillus* spp. are highly susceptible to RIF (Dey and Chatterji, 2012). Our phylogenetic analysis of the RPH protein family revealed orthologous enzymes from a number of Bacilli (FIGURE 4-8). This list also encompassed pathogenic bacteria including *Bacillus cereus*, *Bacillus anthracis* and *Listeria monocytogenes*. These pathogens have been previously reported to be highly susceptible to RIF (Hawkins et al., 1984; Vogler et al., 2002). Indeed, this was confirmed by performing RIF susceptibility testing with *B. cereus* and *L. monocytogenes*, which demonstrated a RIF MIC of 62.5 ng/ml. RPH orthologs from *B. cereus* and *L.*

monocytogenes (RPH-Bc and RPH-Lm respectively) displayed 55% and 52% identity and 74% and 71% similarity, respectively, compared to RPH4747. We selected these two RPH orthologs as representatives from our phylogenetic analysis and evaluated their ability to confer RIF resistance when expressed in a heterologous host. *E. coli* expressing *rph-Bc* or *rph-Lm* exhibited a 64-fold increase in RIF MIC and also conferred high-level resistance towards a variety of rifamycin analogues (TABLE 4-4). This result confirms that RPH orthologs are found in RIF-sensitive pathogenic bacteria and will confer high-level and broad rifamycin resistance when expressed in a heterologous host, although the parent strain is RIF-sensitive.

.

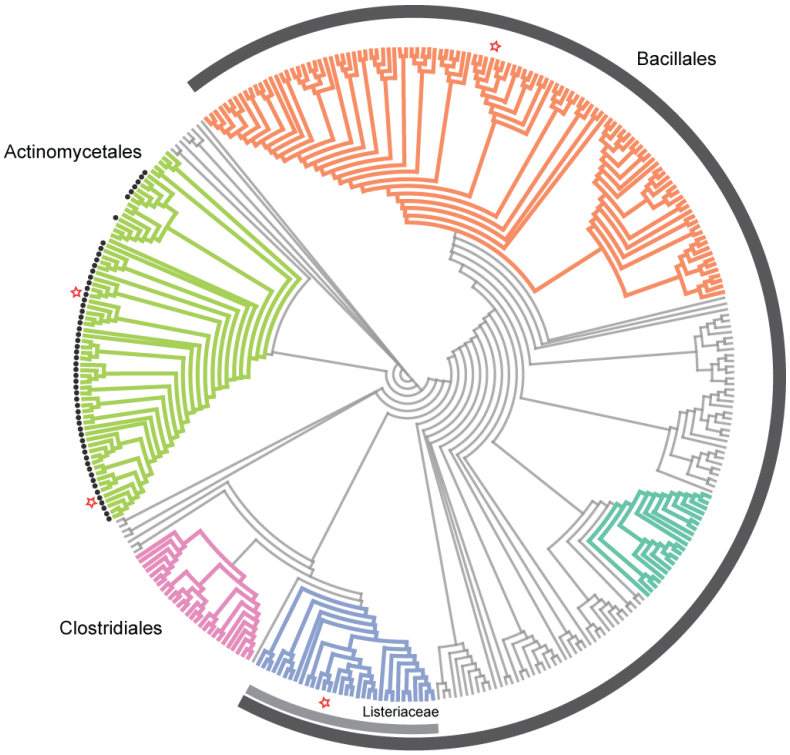

FIGURE 4-8. Cladogram of the RPH protein family. Colored clades represent groups with over 85% bootstrap support, based on maximum likelihood analysis using RAxML. Black circles indicate RPHs that are paired with the RAE. Red stars indicate RPHs selected for characterization: RPH4747 from WAC4747; RPH-Ss from *S. sviceus* ATCC 29083; RPH-Bc from *B. cereus* ATCC14579; RPH-Lm from *L. monocytogenes* str. 4b. F2365. The gray bar represents RPHs from bacteria of the Bacillales order. The light gray bar represents RPHs from the *Listeriaceae* family.

Biochemical Characterization of RPH Activity

Recombinant RPH enzymes were overexpressed and purified from *E. coli* for *in vitro* characterization. Initially, RPH activity was monitored using a thin layer chromatography (TLC) assay, which confirmed ATP served as a cosubstrate (FIGURE 4-9). The RIF-phosphate (RIF-P) product was purified and analyzed using high-resolution mass spectrometry (HR-MS) and nuclear magnetic resonance (NMR) spectroscopy (APPENDIX 4). This analysis confirmed that RIF-P was phosphorylated at the hydroxyl group attached to the C-21 of the ansa-chain, consistent with precedent using whole cell inactivation (FIGURE 4-1) (Yazawa et al., 1994).

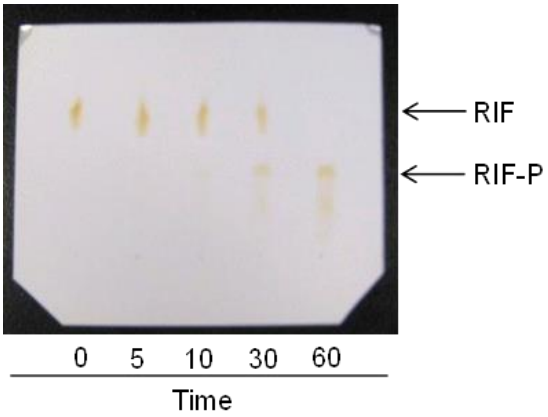

FIGURE 4-9. Thin layer chromatography (TLC) analysis of RPH activity. Purified RPH-Ss enzyme was incubated with RIF and ATP. At specified time intervals, reaction aliquots were quenched with ice-cold methanol and 5 µl was analyzed using silica TLC with methanol:chloroform (50:50).

Liquid chromatography electrospray ionization mass spectrometry (LC-ESI-MS) coupled with multiple reaction monitoring (MRM) were used to quantify RPH activity. Steady-state kinetics were performed for three RPH enzymes from diverse bacterial hosts; RPH-Ss from *S. sviceus*, RPH-Bc from *B. cereus*, and RPH-Lm from *L. monocytogenes*. The gene encoding RPH-Ss is associated with the RAE, whereas the genes encoding RPH-Bc and RPH-Lm are not. All RPHs demonstrated comparable kinetic constants regardless of the host source and RAE association (TABLE 4-4). RPHs

exhibited low K_m values for RIF within the high nanomolar range, indicating a high affinity for RIF. The K_m values for RIF only varied 2-fold among the different RPH enzymes. Similarly, all RPHs displayed comparable k_{cat} constants.

Although PEP synthase and RPH share some amino acid and structural similarities, it is unclear whether these two protein families have similar catalytic mechanisms. In addition to the LC-ESI-MS assay, we further monitored RPH-Bc activity by measuring the generation of free P_i. Steady-state kinetic constants generated using this orthogonal assay were analogous to values obtained with the mass spectrometry method described above (TABLE 4-5), confirming stoichiometric production of RIF-P and P_i by RPH-Bc (FIGURE 4-1). With this assay, RPHs were also assayed for PEP synthase activity and all RPHs failed to phosphorylate pyruvate and showed no PEP synthase activity.

A sequence alignment of the region surrounding the catalytic His residue from PEP synthase and related (structurally and mechanistically) enzymes identified a conserved motif T-X-X-G-G-X-X-X-H; the conserved His is required for formation of a phospho-enzyme intermediate (FIGURE 4-10). A similar motif was found in the RPH family of enzymes fewer than 50 amino acids away from the C-terminus of the protein (FIGURE 4-6 and FIGURE 4-10). A His-827-Ala mutant of RPH-Bc failed to confer RIF resistance in *E. coli* and the enzyme had no *in vitro* enzymatic activity (TABLE 4-4 and FIGURE 4-10). Together, these results suggest that RPH is mechanistically related to PEP synthase, likely using a phosphohistidine (H827) intermediate during catalysis despite having architectural differences with the metabolic enzyme.

A

```
2OLS                408- ASAIVTNRGGRTCHAAIIARE -428
2E28                527- AAAIITEEGGLTSHAAVVGLS -547
2HRO                176- VQGFVTNIGGRTSHSAIMSRS -296
1DIK                441- AEGILTVRGGMTSHAAVVARG -461
1VBG                444- AVGILTERGGMTSHAAVVARG -464
2XOS                469- ACGILTARGGMTSHAAVVARG -589
1ZYM                175- VLGFITDAGGRTSHTSIMARS -295
PPSA (E. coli)      407- ASAIVTNRGGRTCHAAIIARE -427
PPS                 555- IKACVTGVGGVMSHAAIVCRE -575
RPH-Bc              813- IKGLVTEVGGLMTHGAVIARE -833
```

T-X-X-G-G-X-X-X-H

B

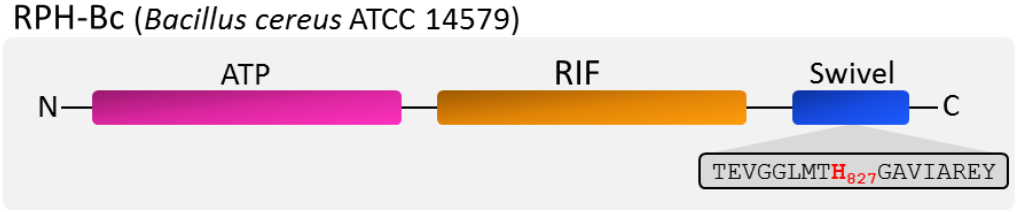

C

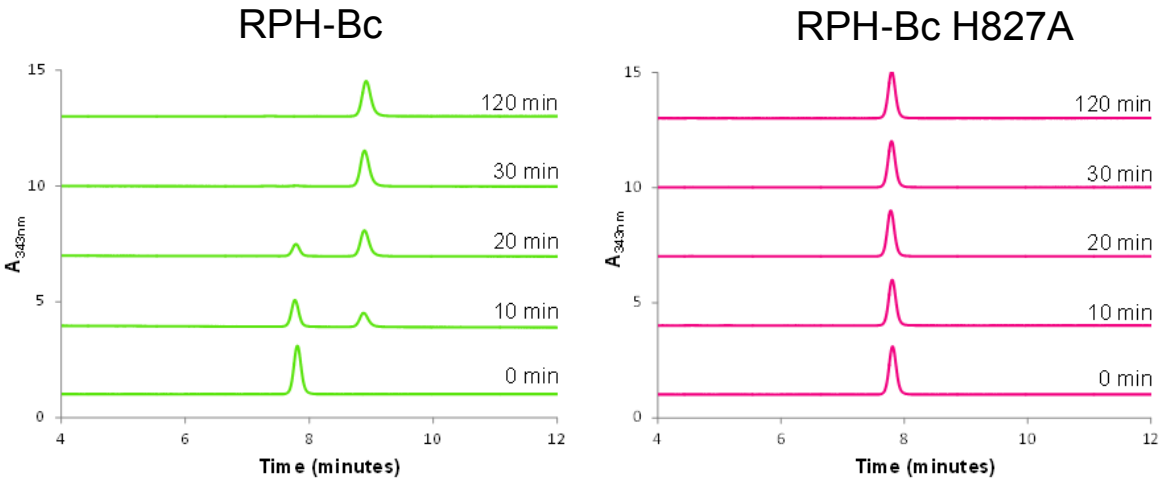

FIGURE 4-10. Characterization of mutant RPH-Bc-H827A. (A) Alignment of amino acids surrounding the catalytic histidine from the catalytic domains of various proteins identifies a conserved motif. PPS, phenylphosphate synthase from *Thauera aromatic* (Schmeling et al., 2004). (B) Histidine-827 from RPH-Bc was mutated to an alanine. (C) HPLC chromatograms comparing the activities of RPH-Bc and RPH-Bc-H827A.

TABLE 4-5. Steady-state kinetic characterization of various RPH enzymes.

Enzyme	Substrate	K_m (μM)	k_{cat} (s^{-1})	k_{cat}/K_m (s^{-1} M^{-1})
RPH-Ss	RIF	0.12 ± 0.04	0.53 ± 0.03	4.42×10^6
	ATP	11.1 ± 1.6		4.79×10^4
RPH-Bc	RIF	0.13 ± 0.05	0.80 ± 0.07	6.15×10^6
	ATP	50.8 ± 4.4		1.57×10^4
RPH-Lm	RIF	0.27 ± 0.03	1.03 ± 0.07	3.81×10^6
	ATP	27.2 ± 4.5		3.79×10^4
RPH-Bc*	ATP	95.3 ± 2.2	0.23 ± 0.02	2.41×10^3

* Assayed using the EnzChek phosphate assay kit.

DISCUSSION

The genetic reservoirs of antibiotic resistance and their regulation are poorly understood. We and others have shown that non-pathogenic environmental bacteria harbor an extensive and ancient resistome that is the likely source of resistance elements circulating in pathogens today (D'Costa et al., 2006; D'Costa et al., 2011; Bhullar et al., 2012; Forsberg et al., 2012). The regulation of resistance genes by target antibiotics has been shown in only a few cases, for example the induction of the efflux protein TetA by tetracycline (Tc) binding to TetR and the complex regulation of beta-lactam resistance by these antibiotics in *Staphylococcus aureus* (Hawkins et al., 1984; Llarrull et al., 2009). In this study we characterize a new family of rifamycin resistance enzymes along with a conserved RIF-associated *cis* regulatory element, the RAE, which is shared amongst genes encoding various RIF-inactivating enzymes from actinomycetes. The RAE is composed of a 19 nucleotide IR that is essential for modulating gene expression. Additional work is required to reveal details of the induction mechanism associated with this RAE and to determine if any additional regulators are involved.

Such IR DNA motifs have long been linked to gene regulation and often interact with protein regulators. One of the best studied examples of IR motifs involved in transcriptional regulation is from the Tc resistance gene pair of *tetA* and *tetR* (Cuthbertson and Nodwell, 2013). The TetA protein is an antiporter membrane protein that couples the efflux of Tc antibiotics with the import of H^+. Expression of *tetA* is tightly regulated by the divergent gene *tetR*, which encodes the Tc repressor protein. In the absence of Tc, TetR forms a complex with an IR operator sequence upstream of both

the *tetA* and *tetR* ORFs, blocking the promoters and thus repressing expression of the corresponding proteins. TetR has a high affinity for Tc and when Tc enters the cell it will bind TetR, causing a conformation change in the protein and loss of affinity for the IR operator sequence. This exposes the promoter of the *tetA* gene, allowing the expression of the efflux protein, resulting in Tc resistance. The IR of the RAE may play a similar role as an operator regulating transcription through a DNA-binding protein such as TetR. An examination of the divergent ORFs associated with RIF inactivating genes (and the RAE) did not reveal any associated conserved ORFs or transcriptional regulators. However, it is possible that the transcriptional regulatory protein responsible for inducing gene expression downstream of the RAE is located elsewhere in the genome.

In addition to the genes encoding the RIF inactivating enzymes, we also demonstrated that other genes are strongly associated with the RAE. These include two distinct proteins predicted to encode helicases. Since they are associated with the RAE, we expect the expression of these helicases to be induced in the presence of RIF and must have an evolutionary role in the Actinomycetes response to RIF. Further work is required to determine the roles of these proteins. For over two decades a number of actinomycetes have been reported to inactivate RIF by phosphorylation, however, the gene encoding the RPH was not known (Yazawa et al., 1994). Our observation of the strong correlation of the RAE with various actinomycete genes known to encode RIF inactivating enzymes suggested a common regulatory mechanism and an entry point to discover the *rph* gene. Indeed, we successfully identified and validated that a gene predicted to encode a PEP synthase was in fact the *rph*. The RPH enzyme does not show

similarity to any previously identified antibiotic phosphotransferases. Instead, RPH is related to the multidomain gluconeogenic enzyme PEP synthase. Although RPH and PEP synthase differ in overall domain architectures, RPH enzymes have been routinely annotated as PEP synthases from sequenced genomes. Therefore, RPH represents a previously unexplored and misannotated protein family. Kinetic analysis and site-directed mutagenesis confirmed the RPH enzyme is mechanistically related to PEP synthase and does not use pyruvate as a substrate. A search of CDART has demonstrated this protein family is widely distributed across bacteria and these enzymes are likely not involved in gluconeogenesis and may have diverse functions, including antibiotic resistance. Additional work is required to decipher their substrates and functions.

RPH orthologs from actinomycetes are colocalized with the RAE. However, the majority of RPHs are found in other Gram positive genera. Interestingly, many of these Gram positives have a RIF-sensitive phenotype. Of particular concern are the orthologs of *rph* that are found within the genomes of pathogens such as *B. anthracis*, *B. cereus* and *L. monocytogenes*. Heterologous expression and *in vitro* enzyme assays confirmed these are *bona fide* RPHs and not PEP synthases and confer high-level and broad spectrum resistance with equivalent competence to their Streptomycete counterparts. This unexpected diversity and prevalence of *rph* genes in a number of bacterial genera is troubling given the renewed interest in expanding the application of these antibiotics outside their use in mycobacterial infections (Huang and DuPont, 2005; Murphy et al., 2006; Rothstein et al., 2007; Cremonini and Lembo, 2012)

Antibiotic resistance genes that do not normally confer resistance for their native host, but are proficient at conferring resistance when expressed in an alternate host are called silent resistance genes (Dantas and Sommer, 2012). The majority of *rph* genes are not from actinomycetes and are not associated with the RAE. Therefore, these bacteria cannot respond to RIF and activate gene expression accordingly. We speculate these non-actinomycete *rph* genes are evolutionary related to *rph*s from actinomycetes but have an alternate function in their native host, which is not associated with antibiotic resistance. Their ability to bind and phosphorylate rifamycins is possibly due to structural similarities with their natural substrates. Silent resistance genes have thus far been largely underappreciated, likely because of their inability to confer an antibiotic resistance phenotype in their native host. Recently, functional metagenomics have revealed numerous novel resistance genes and continued research in this area is likely to uncover additional genes (Torres-Cortes et al., 2011; McGarvey et al., 2012; Pehrsson et al., 2013).

This work has established that RPH enzymes do not discriminate between various rifamycins, and effectively inactivate natural product and semisynthetic derivatives of this family equally. Understanding the molecular interactions between RPH and rifamycin substrates will provide the basis for generating rifamycin analogues that are not susceptible to these enzymes.

CHAPTER FIVE

RESISTANCE-GUIDED DISCOVERY OF ANSAMYCIN NATURAL PRODUCTS

CHAPTER FIVE PREFACE

Sections of the research presented in this chapter have been previously published in:

> Thaker, M.N., Wang, W., Spanogiannopoulos, P., Waglechner, N., King, A.M., Medina, R., and G.D. Wright. 2014. Identifying producers of antibacterial compounds by screening for antibiotic resistance. *Nature Biotechnology*. 31(10):922-927.
>
>

I conducted the majority of the research described in this chapter. Nick Waglechner is credited with the phylogenetic analysis of AHBA synthase.

Acknowledgements:

I am grateful to Dr. Xiao Dong Wang for the isolation of RIF-resistant actinomycete isolates. I thank Dr. Kalinka Koteva for assistance with mass spectrometry analysis.

ABSTRACT

Ansamycins are a family of structurally and biologically diverse of natural products produced by actinomycetes, some of which have experienced great therapeutic success. Due to the clinical importance and diversity of this natural product family, there is desire to discover novel ansamycins. We have developed a new screening method to enrich for ansamycin producing bacteria from the environment. This approach uses rifampin (RIF) resistance as an initial discriminating filter, followed by PCR for an essential and highly conserved gene involved in the biosynthesis of 3-amino-5-hydroxybenzoic acid (AHBA), a precursor to all ansamycins. We successfully identified 16 unique potential ansamycin producers from a screen of 213 RIF-resistant soil isolates. We conducted a phylogenetic analysis of the 16 newly identified AHBA synthases along with 7 from known ansamycin biosynthetic gene clusters. From our phylogenetic analysis we identified four isolates that produce rifamycin antibiotics. Furthermore, one isolate was shown to be a geldanamycin producer. A number of AHBA synthases were identified that did not cluster with any of the known sequences, suggesting they may be involved in the biosynthesis of novel ansamycins. We have demonstrated that this resistance-guided approach increases the probability of identifying ansamycin producing bacteria and continued efforts will likely lead to the discovery of novel ansamycin natural products.

INTRODUCTION

Natural products derived from bacteria are a rich source of therapeutically important drugs, including antibiotics (Berdy, 2012). In the past decade, 80 percent of new antibiotic chemical scaffolds that entered the clinic were from bacterial natural products (Wright, 2012). Although bacteria have been a great source of antibiotics over that past 70 years, a major problem of antibiotic discovery is the rediscovery of known antibiotics. Traditional methodologies of screening bacterial fermentation broths have yielded diminished returns, resulting in a withdrawal by pharmaceutical companies in antibiotic discovery research programs (Baltz, 2006). Today, the discovery and approval of novel antibiotics has stagnated and it has even been suggested that we will soon be entering the post-antibiotic era, a scenario with rampant multi-drug resistant pathogens and no available effective antibiotics (Alanis, 2005).

The ansamycins are a family of structurally and biologically diverse natural products with antibacterial (i.e. rifamycins) and anticancer (i.e. geldanamycin, mitomycin) properties (TABLE 5-1). These natural products share a core aromatic moiety, either benzenic or naphthalenic, which is bridged at nonadjacent positions by an aliphatic ansa chain through an amide linkage (FIGURE 1-2) (Kang et al., 2012). Ansamycins are synthesized by type I modular polyketide synthases (PKS) (Floss and Yu, 2005). The aromatic core of the ansamycins is derived from 3-amino-5-hydroxybenzoic (AHBA), which is synthesized via the amino-shikimate biosynthetic pathway (Floss et al., 2011). AHBA synthase is a key enzyme in the synthesis of AHBA, involved early in transamination and the final step of aromatization (FIGURE 1-7) (Floss et al., 2011). Due

to the indispensability and high sequence conservation of AHBA synthase, this gene has routinely been used as a marker to identify ansamycin biosynthetic gene clusters from genomic (cosmid) libraries (August et al., 1998). Furthermore, the AHBA synthase gene has been a target of PCR screens of soil isolates for the identification of potential ansamycin producers. For example, a study by Huitu *et al*. used a high-throughput PCR method to screen a collection of 2000 randomly isolated soil actinomycetes for the AHBA synthase gene (Huitu et al., 2009). A total of 33 AHBA-positive isolates were identified, which included 26 unique AHBA synthase sequences.

Herein we describe a new methodology for increasing the likelihood of identifying potential ansamycin producing actinomycetes. Using a RIF resistance selection filter, followed by PCR screening for the AHBA synthase gene, we successfully identified a diverse collection of ansamycin producing actinomycetes.

TABLE 5-1. AHBA synthases associated with ansamycin biosynthesis.

Ansamycin	Structure	AHBA Synthase	Accession Number	Mode of Action/ Target
Rifamycin B	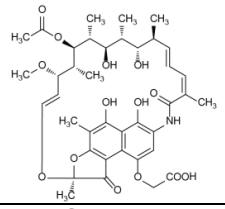	RifK	AAC01720	Antibacterial RNA polymerase
Rubradirin	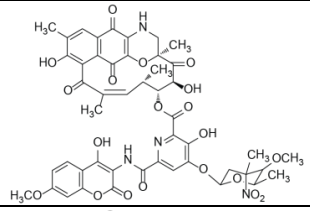	RubK	AJ871581	Antibacterial RNA polymerase and ribosome (aglycone) inhibitors
Naphthomycin A	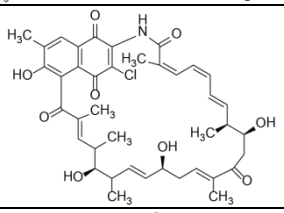	NapF	AF131877	Antibacterial and antineoplastic Fatty acid synthesis and SH-enzyme inhibitor
Ansatrienin A	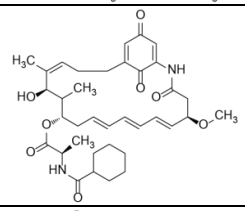	AnsF	AH007725	Anticancer Osteoclastic bone resorption inhibitor
Geldanamycin	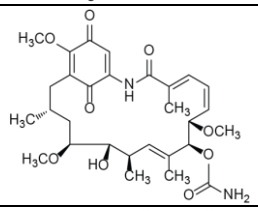	GdnA	AA015906	Anticancer HSP90 inhibitor
Ansamitocin P-3	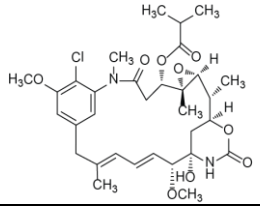	Asm24	AAM54102	Anticancer Tubulin inhibitor
Mitomycin	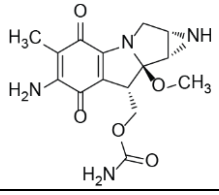	MitA	AAD32723	Anticancer DNA crosslinker

MATERIALS AND METHODS

Isolation of RIF-resistant Soil Actinomycetes

Soil isolates used in this study were from the Wright Actinomycete Collection (WAC). Isolates were derived from soil samples collected from multiple locations across Canada, Cuba, France and Nigeria. Isolation was performed as follows: 1 gram of dry weight soil was treated with dry heat, phenol or rehydrated in 9 ml of sterile water, followed my serial dilutions and plating on Streptomyces isolation media (SIM) (D'Costa et al., 2006), or humic acid vitamin agar (HVA) (Hayakawa and Nonomura, 1987) supplemented with nalidixic acid (100 µg/ml) and RIF (20 or 50 µg/ml).

AHBA Synthase Gene PCR Screen

PCR screening for the AHBA synthase gene was performed using primers AHBA-F and AHBA-R (He et al., 2006). PCR amplification of 16S rRNA and *rpoB* genes was performed as previously described (CHAPTER 2, MATERIALS AND METHODS,). A complete list of primer sequences can be found in APPENDIX 2.

Phylogenetic Analysis of AHBA Synthases

AHBA synthase phylogenetic analysis was conducted using 7 previously identified AHBA synthases from diverse ansamycin biosynthetic gene clusters (TABLE 5-1) and 16 newly identified translated AHBA synthase gene amplicons. AHBA synthase sequences were aligned with MUSCLE using default parameters and manual inspection (Edgar, 2004). This alignment included 23 different partial AHBA synthases. This

alignment served as the input for Bayesian phylogenetic analysis in MrBayes 3.2.0 using a mixed amino acid model with gamma distribution rates and a proportion of invariant sites (Ronquist et al., 2012). Initiating from random trees, two runs of chains were sampled over 5 million generations. Every 200th generation was sampled and a burn-in consisting of the first 1000 samples was discarded. The final average standard deviation of split frequencies was 0.00174, indicating that the two runs were close to convergence.

Biological Assay for Rifamycin Production

Potential rifamycin producing bacterial isolates were grown on three different solid medias for production: Bennett's, IP2 and N6 (Huitu et al., 2009). Cultures were incubated for 10 days at 30°C. Agar plugs from each culture were removed and overlaid on a lawn of *Bacillus subtilis* 168 or RIF-resistant *B. subtilis* (β-subunit H482Y mutation) (see CHAPTER 2, MATERIALS AND METHODS).

Production of Geldanamycin from WAC5038

WAC5038 was inoculated onto Bennett's agar media and incubated for at least 7 days. Agar plates were extracted with acetone overnight at 4°C. The extract was filtered to remove agar pellets and the acetone extract was dried down under reduced pressure. This resulting extract was resuspended in acetonitrile-water (50:50) and analyzed using LC-ESI-MS with an Agilent 1100 series LC system and a QTrap LC/MS/MS system. The geldanamycin standard was supplied by A.G. Scientific (San Diego, CA).

RESULTS

Screening RIF-resistant Soil Bacteria for Ansamycin Biosynthetic Potential

A hallmark of antibiotic producing bacteria is that they must possess mechanisms of resistance to the antibiotic they synthesize to avoid suicide; also called self-resistance (Cundliffe and Demain, 2010). We have been interested in RIF resistance from environmental actinomycetes and therefore have a collection of RIF-resistant actinomycetes. We were intrigued in determining the frequency of rifamycin producers from our collection.

In a previous report, Huitu et al. screened 2000 soil actinomycete isolates by PCR for the AHBA synthase gene to identify potential ansamycin producers (Huitu et al., 2009). They identified 33 positive isolates and 26 unique AHBA synthase sequences (TABLE 5-2). Their hits included 2 rifamycin producers, representing a hit rate of 1 in 1 000 (0.1%). We reasoned the hit rate of rifamycin producers could be greatly increased by first performing a RIF resistance phenotypic screen.

In addition to our previously described collection of RIF-resistant actinomycetes (APPENDIX 2), we isolated additional actinomycetes by plating soil samples directly on RIF-containing media. Following dereplication by BOX-PCR (see CHAPTER 2), we possessed a collection of 213 unique RIF-resistant actinomycetes. Potential ansamycin producers were identified by amplification of the AHBA synthase gene using PCR and AHBA gene specific degenerate primers (He et al., 2006). A positive PCR resulted in the amplification of a 750 bp product (FIGURE 5-1). We identified 16 AHBA synthase positive isolates, representing 7.5% of our RIF-resistant collection (TABLE 5-2).

FIGURE 5-1. PCR screen for the AHBA synthase gene. gDNA from 213 RIF-resistant soil actinomycete isolates was used as template for AHBA synthase gene amplification and the resulting reactions were resolved using agarose gel electrophoresis. A positive reaction amplified a 750 bp PCR product. Isolates positive for AHBA synthase genes include WAC7278 (1) and WAC7295 (2). C1 and C2 are PCR reactions using *A. mediterranei* gDNA (positive controls). C3 is a negative control.

TABLE 5-2. Number of AHBA-positive actinomycete isolates.

Study	No. of Isolates Screened	No. of AHBA synthase positive isolates	No. of unique AHBA synthase sequences (%)
Huitu *et al.*	2 000	33	26 (1.3)
This study	213	16	16 (7.5)
Fold-difference			(5.8)

Phylogenetic Analysis of AHBA Synthase

We sequenced the partial AHBA synthase gene sequences identified from our screen and using the translated sequences, constructed a phylogenetic tree to determine the diversity of AHBA synthases. We also included seven AHBA synthases from various

characterized ansamycin biosynthetic gene clusters (TABLE 5-1). Consistent with previous phylogenetic analyses of AHBA synthase, the known AHBA synthases are clearly divided into two groups; one that is involved in the biosynthesis of the benzenic ansamycins and the other with the naphthalenic ansamycins (FIGURE 5-2) (Huitu et al., 2009; Kang et al., 2012). Unexpectedly, the majority of AHBA synthases identified from our screen did not cluster with RifK, the AHBA synthase involved in rifamycin biosynthesis. Four isolates (WAC6369, WAC6767, WAC6771 and WAC7295) clustered with RifK. Two isolates (WAC5060 and WAC6356) carry AHBA synthases similar to the naphthalenic ansamycins rubradirin and naphthomycin. Five isolates (WAC5038, WAC6321, WAC5323, WAC6756 and WAC6759) are closely associated with GdnA from the geldanamycin biosynthetic gene cluster. Four isolates (WAC6321, WAC6322, WAC6781 and WA7278) carry very similar AHBA synthases but do not appear to cluster with any previously characterized enzymes. Furthermore, WAC5122 appears to carry a unique AHBA synthase. These AHBA synthases may be involved in the biosynthesis of novel ansamycins.

Ansamycin Production

We pursued validation of our phylogeny-based classification of AHBA synthase by sampling fermentation products of our isolates from various clades. For sampling of the naphthalenic ansamycins, we selected WAC6369, WAC6768, WAC6771 and WAC7295, which cluster with RifK. We inoculated solid media agar with spores derived from these isolates, grew them for 10 days and analyzed agar plugs for bioactivity. All

isolates produced significant quantities of antibiotic active against RIF-sensitive *Bacillus subtilis* but failed to inhibit the growth of RIF-resistant *B. subtilis* (*rpoB* mutant) (FIGURE 5-3). These actinomycetes strains are likely producing antibiotics that are targeting RNA polymerase (RNAP), consistent with the production of rifamycins. The rifamycin producer *A. mediterranei* is known to possess a unique RNAP that is highly resistant to rifamycin antibiotics due to a triple amino acid polymorphism (Q516, D522, and N531) within the RRDR of the β-subunit (Figure 1-5) (Floss and Yu, 2005; Tang et al., 2012). Substitutions in just one of these positions is sufficient to confer high-level rifamycin resistance (Floss and Yu, 2005). We amplified and sequenced RRDR of the *rpoB* gene from each actinomycete isolate. All isolates contained the signature triple amino acid polymorphism identical to *A. mediterranei* (FIGURE 5-4), further supporting their rifamycin production capabilities.

We next focused on the benzenic ansamycins and selected WAC5038 for follow-up studies. According to our phylogenetic analysis, WAC5038 is closely related to GdnA, which is involved in geldanamycin biosynthesis. We prepared fermentation extracts of WAC5038 and analyzed secondary metabolites using LC-ESI-MS. A natural product with a HPLC retention time, UV-visible spectrum and, *m/z* ratio consistent with geldanamycin was identified.

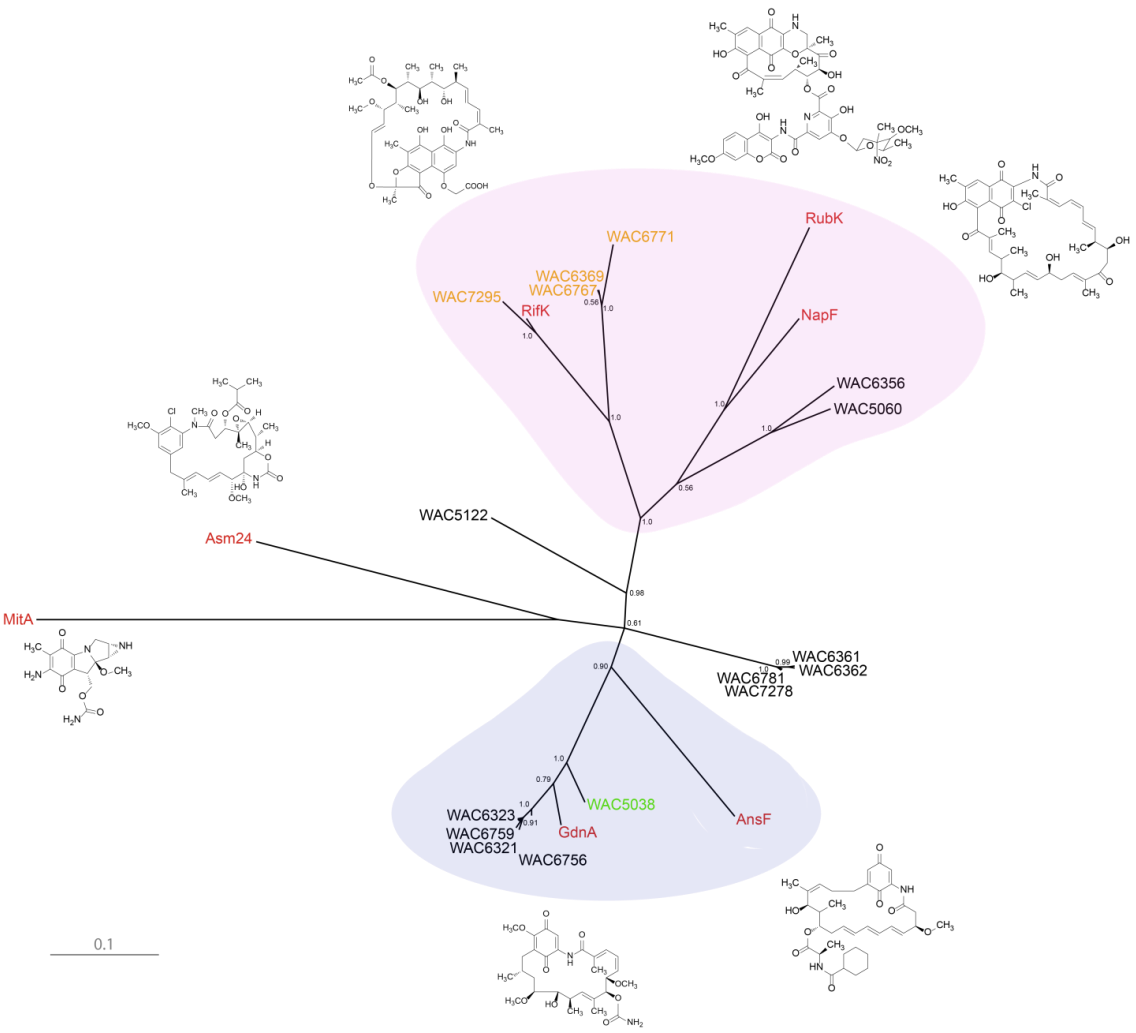

FIGURE 5-2. Phylogenetic analysis of AHBA synthase sequences. A phylogenetic analysis of partial AHBA synthases was constructed from 7 known ansamycin biosynthetic gene clusters and 16 identified in this study. The AHBA synthases are divided into two main groups according to the aromatic core moiety, benzenic (blue region) and naphthalenic (pink region). AHBA synthases in red are from characterized ansamycin biosynthetic gene clusters (TABLE 5-1). AHBA synthases highlighted in orange are those that produce rifamycin antibiotics (FIGURE 5-2 and FIGURE 5-3). The AHBA synthase in green is involved in the production of geldanamycin.

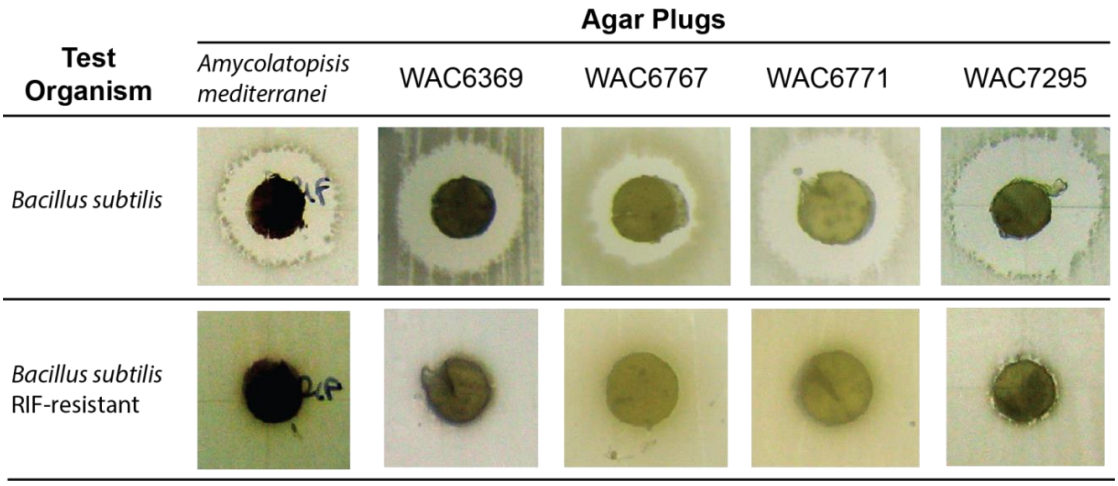

FIGURE 5-3. Rifamycin production bioassay. Agar plugs from the rifamycin producer *A. mediterranei* and putative rifamycin producers were overlaid on a lawn of RIF-sensitive *B. subtilis* and RIF-resistant *B. subtilis* (*rpoB* mutant). All strains inhibit the RIF-sensitive *B. subtilis* but fail to inhibit the RIF-resistant mutant strain.

```
E. coli          505-FFGSSQLSQFMDQNNPLSEITHKRRISALGPGG-537
M. tuberculosis     -FFGTSQLSQFMDQNNPLSGLTHKRRLSALGPGG-
S. coelicolor       -FFGTSGLSQFMDQNNPLSGLTHKRRLNALGPGG-
A. mediterranei     -FFGTSQLSQFMQQTNPIDGLTHKRRLNALGPGG-
WAC6369             -FFGTSQLSQFMQQTNPIDGLTHKRRLNALGPGG-
WAC6767             -FFGTSQLSQFMQQTNPIDGLTHKRRLNALGPGG-
WAC6771             -FFGTSQLSQFMQQTNPIDGLTHKRRLNALGPGG-
WAC7295             -FFGTSQLSQFMQQTNPIDGLTHKRRLNALGPGG-
```

FIGURE 5-4. β-subunit protein alignment from rifamycin producers. A partial region of the *rpoB* gene from each rifamycin producing isolate was amplified and sequenced. The translated sequence was aligned to reference β-subunits. Highlighted in red are the amino acid residues known to confer high-level RIF resistance in the rifamycin producer *A. mediterranei* (Floss and Yu, 2005). These positions are Q516, D522, and N531.

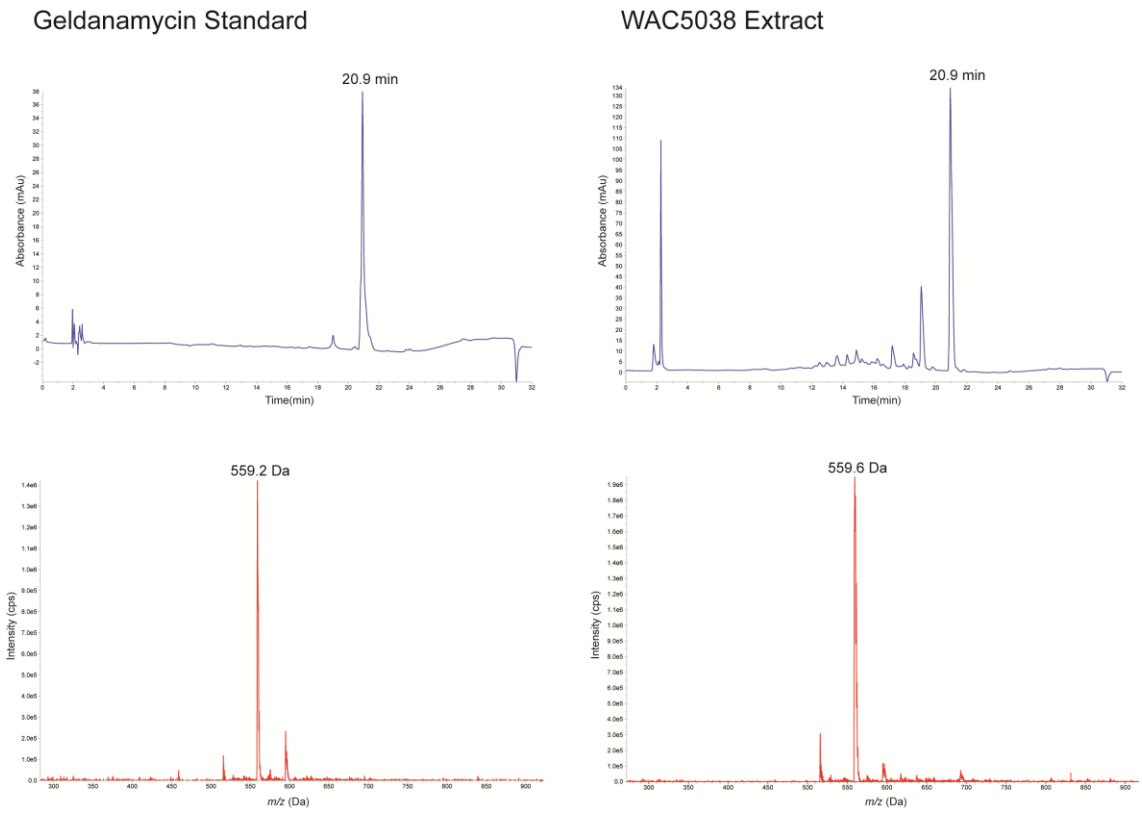

FIGURE 5-5. LC-ESI-MS analysis of geldanamycin produced by WAC5038 extract. Acetone extracts of WAC5038 grown on solid Bennett's media were analyzed using LC-ESI-MS. A natural product with a UV-visible spectrum and a molecular anion $[M-H]^-$ consistent with geldanamycin was identified. Liquid chromatography (LC) chromatograms are shown at 310 nm.

DISCUSSION

The ansamycins are a diverse family of natural products and have therapeutic importance in antibiotic therapy (e.g. rifamycins) and anticancer therapy (e.g. geldanamycin and mitomycin) (Kang et al., 2012). Therefore, there is promise in identifying novel ansamycins that may provide new drug leads. Previous studies using PCR based screening methods have shown that ansamycin producers can be identified from random sampling of soil actinomycetes at a frequency of 1.6% (Huitu et al., 2009). Herein we demonstrate that applying a RIF resistance filter prior to PCR screening will increase the hit rate of identifying ansamycin producers by 6-fold (TABLE 5-2). This approach led to the discovery of four rifamycin producers, representing a hit rate of 1.9%, compared to 0.1% without using a resistance filter. Interestingly, the majority of AHBA synthases identified were not related to rifamycin biosynthesis but represented a diverse set of ansamycin natural products, which we confirmed by identifying a geldanamycin producer. In addition to the antibacterial properties of the rifamycins, ansamycin natural products display diverse bioactivities (Table 5-1). Additional work is required to determine if there is correlation with the degree ansamycin producers show resistance to other ansamycin natural products. Another explanation could be that ansamycin producers are rare in the soil and outcompeted by abundant microbes using traditional isolation methods. The use of RIF might suppress the growth of most soil bacteria allowing the isolation of rarer species. From there isolates a number of AHBA synthases were identified that showed no relation to any previously identified enzyme. Isolates with these enzymes are prospective leads towards discovering novel ansamycins.

The resistance-guided screen approach was also applied to the vancomycin family of antibiotics (Thaker et al., 2013). By selecting vancomycin-resistant bacteria directly from soil, this study achieved a hit rate of 11%, which is dramatically enhanced in comparison to screening randomly isolated soil bacteria using PCR for vancomycin biosynthetic capabilities (0.1% hit rate). Using phylogenetics, this study was also successful at identifying a novel glycopeptide antibiotic called pekiskomycin. The extension of this method to other classes of antibiotics is likely to expand the chemical diversity of natural products and hopefully provide leads for new antibiotics and other therapeutic compounds.

CHAPTER 6

DISCUSSION AND FUTURE DIRECTIONS

DISCUSSION

Antibiotics are ancient products of environmental microorganisms, presumed to deter competitors and thus providing an advantage to the producing organism. Over millennia, neighboring bacteria evolved many diverse mechanisms to resist the noxious effects of antibiotics in order to survive. It should therefore be no surprise that contemporary environmental bacteria are multidrug resistant (D'Costa et al., 2006). The environment represents a diverse reservoir of antibiotic resistance determinants. The main concern with this environmental gene pool is bacteria's ability to horizontally transfer DNA, which could find its way into the clinic with the appropriate selection pressure. There are now a number of examples highlighting the link between resistance genes in environmental and pathogenic bacteria (Benveniste and Davies, 1973; Marshall et al., 1997; Forsberg et al., 2012). However, there is paucity of supporting evidence linking a direct transfer of antibiotic resistance genes from the environment to clinical pathogens, based on minimal sequence identity between the two.

The rifamycins are natural product antibiotics produced by actinomycetes, which have experienced great success in the clinic. Our group has demonstrated that RIF resistance is prevalent from soil actinomycetes (D'Costa et al., 2006). Furthermore, we have shown that many of these isolates are capable of inactivating RIF (D'Costa et al., 2006; Spanogiannopoulos et al., 2012). These RIF inactivating enzymes are of particular concern because their corresponding genes have the potential to be mobilized. The emergence of these RIF resistance genes into clinically relevant bacteria would threaten the efficacy of this entire family of antibiotics. With an increase of RIF usage, along with

a renewed interest in the rifamycin scaffold for the development of derivatives against a broader repertoire of bacterial pathogens, it is likely there be an increase in the frequency and diversity of resistance determinants surfacing in the clinic. For example, *arr*, encoding a RIF-inactivating ADP-ribosyltransferase, was initially discovered from *Mycobacterium smegmatis*, a normally benign soil actinomycete (Morisaki et al., 1995; Quan et al., 1999). However, this gene is now mobile and found on a variety of transmissible genetic elements clustered with other antibiotic resistance genes from a number of pathogens (Arlet et al., 2001; Houang et al., 2003; da Fonseca et al., 2008). More troubling, the Arr enzyme has broad substrate specificity and is effective at inactivating all clinically approved rifamycins (Baysarowich et al., 2008).

The main goal of this dissertation was to explore the rifamycin resistome from environmental bacteria, as it has evolved over millennia, with particular focus on unidentified resistance genes encoding RIF-inactivating enzymes. Herein, we have identified the *rgt* and *rph* genes, encoding a RIF-inactivating glycosyltransferase and phosphotransferase respectively. We have demonstrated that that both genes are capable of conferring high-level and broad RIF resistance when expressed in a heterologous host. Orthologs of RGT are distributed across actinomycete genomes. Interestingly, orthologs of RPH are much more widely distributed. In addition to actinomycetes, RPHs are found in many Gram positive bacteria, including pathogens. Using heterologous expression and enzyme assays with purified RPHs, we have verified orthologs from *B. cereus* and *L. monocytogenes* confer RIF resistance. However, these nonactinomycete Gram positives display a RIF-sensitive phenotype, highlighting the existence of a 'silent' rifamycin

resistome. These enzymes likely have alternate functions in their respective host and their ability to confer RIF resistance when overexpressed is perhaps an artifact of their ancestral relatedness (FIGURE 6-1). These silent resistance enzymes may be the link between antibiotic resistance enzymes found in the environment and those from pathogens. A mutation affecting the expression of *rph* or mobilization of *rph* to another host would enable this silent gene to confer antibiotic resistance (FIGURE 6-1).

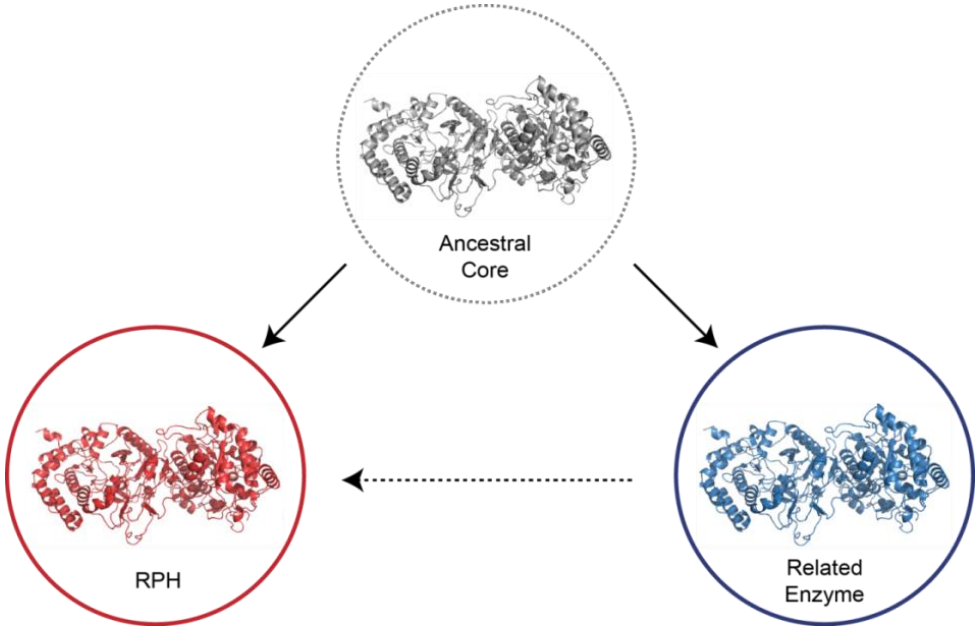

FIGURE 6-1. Genomic enzymology of RPH. RPH (red) and 'silent' RPH (blue) share a common ancestral protein. The silent RPH is able to confer RIF resistance, however it is not expressed. A change in gene expression affecting expression of the silent *rph* gene, such as a mutation in the promoter, would allow the host to survive in the presence of RIF.

This study has identified two genes that threaten the clinical efficacy of rifamycin antibiotics. Although these resistance genes have not yet emerged into the clinic, they should be included in antibiotic resistance gene surveillance programs. This study serves as a warning that rifamycin resistance determinants are widespread in environmental and clinically relevant bacteria. Of course, antibiotic use selects for resistance, therefore we should consider prudent administration programs for the rifamycins.

A number of strategies have been used in the past to lengthen the clinical shelf life of particular antibiotics threatened by resistance. Considering the decline of new antibiotics entering the clinic, attention has been focused on identifying antibiotic adjuvants that would revive the utility of our classic antibiotics (Kalan and Wright, 2011). The co-administration of antibiotic and inactivating enzyme inhibitor has experienced success in the clinic, exemplified by Augmentin, amoxicillin (β-lactam) and clavulanate (β-lactamase inhibitor) (White et al., 2004). This approach may be useful in preventing the dissemination of rifamycin-inactivating enzymes. There are a number of glycosyltransferase inhibitors, of both natural product and synthetic origin, that have been identified in the literature, and would be a good starting point for finding RGT inhibitors (Schutzbach and Brockhausen, 2009). Recently, a number of flavone small molecules were discovered to inhibit PPDK from *Clostridium symbiosum* by binding to the ATP-grasp domain, which is structurally and mechanistically related to RPH (Wu et al., 2013) (FIGURE 4-6). We may expect these inhibitors to also inhibit RPH activity.

As discussed in CHAPTER 5, we used a novel screening approach using RIF resistance as a selection filter followed by diagnostic PCR screening to identify potential

ansamycin producers. Considering the therapeutic success of ansamycin natural products, the continued discovery of novel ansamycins may lead to new clinical candidates. We have succeeded in identifying many potential ansamycin producers. Follow up experiments have showed that a number of our isolates are producers of rifamycin antibiotics. A number of rifamycin derivatives have been previously reported from various actinomycetes (Floss and Yu, 2005; Kang et al., 2012). Assuming antibiotics are products of a chemical arms race between bacteria in the environment, there is a possibility that nature has selected for a rifamycin derivative that is not susceptible to enzymatic inactivation. Indeed, the discovery of the naturally produced carbapenem thienamycin inspired the generation of β-lactams antibiotics that evaded inactivation by β-lactamases and have been very successful in the clinic (Kahan et al., 1983). Tolypomycin Y, which was reported in the literature in the late 1960s as a product of *Amycolatopsis tolypomycina*, is a rifamycin derivative with a cyclopropane on the ansa bridge adjacent to the C-21 and C-23 hydroxyls (FIGURE 6-2) (Kishi et al., 1969; Kondo et al., 1972). It would be interesting to determine if tolypomycin Y evades modification by the various rifamycin inactivating enzymes. Identifying new rifamycin antibiotics in nature could inspire or provide leads for resistance-proof antibiotics.

The use of semisynthesis has been a successful strategy for designing antibiotics that evade resistance. This approach has focused on the addition of chemical groups to an antibiotic scaffold that prevent resistance enzymes from binding. The first such example was the semisynthetic β-lactam methicillin, which evaded inactivation by penicillinases (Sheehan, 1967). In addition, a number of semisynthetic aminoglycosides

have been developed that evade aminoglycoside modifying enzymes (Shi et al., 2013). The generation of such resistance-proof antibiotics continues to be the focus of many drug development programs. The development of rifamycin derivatives that evade rifamycin inactivating enzymes should be useful if these enzymes become prevalent in pathogenic bacteria. Recently, scientists at Cumbre Pharmaceuticals developed a series of rifamycin derivatives substituted at the C-25 position, which retained activity against bacteria expressing Arr (FIGURE 6-2) (Combrink et al., 2007). These derivatives should also be tested to determine if they retain activity against bacteria expressing *rgt* or *rph*.

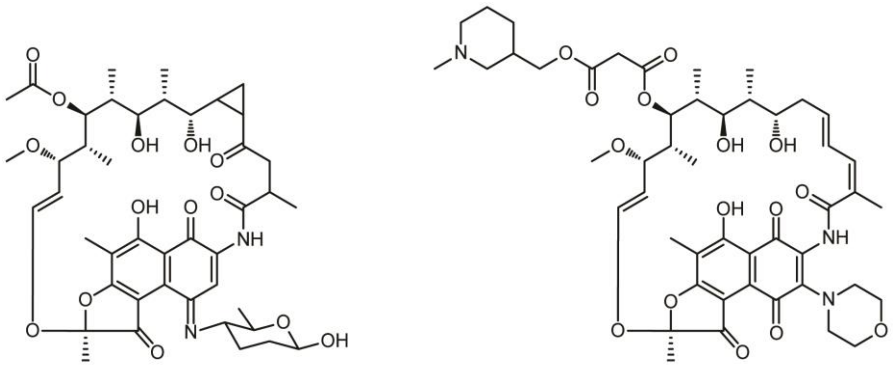

FIGURE 6-2. Structures of tolypomycin Y and CGP 4832.

In this study we describe a novel bioinformatics approach used to identify antibiotic resistance genes. A conserved regulatory motif, the RAE, was found associated with all RIF-inactivating enzymes from the actinomycete group of bacteria and this motif led the identification of the *rph* gene. The mechanism of gene regulation is unknown but appears to be conserved across *Streptomyces* spp. (FIGURE 4-6).

Furthermore, a number of other genes appear to be associated with the RAE, which encode putative helicases. Deciphering the mechanism of gene induction and the role of these putative helicases will reveal how soil bacteria have evolved to sense and respond to rifamycins in the environment, providing details about the evolution of antibiotic resistance. Additionally, the approach of using conserved regulatory motifs to interrogate gene function might also be promising for identifying other antibiotic resistance determinants or studying bacteria's regulatory response to antibiotics.

FUTURE DIRECTIONS

1. Determine the mechanism of RAE induction.
2. Investigate the role of the two putative helicase proteins in response to RIF.
3. Obtain crystals structures of RGT and RPH in complex with RIF.
4. Identify potential ansamycin and rifamycin natural products and corresponding biosynthetic gene clusters.

CONCLUDING REMARKS

We are losing the battle against pathogenic bacteria due to the rise in antibiotic resistance and the abating number of new antibiotics entering the clinic. Identifying and characterizing the antibiotic resistome will reveal the true vulnerability of our current antibiotic arsenal and provide insight for future drug development programs. This strategy will place us ahead of antibiotic resistance. We have expanded the rifamycin resistome and this information should be a warning of what we may encounter in the not so distant future.

REFERENCES

Abraham, E. P. and Chain, E. (1940). An Enzyme from Bacteria able to Destroy Penicillin. Nature. 146837.

Alanis, A. J. (2005). Resistance to antibiotics: are we in the post-antibiotic era? Arch Med Res. 36(6): 697-705.

Alekshun, M., Kashlev, M. and Schwartz, I. (1997). Molecular cloning and characterization of *Borrelia burgdorferi rpoB*. Gene. 186(2): 227-235.

Allen, H. K., Moe, L. A., Rodbumrer, J., Gaarder, A. and Handelsman, J. (2009). Functional metagenomics reveals diverse beta-lactamases in a remote Alaskan soil. ISME J. 3(2): 243-251.

Altschul, S. F., Gish, W., Miller, W., Myers, E. W. and Lipman, D. J. (1990). Basic local alignment search tool. J Mol Biol. 215(3): 403-410.

Altschul, S. F., Madden, T. L., Schaffer, A. A., Zhang, J., Zhang, Z., Miller, W. and Lipman, D. J. (1997). Gapped BLAST and PSI-BLAST: a new generation of protein database search programs. Nucleic Acids Res. 25(17): 3389-3402.

Andersen, S. J., Quan, S., Gowan, B. and Dabbs, E. R. (1997). Monooxygenase-like sequence of a *Rhodococcus equi* gene conferring increased resistance to rifampin by inactivating this antibiotic. Antimicrob Agents Chemother. 41(1): 218-221.

Aristoff, P. A., Garcia, G. A., Kirchhoff, P. D. and Hollis Showalter, H. D. (2010). Rifamycins--obstacles and opportunities. Tuberculosis (Edinb). 90(2): 94-118.

Arlet, G., Nadjar, D., Herrmann, J. L., Donay, J. L., Lagrange, P. H. and Philippon, A. (2001). Plasmid-mediated rifampin resistance encoded by an *arr-2*-like gene cassette in *Klebsiella pneumoniae* producing an ACC-1 class C beta-lactamase. Antimicrob Agents Chemother. 45(10): 2971-2972.

Artsimovitch, I., Vassylyeva, M. N., Svetlov, D., Svetlov, V., Perederina, A., Igarashi, N., Matsugaki, N., Wakatsuki, S., Tahirov, T. H. and Vassylyev, D. G. (2005). Allosteric modulation of the RNA polymerase catalytic reaction is an essential component of transcription control by rifamycins. Cell. 122(3): 351-363.

August, P. R., Tang, L., Yoon, Y. J., Ning, S., Muller, R., Yu, T. W., Taylor, M., Hoffmann, D., Kim, C. G., Zhang, X., Hutchinson, C. R. and Floss, H. G. (1998). Biosynthesis of the ansamycin antibiotic rifamycin: deductions from the molecular analysis of the rif biosynthetic gene cluster of *Amycolatopsis mediterranei* S699. Chem Biol. 5(2): 69-79.

Baltz, R. H. (2006). Marcel Faber Roundtable: is our antibiotic pipeline unproductive because of starvation, constipation or lack of inspiration? J Ind Microbiol Biotechnol. 33(7): 507-513.

Bass, J. B., Jr., Farer, L. S., Hopewell, P. C., O'Brien, R., Jacobs, R. F., Ruben, F., Snider, D. E., Jr. and Thornton, G. (1994). Treatment of tuberculosis and tuberculosis infection in adults and children. American Thoracic Society and The Centers for Disease Control and Prevention. Am J Respir Crit Care Med. 149(5): 1359-1374.

Bass, N. M., Mullen, K. D., Sanyal, A., Poordad, F., Neff, G., Leevy, C. B., Sigal, S., Sheikh, M. Y., Beavers, K., Frederick, T., Teperman, L., Hillebrand, D., Huang, S., Merchant, K., Shaw, A., Bortey, E. and Forbes, W. P. (2010). Rifaximin treatment in hepatic encephalopathy. N Engl J Med. 362(12): 1071-1081.

Baysarowich, J., Koteva, K., Hughes, D. W., Ejim, L., Griffiths, E., Zhang, K., Junop, M. and Wright, G. D. (2008). Rifamycin antibiotic resistance by ADP-ribosylation: Structure and diversity of Arr. Proc Natl Acad Sci U S A. 105(12): 4886-4891.

Bentley, S. D., Chater, K. F., Cerdeno-Tarraga, A. M., Challis, G. L., Thomson, N. R., James, K. D., Harris, D. E., Quail, M. A., Kieser, H., Harper, D., Bateman, A., Brown, S., Chandra, G., Chen, C. W., Collins, M., Cronin, A., Fraser, A., Goble, A., Hidalgo, J., Hornsby, T., Howarth, S., Huang, C. H., Kieser, T., Larke, L., Murphy, L., Oliver, K., O'Neil, S., Rabbinowitsch, E., Rajandream, M. A., Rutherford, K., Rutter, S., Seeger, K., Saunders, D., Sharp, S., Squares, R., Squares, S., Taylor, K., Warren, T., Wietzorrek, A., Woodward, J., Barrell, B. G., Parkhill, J. and Hopwood, D. A. (2002). Complete genome sequence of the model actinomycete *Streptomyces coelicolor* A3(2). Nature. 417(6885): 141-147.

Benveniste, R. and Davies, J. (1973). Aminoglycoside antibiotic-inactivating enzymes in actinomycetes similar to those present in clinical isolates of antibiotic-resistant bacteria. Proc Natl Acad Sci U S A. 70(8): 2276-2280.

Berdy, J. (2005). Bioactive microbial metabolites. J Antibiot (Tokyo). 58(1): 1-26.

Berdy, J. (2012). Thoughts and facts about antibiotics: where we are now and where we are heading. J Antibiot (Tokyo). 65(8): 385-395.

Bergamini, N. and Fowst, G. (1965). Rifamycin SV. A review. Arzneimittelforschung. 15(8): Suppl:951-1002.

Bhullar, K., Waglechner, N., Pawlowski, A., Koteva, K., Banks, E. D., Johnston, M. D., Barton, H. A. and Wright, G. D. (2012). Antibiotic resistance is prevalent in an isolated cave microbiome. PLoS One. 7(4): e34953.

Bolam, D. N., Roberts, S., Proctor, M. R., Turkenburg, J. P., Dodson, E. J., Martinez-Fleites, C., Yang, M., Davis, B. G., Davies, G. J. and Gilbert, H. J. (2007). The crystal structure of two macrolide glycosyltransferases provides a blueprint for host cell antibiotic immunity. Proc Natl Acad Sci U S A. 104(13): 5336-5341.

Bortoluzzi, A., Muskett, F. W., Waters, L. C., Addis, P. W., Rieck, B., Munder, T., Schleier, S., Forti, F., Ghisotti, D., Carr, M. D. and O'Hare, H. M. (2013). *Mycobacterium tuberculosis* RNA polymerase-binding protein A (RbpA) and its interactions with sigma factors. J Biol Chem. 288(20): 14438-14450.

Brufani, M., Fedeli, W., Giacomello, G. and Vaciago, A. (1964). The x-ray analysis of the structure of rifamycin B. Experientia. 20(6): 339-342.

Calvori, C., Frontali, L., Leoni, L. and Tecce, G. (1965). Effect of rifamycin on protein synthesis. Nature. 207(995): 417-418.

Campbell, E. A., Korzheva, N., Mustaev, A., Murakami, K., Nair, S., Goldfarb, A. and Darst, S. A. (2001). Structural mechanism for rifampicin inhibition of bacterial rna polymerase. Cell. 104(6): 901-912.

Casali, N., Nikolayevskyy, V., Balabanova, Y., Harris, S. R., Ignatyeva, O., Kontsevaya, I., Corander, J., Bryant, J., Parkhill, J., Nejentsev, S., Horstmann, R. D., Brown, T. and Drobniewski, F. (2014). Evolution and transmission of drug-resistant tuberculosis in a Russian population. Nat Genet. 46(3): 279-286.

Cavusoglu, C., Karaca-Derici, Y. and Bilgic, A. (2004). In-vitro activity of rifabutin against rifampicin-resistant *Mycobacterium tuberculosis* isolates with known *rpoB* mutations. Clin Microbiol Infect. 10(7): 662-665.

Chevreux, B., Wetter, T., Suhai, S. (1999). Genome sequence assembly using trace signals and addiional sequence information. . Proceedings of the German Conference on Bioinformatics (GCB), Universitat Trier, Hanover, Germany

CLSI (2012). Methods for dilution antimicrobial susceptibility testing of bacteria that grow aerobically. Wayne, PA.

Comas, I., Borrell, S., Roetzer, A., Rose, G., Malla, B., Kato-Maeda, M., Galagan, J., Niemann, S. and Gagneux, S. (2012). Whole-genome sequencing of rifampicin-

resistant *Mycobacterium tuberculosis* strains identifies compensatory mutations in RNA polymerase genes. Nat Genet. 44(1): 106-110.

Combrink, K. D., Denton, D. A., Harran, S., Ma, Z., Chapo, K., Yan, D., Bonventre, E., Roche, E. D., Doyle, T. B., Robertson, G. T. and Lynch, A. S. (2007). New C25 carbamate rifamycin derivatives are resistant to inactivation by ADP-ribosyl transferases. Bioorg Med Chem Lett. 17(2): 522-526.

Cooper, M. A. and Shlaes, D. (2011). Fix the antibiotics pipeline. Nature. 472(7341): 32.

Cooper, R. A. and Kornberg, H. L. (1967). The mechanism of the phosphoenolpyruvate synthase reaction. Biochim Biophys Acta. 141(1): 211-213.

Cox, G., Koteva, K. and Wright G.D. (2014). An unusual class of anthracyclines potentiate Gram-postive antibiotics in intrisnically resistant Gram-negative bacteria. J. Antimicrob. Chemothear. 2014. 69(7):1844-1855.

Coutinho, P. M., Deleury, E., Davies, G. J. and Henrissat, B. (2003). An evolving hierarchical family classification for glycosyltransferases. J Mol Biol. 328(2): 307-317.

Cremonini, F. and Lembo, A. (2012). Rifaximin for the treatment of irritable bowel syndrome. Expert Opin Pharmacother. 13(3): 433-440.

Crooks, G. E., Hon, G., Chandonia, J. M. and Brenner, S. E. (2004). WebLogo: a sequence logo generator. Genome Res. 14(6): 1188-1190.

Cundliffe, E. and Demain, A. L. (2010). Avoidance of suicide in antibiotic-producing microbes. J Ind Microbiol Biotechnol. 37(7): 643-672.

Cunha, B. A. (2004). The cause of the plague of Athens: plague, typhoid, typhus, smallpox, or measles? Infect Dis Clin North Am. 18(1): 29-43.

Cuthbertson, L. and Nodwell, J.R. The TetR family of regulators. (2013). Microbiol. Mol. Biol. Rev. 77(3):440-475.

D'Costa, V. M., King, C. E., Kalan, L., Morar, M., Sung, W. W., Schwarz, C., Froese, D., Zazula, G., Calmels, F., Debruyne, R., Golding, G. B., Poinar, H. N. and Wright, G. D. (2011). Antibiotic resistance is ancient. Nature. 477(7365): 457-461.

D'Costa, V. M., McGrann, K. M., Hughes, D. W. and Wright, G. D. (2006). Sampling the antibiotic resistome. Science. 311(5759): 374-377.

da Fonseca, E. L., Freitas Fdos, S., de Amorim, J. C. and Vicente, A. C. (2008). Detection of new *arr-4* and *arr-5* gene cassettes in clinical *Pseudomonas aeruginosa* and *Klebsiella pneumoniae* strains from Brazil. Antimicrob Agents Chemother. 52(5): 1865-1867.

Dabbs, E. R. (1987). Rifampicin inactivation by *Rhodococcus* and *Mycobacterium* species. FEMS Microbiology Letters. 44(3): 395-399.

Dabbs, E. R., Yazawa, K., Mikami, Y., Miyaji, M., Morisaki, N., Iwasaki, S. and Furihata, K. (1995). Ribosylation by mycobacterial strains as a new mechanism of rifampin inactivation. Antimicrob Agents Chemother. 39(4): 1007-1009.

Dabbs, E. R., Yazawa, K., Tanaka, Y., Mikami, Y., Miyaji, M., Andersen, S. J., Morisaki, N., Iwasaki, S., Shida, O., Takagi, H. and et al. (1995). Rifampicin inactivation by *Bacillus* species. J Antibiot (Tokyo). 48(8): 815-819.

Dantas, G. and Sommer, M. O. (2012). Context matters - the complex interplay between resistome genotypes and resistance phenotypes. Curr Opin Microbiol. 15(5): 577-582.

David, H. L. (1970). Probability distribution of drug-resistant mutants in unselected populations of *Mycobacterium tuberculosis*. Appl Microbiol. 20(5): 810-814.

de Knegt, G. J., Bruning, O., ten Kate, M. T., de Jong, M., van Belkum, A., Endtz, H. P., Breit, T. M., Bakker-Woudenberg, I. A. and de Steenwinkel, J. E. (2013). Rifampicin-induced transcriptome response in rifampicin-resistant *Mycobacterium tuberculosis*. Tuberculosis (Edinb). 93(1): 96-101.

Desomer, J., Dhaese, P. and Montagu, M. V. (1990). Transformation of *Rhodococcus fascians* by High-Voltage Electroporation and Development of R. fascians Cloning Vectors. Appl Environ Microbiol. 56(9): 2818-2825.

Dey, A. and Chatterji, D. (2012). Tracing the variation in physiological response to rifampicin across the microbial spectrum. Journal of Bacteriology and Virology. 42(2): 87-100.

Dey, A., Verma, A. K. and Chatterji, D. (2010). Role of an RNA polymerase interacting protein, MsRbpA, from *Mycobacterium smegmatis* in phenotypic tolerance to rifampicin. Microbiology. 156(Pt 3): 873-883.

Dey, A., Verma, A. K. and Chatterji, D. (2011). Molecular insights into the mechanism of phenotypic tolerance to rifampicin conferred on mycobacterial RNA polymerase by MsRbpA. Microbiology. 157(Pt 7): 2056-2071.

Dubos, R. J. and Hotchkiss, R. D. (1941). The Production of Bactericidal Substances by Aerobic Sporulating Bacilli. J Exp Med. 73(5): 629-640.

DuPont, H. L., Ericsson, C. D., Mathewson, J. J., Palazzini, E., DuPont, M. W., Jiang, Z. D., Mosavi, A. and de la Cabada, F. J. (1998). Rifaximin: a nonabsorbed antimicrobial in the therapy of travelers' diarrhea. Digestion. 59(6): 708-714.

Edgar, R. C. (2004). MUSCLE: multiple sequence alignment with high accuracy and high throughput. Nucleic Acids Res. 32(5): 1792-1797.

Edgar, R. C. (2010). Search and clustering orders of magnitude faster than BLAST. Bioinformatics. 26(19): 2460-2461.

Feklistov, A., Mekler, V., Jiang, Q., Westblade, L. F., Irschik, H., Jansen, R., Mustaev, A., Darst, S. A. and Ebright, R. H. (2008). Rifamycins do not function by allosteric modulation of binding of Mg2+ to the RNA polymerase active center. Proc Natl Acad Sci U S A. 105(39): 14820-14825.

Fleming, A. (1945). Penicillin. Nobel Lecture.

Fleming, A. (1980). Classics in infectious diseases: on the antibacterial action of cultures of a penicillium, with special reference to their use in the isolation of *B. influenzae* by Alexander Fleming, Reprinted from the British Journal of Experimental Pathology 10:226-236, 1929. Rev Infect Dis. 2(1): 129-139.

Floss, H. G. and Yu, T. W. (2005). Rifamycin-mode of action, resistance, and biosynthesis. Chem Rev. 105(2): 621-632.

Floss, H. G., Yu, T. W. and Arakawa, K. (2011). The biosynthesis of 3-amino-5-hydroxybenzoic acid (AHBA), the precursor of mC7N units in ansamycin and mitomycin antibiotics: a review. J Antibiot (Tokyo). 64(1): 35-44.

Forrest, G. N. and Tamura, K. (2010). Rifampin combination therapy for nonmycobacterial infections. Clin Microbiol Rev. 23(1): 14-34.

Forsberg, K. J., Reyes, A., Wang, B., Selleck, E. M., Sommer, M. O. and Dantas, G. (2012). The shared antibiotic resistome of soil bacteria and human pathogens. Science. 337(6098): 1107-1111.

Gagneux, S., Long, C. D., Small, P. M., Van, T., Schoolnik, G. K. and Bohannan, B. J. (2006). The competitive cost of antibiotic resistance in *Mycobacterium tuberculosis*. Science. 312(5782): 1944-1946.

Gaurivaud, P., Laigret, F. and Bove, J. M. (1996). Insusceptibility of members of the class Mollicutes to rifampin: studies of the *Spiroplasma citri* RNA polymerase beta-subunit gene. Antimicrob Agents Chemother. 40(4): 858-862.

Geer, L. Y., Domrachev, M., Lipman, D. J. and Bryant, S. H. (2002). CDART: protein homology by domain architecture. Genome Res. 12(10): 1619-1623.

Gill, S. K. and Garcia, G. A. (2011). Rifamycin inhibition of WT and Rif-resistant *Mycobacterium tuberculosis* and *Escherichia coli* RNA polymerases in vitro. Tuberculosis (Edinb). 91(5): 361-369.

Gillespie, S. H. (2002). Evolution of drug resistance in *Mycobacterium tuberculosis*: clinical and molecular perspective. Antimicrob Agents Chemother. 46(2): 267-274.

Girlich, D., Poirel, L., Leelaporn, A., Karim, A., Tribuddharat, C., Fennewald, M. and Nordmann, P. (2001). Molecular epidemiology of the integron-located VEB-1 extended-spectrum beta-lactamase in nosocomial enterobacterial isolates in Bangkok, Thailand. J Clin Microbiol. 39(1): 175-182.

Gouet, P., Robert, X. and Courcelle, E. (2003). ESPript/ENDscript: Extracting and rendering sequence and 3D information from atomic structures of proteins. Nucleic Acids Res. 31(13): 3320-3323.

Gupta, A. K., Chauhan, D. S., Srivastava, K., Das, R., Batra, S., Mittal, M., Goswami, P., Singhal, N., Sharma, V. D., Venkatesan, K., Hasnain, S. E. and Katoch, V. M. (2006). Estimation of efflux mediated multi-drug resistance and its correlation with expression levels of two major efflux pumps in mycobacteria. J Commun Dis. 38(3): 246-254.

Gupta, A. K., Katoch, V. M., Chauhan, D. S., Sharma, R., Singh, M., Venkatesan, K. and Sharma, V. D. (2010). Microarray analysis of efflux pump genes in multidrug-resistant *Mycobacterium tuberculosis* during stress induced by common anti-tuberculous drugs. Microb Drug Resist. 16(1): 21-28.

Hagman, K. E., Pan, W., Spratt, B. G., Balthazar, J. T., Judd, R. C. and Shafer, W. M. (1995). Resistance of *Neisseria gonorrhoeae* to antimicrobial hydrophobic agents is modulated by the mtrRCDE efflux system. Microbiology. 141 (Pt 3)611-622.

Hannula, M. and Hanninen, M. L. (2008). Effect of putative efflux pump inhibitors and inducers on the antimicrobial susceptibility of *Campylobacter jejuni* and *Campylobacter coli*. J Med Microbiol. 57(Pt 7): 851-855.

Hartmann, G., Behr, W., Beissner, K. A., Honikel, K. and Sippel, A. (1968). Antibiotics as inhibitors of nucleic acid and protein synthesis. Angew Chem Int Ed Engl. 7(9): 693-701.

Hartmann, G., Honikel, K. O., Knusel, F. and Nuesch, J. (1967). The specific inhibition of the DNA-directed RNA synthesis by rifamycin. Biochim Biophys Acta. 145(3): 843-844.

Hawkins, A. E., Bortolussi, R. and Issekutz, A. C. (1984). In vitro and in vivo activity of various antibiotics against *Listeria monocytogenes* type 4b. Clin Invest Med. 7(4): 335-341.

Hayakawa, M. and Nonomura, H. (1987). Humic acid-vitamin agar, a new medium for the selective isolation of soil actinomycetes. Journal of Fermentation Technology. 65(5): 501-509.

He, W., Wu, L., Gao, Q., Du, Y. and Wang, Y. (2006). Identification of AHBA biosynthetic genes related to geldanamycin biosynthesis in *Streptomyces hygroscopicus* 17997. Curr Microbiol. 52(3): 197-203.

Heuer, H., Krsek, M., Baker, P., Smalla, K. and Wellington, E. M. (1997). Analysis of actinomycete communities by specific amplification of genes encoding 16S rRNA and gel-electrophoretic separation in denaturing gradients. Appl Environ Microbiol. 63(8): 3233-3241.

Hon, W. C., McKay, G. A., Thompson, P. R., Sweet, R. M., Yang, D. S., Wright, G. D. and Berghuis, A. M. (1997). Structure of an enzyme required for aminoglycoside antibiotic resistance reveals homology to eukaryotic protein kinases. Cell. 89(6): 887-895.

Hopwood, D. A., Levy, S., Wenzel, R. P., Georgopapadako, N., Baltz, R. H., Bhavnani, S. and Cox, E. (2007). News Feature: A call to arms. Nat Rev Drug Discov. 6(6): 8-12.

Hosaka, T., Ohnishi-Kameyama, M., Muramatsu, H., Murakami, K., Tsurumi, Y., Kodani, S., Yoshida, M., Fujie, A. and Ochi, K. (2009). Antibacterial discovery in actinomycetes strains with mutations in RNA polymerase or ribosomal protein S12. Nat Biotechnol. 27(5): 462-464.

Hoshino, Y., Fujii, S., Shinonaga, H., Arai, K., Saito, F., Fukai, T., Satoh, H., Miyazaki, Y. and Ishikawa, J. (2010). Monooxygenation of rifampicin catalyzed by the *rox* gene product of *Nocardia farcinica*: structure elucidation, gene identification and role in drug resistance. J Antibiot (Tokyo). 63(1): 23-28.

Houang, E. T., Chu, Y. W., Lo, W. S., Chu, K. Y. and Cheng, A. F. (2003). Epidemiology of rifampin ADP-ribosyltransferase (*arr-2*) and metallo-beta-lactamase (*blaIMP-4*) gene cassettes in class 1 integrons in Acinetobacter strains isolated from blood cultures in 1997 to 2000. Antimicrob Agents Chemother. 47(4): 1382-1390.

Hu, Y., Morichaud, Z., Chen, S., Leonetti, J. P. and Brodolin, K. (2012). *Mycobacterium tuberculosis* RbpA protein is a new type of transcriptional activator that stabilizes the sigma A-containing RNA polymerase holoenzyme. Nucleic Acids Res. 40(14): 6547-6557.

Huang, D. B. and DuPont, H. L. (2005). Rifaximin--a novel antimicrobial for enteric infections. J Infect. 50(2): 97-106.

Hudson, A., Imamura, T., Gutteridge, W., Kanyok, T. and Nunn, P. (2003). The current anti-TB drug research and development pipeline. World Health Organization: Special Programme for Research and Training in Tropical Diseases (TDR).

Huitu, Z., Linzhuan, W., Aiming, L., Guizhi, S., Feng, H., Qiuping, L., Yuzhen, W., Huanzhang, X., Qunjie, G. and Yiguang, W. (2009). PCR screening of 3-amino-5-hydroxybenzoic acid synthase gene leads to identification of ansamycins and AHBA-related antibiotic producers in Actinomycetes. J Appl Microbiol. 106:755-763.

Inaoka, T. and Ochi, K. (2011). Activation of dormant secondary metabolism neotrehalosadiamine synthesis by an RNA polymerase mutation in *Bacillus subtilis*. Biosci Biotechnol Biochem. 75(4): 618-623.

Institute, T. B. (2010). The Actinomycetales group Database. From www.broadinstitute.org/annotation/genome/streptomyces_group/Info.html.

Ishikawa, J., Chiba, K., Kurita, H. and Satoh, H. (2006). Contribution of *rpoB2* RNA polymerase beta subunit gene to rifampin resistance in *Nocardia* species. Antimicrob Agents Chemother. 50(4): 1342-1346.

Izard, T. and Ellis, J. (2000). The crystal structures of chloramphenicol phosphotransferase reveal a novel inactivation mechanism. EMBO J. 19(11): 2690-2700.

Janda, J. M. and Abbott, S. L. (2007). 16S rRNA gene sequencing for bacterial identification in the diagnostic laboratory: pluses, perils, and pitfalls. J Clin Microbiol. 45(9): 2761-2764.

Jiang, X., Zhang, W., Zhang, Y., Gao, F., Lu, C., Zhang, X. and Wang, H. (2008). Assessment of efflux pump gene expression in a clinical isolate *Mycobacterium tuberculosis* by real-time reverse transcription PCR. Microb Drug Resist. 14(1): 7-11.

Kahan, F. M., Kropp, H., Sundelof, J. G. and Birnbaum, J. (1983). Thienamycin: development of imipenen-cilastatin. J Antimicrob Chemother. 12 Suppl D1-35.

Kalan, L. and Wright, G. D. (2011). Antibiotic adjuvants: multicomponent anti-infective strategies. Expert Rev Mol Med. 13e5.

Kang, Q., Shen, Y. and Bai, L. (2012). Biosynthesis of 3,5-AHBA-derived natural products. Nat Prod Rep. 29(2): 243-263.

Kieser, T., Bibb M.J., Buttner, M.J., Chater, K.F., Hopwood, D.A. (2000). Practical Streptomyces Genetics., John Innes Foundation Press, Norwich, United Kingdom.

Kim, H., Kim, S. H., Ying, Y. H., Kim, H. J., Koh, Y. H., Kim, C. J., Lee, S. H., Cha, C. Y., Kook, Y. H. and Kim, B. J. (2005). Mechanism of natural rifampin resistance of *Streptomyces* spp. Syst Appl Microbiol. 28(5): 398-404.

Kingston, W. (2008). Irish contributions to the origins of antibiotics. Ir J Med Sci. 177(2): 87-92.

Kishi, T., Asai, M., Muroi, M., Harada, S. and Mizuta, E. (1969). Tolypomycin. I. Structure of tolypomycinone. Tetrahedron Lett.(2): 91-95.

Klopper, M., Warren, R. M., Hayes, C., Gey van Pittius, N. C., Streicher, E. M., Muller, B., Sirgel, F. A., Chabula-Nxiweni, M., Hoosain, E., Coetzee, G., David van Helden, P., Victor, T. C. and Trollip, A. P. (2013). Emergence and spread of extensively and totally drug-resistant tuberculosis, South Africa. Emerg Infect Dis. 19(3): 449-455.

Kondo, M., Oishi, T. and Tsuchiya, K. (1972). Tolypomycin, a new antibiotic. V. In vitro and in vivo antimicrobial activity. J Antibiot (Tokyo). 25(1): 16-24.

Kump, W. and Bickel, H. (1973). [Understanding of rifamycin S. Reactions of the ansa-rings. Modifications of antibiotics. 8]. Helv Chim Acta. 56(7): 2323-2347.

Lairson, L. L., Henrissat, B., Davies, G. J. and Withers, S. G. (2008). Glycosyltransferases: structures, functions, and mechanisms. Annu Rev Biochem. 77521-555.

Landsberg, H. (1949). Prelude to the discovery of penicillin. Isis. 40(3): 225-227.

Lanoot, B., Vancanneyt, M., Dawyndt, P., Cnockaert, M., Zhang, J., Huang, Y., Liu, Z. and Swings, J. (2004). BOX-pCR fingerprinting as a powerful tool to reveal synonymous names in the genus Streptomyces. Emended descriptions are proposed for the species *Streptomyces cinereorectus*, *S. fradiae*, *S. tricolor*, *S. colombiensis*, *S. filamentosus*, *S. vinaceus* and *S. phaeopurpureus*. Syst Appl Microbiol. 27(1): 84-92.

Larkin, M. A., Blackshields, G., Brown, N. P., Chenna, R., McGettigan, P. A., McWilliam, H., Valentin, F., Wallace, I. M., Wilm, A., Lopez, R., Thompson, J. D., Gibson, T. J. and Higgins, D. G. (2007). Clustal W and Clustal X version 2.0. Bioinformatics. 23(21): 2947-2948.

Laxminarayan, R., Duse, A., Wattal, C., Zaidi, A. K., Wertheim, H. F., Sumpradit, N., Vlieghe, E., Hara, G. L., Gould, I. M., Goossens, H., Greko, C., So, A. D., Bigdeli, M., Tomson, G., Woodhouse, W., Ombaka, E., Peralta, A. Q., Qamar, F. N., Mir, F., Kariuki, S., Bhutta, Z. A., Coates, A., Bergstrom, R., Wright, G. D., Brown, E. D. and Cars, O. (2013). Antibiotic resistance - the need for global solutions. Lancet Infect Dis. 13(12): 1057-1098.

Llarrull, L. I., Fisher, J. F. and Mobashery, S. (2009). Molecular basis and phenotype of methicillin resistance in *Staphylococcus aureus* and insights into new beta-lactams that meet the challenge. Antimicrob Agents Chemother. 53(10): 4051-4063.

Louw, G. E., Warren, R. M., Gey van Pittius, N. C., McEvoy, C. R., Van Helden, P. D. and Victor, T. C. (2009). A balancing act: efflux/influx in mycobacterial drug resistance. Antimicrob Agents Chemother. 53(8): 3181-3189.

Maness, M. J. and Sparling, P. F. (1973). Multiple antibiotic resistance due to a single mutation in Neisseria gonorrhoeae. J Infect Dis. 128(3): 321-330.

Marchler-Bauer, A., Zheng, C., Chitsaz, F., Derbyshire, M. K., Geer, L. Y., Geer, R. C., Gonzales, N. R., Gwadz, M., Hurwitz, D. I., Lanczycki, C. J., Lu, F., Lu, S., Marchler, G. H., Song, J. S., Thanki, N., Yamashita, R. A., Zhang, D. and Bryant, S. H. (2013). CDD: conserved domains and protein three-dimensional structure. Nucleic Acids Res. 41(Database issue): D348-352.

Mariam, D. H., Mengistu, Y., Hoffner, S. E. and Andersson, D. I. (2004). Effect of rpoB mutations conferring rifampin resistance on fitness of *Mycobacterium tuberculosis*. Antimicrob Agents Chemother. 48(4): 1289-1294.

Marshall, C. G., Broadhead, G., Leskiw, B. K. and Wright, G. D. (1997). D-Ala-D-Ala ligases from glycopeptide antibiotic-producing organisms are highly homologous to the enterococcal vancomycin-resistance ligases VanA and VanB. Proc Natl Acad Sci U S A. 94(12): 6480-6483.

McClure, W. R. and Cech, C. L. (1978). On the mechanism of rifampicin inhibition of RNA synthesis. J Biol Chem. 253(24): 8949-8956.

McGarvey, K. M., Queitsch, K. and Fields, S. (2012). Wide variation in antibiotic resistance proteins identified by functional metagenomic screening of a soil DNA library. Appl Environ Microbiol. 78(6): 1708-1714.

Mitani, Y., Meng, X., Kamagata, Y. and Tamura, T. (2005). Characterization of LtsA from *Rhodococcus erythropolis*, an enzyme with glutamine amidotransferase activity. J Bacteriol. 187(8): 2582-2591.

Morar, M. and Wright, G. D. (2010). The genomic enzymology of antibiotic resistance. Annu Rev Genet. 4425-51.

Morisaki, N., Hashimoto, Y., Furihata, K., Imai, T., Watanabe, K., Mikami, Y., Yazawa, K., Ando, A., Nagata, Y. and Dabbs, E. R. (2000). Structures of ADP-ribosylated rifampicin and its metabolite: intermediates of rifampicin-ribosylation by *Mycobacterium smegmatis* DSM43756. J Antibiot (Tokyo). 53(3): 269-275.

Morisaki, N., Iwasaki, S., Yazawa, K., Mikami, Y. and Maeda, A. (1993). Inactivated products of rifampicin by pathogenic *Nocardia* spp.: structures of glycosylated and phosphorylated metabolites of rifampicin and 3-formylrifamycin SV. J Antibiot (Tokyo). 46(10): 1605-1610.

Morisaki, N., Kobayashi, H., Iwasaki, S., Furihata, K., Dabbs, E. R., Yazawa, K. and Mikami, Y. (1995). Structure determination of ribosylated rifampicin and its derivative: new inactivated metabolites of rifampicin by mycobacterial strains. J Antibiot (Tokyo). 48(11): 1299-1303.

Mosher, R. H., Camp, D. J., Yang, K., Brown, M. P., Shaw, W. V. and Vining, L. C. (1995). Inactivation of chloramphenicol by O-phosphorylation. A novel resistance mechanism in *Streptomyces venezuelae* ISP5230, a chloramphenicol producer. J Biol Chem. 270(45): 27000-27006.

Mulichak, A. M., Losey, H. C., Walsh, C. T. and Garavito, R. M. (2001). Structure of the UDP-glucosyltransferase GtfB that modifies the heptapeptide aglycone in the biosynthesis of vancomycin group antibiotics. Structure. 9(7): 547-557.

Mulichak, A. M., Lu, W., Losey, H. C., Walsh, C. T. and Garavito, R. M. (2004). Crystal structure of vancosaminyltransferase GtfD from the vancomycin biosynthetic pathway: interactions with acceptor and nucleotide ligands. Biochemistry. 43(18): 5170-5180.

Murphy, C. K., Mullin, S., Osburne, M. S., van Duzer, J., Siedlecki, J., Yu, X., Kerstein, K., Cynamon, M. and Rothstein, D. M. (2006). In vitro activity of novel rifamycins against rifamycin-resistant *Staphylococcus aureus*. Antimicrob Agents Chemother. 50(3): 827-834.

Naas, T., Mikami, Y., Imai, T., Poirel, L. and Nordmann, P. (2001). Characterization of In53, a class 1 plasmid- and composite transposon-located integron of *Escherichia coli* which carries an unusual array of gene cassettes. J Bacteriol. 183(1): 235-249.

Nakashima, N. and Tamura, T. (2004). Isolation and characterization of a rolling-circle-type plasmid from *Rhodococcus erythropolis* and application of the plasmid to multiple-recombinant-protein expression. Appl Environ Microbiol. 70(9): 5557-5568.

Narayanan, C. S. and Dubnau, D. (1985). Evidence for the translational attenuation model: ribosome-binding studies and structural analysis with an in vitro run-off transcript of *ermC*. Nucleic Acids Res. 13(20): 7307-7326.

Narindrasorasak, S. and Bridger, W. A. (1977). Phosphoenolypyruvate synthetase of *Escherichia coli*: molecular weight, subunit composition, and identification of phosphohistidine in phosphoenzyme intermediate. J Biol Chem. 252(10): 3121-3127.

Newell, K. V., Thomas, D. P., Brekasis, D. and Paget, M. S. (2006). The RNA polymerase-binding protein RbpA confers basal levels of rifampicin resistance on *Streptomyces coelicolor*. Mol Microbiol. 60(3): 687-696.

Nicholson, W. L. and Maughan, H. (2002). The spectrum of spontaneous rifampin resistance mutations in the *rpoB* gene of *Bacillus subtilis* 168 spores differs from that of vegetative cells and resembles that of *Mycobacterium tuberculosis*. J Bacteriol. 184(17): 4936-4940.

Okusu, H., Ma, D. and Nikaido, H. (1996). AcrAB efflux pump plays a major role in the antibiotic resistance phenotype of *Escherichia coli* multiple-antibiotic-resistance (Mar) mutants. J Bacteriol. 178(1): 306-308.

Pallanza, R., Furesz, S., Timbal, M. T. and Carniti, G. (1965). In vitro bacteriological studies on rifamycin B diethylamide (rifamide). Arzneimittelforschung. 15(7): 800-802.

Papagrigorakis, M. J., Yapijakis, C., Synodinos, P. N. and Baziotopoulou-Valavani, E. (2006). DNA examination of ancient dental pulp incriminates typhoid fever as a probable cause of the Plague of Athens. Int J Infect Dis. 10(3): 206-214.

Pehrsson, E. C., Forsberg, K. J., Gibson, M. K., Ahmadi, S. and Dantas, G. (2013). Novel resistance functions uncovered using functional metagenomic investigations of resistance reservoirs. Front Microbiol. 4145.

Perez, F. and Van Duin, D. (2013). Carbapenem-resistant Enterobacteriaceae: a menace to our most vulnerable patients. Cleve Clin J Med. 80(4): 225-233.

Perkins, A. E. and Nicholson, W. L. (2008). Uncovering new metabolic capabilities of *Bacillus subtilis* using phenotype profiling of rifampin-resistant *rpoB* mutants. J Bacteriol. 190(3): 807-814.

Perry, J. A. and Wright, G. D. (2013). The antibiotic resistance "mobilome": searching for the link between environment and clinic. Front Microbiol. 4138.

Phuc Nguyen, M. C., Woerther, P. L., Bouvet, M., Andremont, A., Leclercq, R. and Canu, A. (2009). *Escherichia coli* as reservoir for macrolide resistance genes. Emerg Infect Dis. 15(10): 1648-1650.

Pimentel, M., Lembo, A., Chey, W. D., Zakko, S., Ringel, Y., Yu, J., Mareya, S. M., Shaw, A. L., Bortey, E. and Forbes, W. P. (2011). Rifaximin therapy for patients with irritable bowel syndrome without constipation. N Engl J Med. 364(1): 22-32.

Powers, J. H. (2004). Antimicrobial drug development - the past, the present, and the future. Clin Microbiol Infect. 10 Suppl 423-31.

Quan, S., Imai, T., Mikami, Y., Yazawa, K., Dabbs, E. R., Morisaki, N., Iwasaki, S., Hashimoto, Y. and Furihata, K. (1999). ADP-ribosylation as an intermediate step in inactivation of rifampin by a mycobacterial gene. Antimicrob Agents Chemother. 43(1): 181-184.

Quan, S., Venter, H. and Dabbs, E. R. (1997). Ribosylative inactivation of rifampin by *Mycobacterium smegmatis* is a principal contributor to its low susceptibility to this antibiotic. Antimicrob Agents Chemother. 41(11): 2456-2460.

Ramaswamy, S. and Musser, J. M. (1998). Molecular genetic basis of antimicrobial agent resistance in *Mycobacterium tuberculosis*: 1998 update. Tuber Lung Dis. 79(1): 3-29.

Retief, F. P. and Cilliers, L. (2007). Mesopotamian medicine. S Afr Med J. 97(1): 27-30.

Reynolds, M. G. (2000). Compensatory evolution in rifampin-resistant *Escherichia coli*. Genetics. 156(4): 1471-1481.

Roesch, L. F., Fulthorpe, R. R., Riva, A., Casella, G., Hadwin, A. K., Kent, A. D., Daroub, S. H., Camargo, F. A., Farmerie, W. G. and Triplett, E. W. (2007). Pyrosequencing enumerates and contrasts soil microbial diversity. ISME J. 1(4): 283-290.

Ronquist, F., Teslenko, M., van der Mark, P., Ayres, D. L., Darling, A., Hohna, S., Larget, B., Liu, L., Suchard, M. A. and Huelsenbeck, J. P. (2012). MrBayes 3.2: efficient Bayesian phylogenetic inference and model choice across a large model space. Syst Biol. 61(3): 539-542.

Rothstein, D. M., van Duzer, J., Sternlicht, A. and Gilman, S. C. (2007). Rifalazil and other benzoxazinorifamycins in the treatment of chlamydia-based persistent infections. Arch Pharm (Weinheim). 340(10): 517-529.

Roy, A., Kucukural, A. and Zhang, Y. (2010). I-TASSER: a unified platform for automated protein structure and function prediction. Nat Protoc. 5(4): 725-738.

Russell, C. D., Lawson McLean, A., Saunders, C. and Laurenson, I. F. (2014). Adjunctive rifampicin may improve outcomes in *Staphylococcus aureus* bacteraemia: a systematic review. J Med Microbiol.

Sadaie, Y. and Kada, T. (1983). Formation of competent *Bacillus subtilis* cells. J Bacteriol. 153(2): 813-821.

Sanchez-Hidalgo, M., Nunez, L. E., Mendez, C. and Salas, J. A. (2010). Involvement of the beta subunit of RNA polymerase in resistance to streptolydigin and streptovaricin in the producer organisms *Streptomyces lydicus* and *Streptomyces spectabilis*. Antimicrob Agents Chemother. 54(5): 1684-1692.

Schmeling, S., Narmandakh, A., Schmitt, O., Gad'on, N., Schuhle, K. and Fuchs, G. (2004). Phenylphosphate synthase: a new phosphotransferase catalyzing the first step in anaerobic phenol metabolism in *Thauera aromatica*. J Bacteriol. 186(23): 8044-8057.

Schupp, T., Toupet, C., Engel, N. and Goff, S. (1998). Cloning and sequence analysis of the putative rifamycin polyketide synthase gene cluster from *Amycolatopsis mediterranei*. FEMS Microbiol Lett. 159(2): 201-207.

Schutzbach, J. and Brockhausen, I. (2009). Inhibition of glycosyltransferase activities as the basis for drug development. Methods Mol Biol. 534359-373.

Sensi, P. (1983). History of the development of rifampin. Rev Infect Dis. 5 Suppl 3S402-406.

Sensi, P., Margalith, P. and Timbal, M. T. (1959). Rifomycin, a new antibiotic; preliminary report. Farmaco Sci. 14(2): 146-147.

Shakya, T., Stogios, P. J., Waglechner, N., Evdokimova, E., Ejim, L., Blanchard, J. E., McArthur, A. G., Savchenko, A. and Wright, G. D. (2011). A small molecule discrimination map of the antibiotic resistance kinome. Chem Biol. 18(12): 1591-1601.

Shao, Z., Dick, W. A. and Behki, R. M. (1995). An improved *Escherichia coli-Rhodococcus* shuttle vector and plasmid transformation in *Rhodococcus* spp. using electroporation. Lett Appl Microbiol. 21(4): 261-266.

Sheehan, J. C. (1967). The chemistry of synthetic and semisynthetic penicillins. Ann N Y Acad Sci. 145(2): 216-223.

Shi, K., Caldwell, S. J., Fong, D. H. and Berghuis, A. M. (2013). Prospects for circumventing aminoglycoside kinase mediated antibiotic resistance. Front Cell Infect Microbiol. 322.

Siddiqi, N., Das, R., Pathak, N., Banerjee, S., Ahmed, N., Katoch, V. M. and Hasnain, S. E. (2004). *Mycobacterium tuberculosis* isolate with a distinct genomic identity overexpresses a tap-like efflux pump. Infection. 32(2): 109-111.

Singleton, M. R., Dillingham, M. S. and Wigley, D. B. (2007). Structure and mechanism of helicases and nucleic acid translocases. Annu Rev Biochem. 7623-50.

Sippel, A. and Hartmann, G. (1968). Mode of action of rifamycin on the RNA polymerase reaction. Biochim Biophys Acta. 157(1): 218-219.

Skinner, R. H. and Cundliffe, E. (1980). Resistance to the antibiotics viomycin and capreomycin in the *Streptomyces* species which produce them. J Gen Microbiol. 120(1): 95-104.

Solecki, R. S. (1975). Shanidar IV, a Neanderthal Flower Burial in Northern Iraq. Science. 190(4217): 880-881.

Spanogiannopoulos, P., Thaker, M., Koteva, K., Waglechner, N. and Wright, G. D. (2012). Characterization of a rifampin-inactivating glycosyltransferase from a screen of environmental actinomycetes. Antimicrob Agents Chemother. 56(10): 5061-5069.

Spellberg, B. (2008). Dr. William H. Stewart: mistaken or maligned? Clin Infect Dis. 47(2): 294.

Stamatakis, A. (2014). RAxML Version 8: A tool for Phylogenetic Analysis and Post-Analysis of Large Phylogenies. Bioinformatics.

Stamm, L. V., Bergen, H. L. and Shangraw, K. A. (2001). Natural rifampin resistance in *Treponema* spp. correlates with presence of N531 in RpoB rif cluster I. Antimicrob Agents Chemother. 45(10): 2973-2974.

Studier, F. W. (2005). Protein production by auto-induction in high density shaking cultures. Protein Expr Purif. 41(1): 207-234.

Sun, J., Zhou, M., Wu, Q. and Ni, Y. (2010). Characterization of two novel gene cassettes, *dfrA27* and *aadA16*, in a non-O1, non-O139 *Vibrio cholerae* isolate from China. Clin Microbiol Infect. 16(8): 1125-1129.

Tala, A., Wang, G., Zemanova, M., Okamoto, S., Ochi, K. and Alifano, P. (2009). Activation of dormant bacterial genes by *Nonomuraea* sp. strain ATCC 39727 mutant-type RNA polymerase. J Bacteriol. 191(3): 805-814.

Tanaka, Y., Kasahara, K., Hirose, Y., Murakami, K., Kugimiya, R. and Ochi, K. (2013). Activation and products of the cryptic secondary metabolite biosynthetic gene clusters by rifampin resistance (*rpoB*) mutations in actinomycetes. J Bacteriol. 195(13): 2959-2970.

Tanaka, Y., Yazawa, K., Dabbs, E. R., Nishikawa, K., Komaki, H., Mikami, Y., Miyaji, M., Morisaki, N. and Iwasaki, S. (1996). Different rifampicin inactivation mechanisms in *Nocardia* and related taxa. Microbiol Immunol. 40(1): 1-4.

Tang, B., Zhao, W., Zheng, H., Zhuo, Y., Zhang, L. and Zhao, G. P. (2012). Complete genome sequence of *Amycolatopsis mediterranei* S699 based on de novo assembly via a combinatorial sequencing strategy. J Bacteriol. 194(20): 5699-5700.

Taniguchi, K., Nakamura, A., Tsurubuchi, K., Ishii, A., O'Hara, K. and Sawai, T. (1999). Identification of functional amino acids in the macrolide 2'-phosphotransferase II. Antimicrob Agents Chemother. 43(8): 2063-2065.

Temple, M. E. and Nahata, M. C. (1999). Rifapentine: its role in the treatment of tuberculosis. Ann Pharmacother. 33(11): 1203-1210.

Thaker, M. N., Wang, W., Spanogiannopoulos, P., Waglechner, N., King, A. M., Medina, R. and Wright, G. D. (2013). Identifying producers of antibacterial compounds by screening for antibiotic resistance. Nat Biotechnol. 31(10): 922-927.

Torres-Cortes, G., Millan, V., Ramirez-Saad, H. C., Nisa-Martinez, R., Toro, N. and Martinez-Abarca, F. (2011). Characterization of novel antibiotic resistance genes identified by functional metagenomics on soil samples. Environ Microbiol. 13(4): 1101-1114.

Tribuddharat, C. and Fennewald, M. (1999). Integron-mediated rifampin resistance in *Pseudomonas aeruginosa*. Antimicrob Agents Chemother. 43(4): 960-962.

Tupin, A., Gualtieri, M., Roquet-Baneres, F., Morichaud, Z., Brodolin, K. and Leonetti, J. P. (2010). Resistance to rifampicin: at the crossroads between ecological, genomic and medical concerns. Int J Antimicrob Agents. 35(6): 519-523.

Vierling, S., Weber, T., Wohlleben, W. and Muth, G. (2001). Evidence that an additional mutation is required to tolerate insertional inactivation of the *Streptomyces lividans recA* gene. J Bacteriol. 183(14): 4374-4381.

Vigliotta, G., Tredici, S. M., Damiano, F., Montinaro, M. R., Pulimeno, R., di Summa, R., Massardo, D. R., Gnoni, G. V. and Alifano, P. (2005). Natural merodiploidy involving duplicated *rpoB* alleles affects secondary metabolism in a producer actinomycete. Mol Microbiol. 55(2): 396-412.

Vilches, C., Hernandez, C., Mendez, C. and Salas, J. A. (1992). Role of glycosylation and deglycosylation in biosynthesis of and resistance to oleandomycin in the producer organism, *Streptomyces antibioticus*. J Bacteriol. 174(1): 161-165.

Vogler, A. J., Busch, J. D., Percy-Fine, S., Tipton-Hunton, C., Smith, K. L. and Keim, P. (2002). Molecular analysis of rifampin resistance in *Bacillus anthracis* and *Bacillus cereus*. Antimicrob Agents Chemother. 46(2): 511-513.

Wainwright, M. (1989). Moulds in ancient and more recent medicine. Mycologist. 3(1): 21-23.

Wang, H. X., Chen, Y. Y., Ge, L., Fang, T. T., Meng, J., Liu, Z., Fang, X. Y., Ni, S., Lin, C., Wu, Y. Y., Wang, M. L., Shi, N. N., He, H. G., Hong, K. and Shen, Y. M. (2013). PCR screening reveals considerable unexploited biosynthetic potential of ansamycins and a mysterious family of AHBA-containing natural products in actinomycetes. J Appl Microbiol. 115(1): 77-85.

Watve, M. G., Tickoo, R., Jog, M. M. and Bhole, B. D. (2001). How many antibiotics are produced by the genus *Streptomyces*? Arch Microbiol. 176(5): 386-390.

Wehrli, W. (1977). Ansamycins. Chemistry, biosynthesis and biological activity. Top Curr Chem. 7221-49.

Wehrli, W., Knusel, F., Schmid, K. and Staehelin, M. (1968). Interaction of rifamycin with bacterial RNA polymerase. Proc Natl Acad Sci U S A. 61(2): 667-673.

Wehrli, W. and Staehelin, M. (1971). Actions of the rifamycins. Bacteriol Rev. 35(3): 290-309.

White, A. R., Kaye, C., Poupard, J., Pypstra, R., Woodnutt, G. and Wynne, B. (2004). Augmentin (amoxicillin/clavulanate) in the treatment of community-acquired respiratory tract infection: a review of the continuing development of an innovative antimicrobial agent. J Antimicrob Chemother. 53 Suppl 1i3-20.

Wikler, M. A., Cockerill III, F. R., Craig, W. A., Dudley, M. N., Eliopoulos, G. M., Hecht, D. W., Hindler, J. F., Low, D. E., Sheehan, D. J., Tonever, F. C., Turnidge, J. D., Weinstein, M. P. and Zimmer, B. L. (2006). Performance Standards for Antimicrobial Disk Susceptibility Tests; Approved Standard-Ninth Edition. Clinical and Laboratory Standards Institute. 26(1): M2-A9.

Wood, S. A., Kirby, B. M., Goodwin, C. M., Le Roes, M. and Meyers, P. R. (2007). PCR screening reveals unexpected antibiotic biosynthetic potential in *Amycolatopsis* sp. strain UM16. J Appl Microbiol. 102(1): 245-253.

Wright, G. D. (2005). Bacterial resistance to antibiotics: enzymatic degradation and modification. Adv Drug Deliv Rev. 57(10): 1451-1470.

Wright, G. D. (2007). The antibiotic resistome: the nexus of chemical and genetic diversity. Nat Rev Microbiol. 5(3): 175-186.

Wright, G. D. (2012). Antibiotics: a new hope. Chem Biol. 19(1): 3-10.

Wu, C., Dunaway-Mariano, D. and Mariano, P. S. (2013). Design, synthesis, and evaluation of inhibitors of pyruvate phosphate dikinase. J Org Chem. 78(5): 1910-1922.

Yazawa, K., Mikami, Y., Maeda, A., Akao, M., Morisaki, N. and Iwasaki, S. (1993). Inactivation of rifampin by *Nocardia brasiliensis*. Antimicrob Agents Chemother. 37(6): 1313-1317.

Yazawa, K., Mikami, Y., Maeda, A., Morisaki, N. and Iwasaki, S. (1994). Phosphorylative inactivation of rifampicin by *Nocardia otitidiscaviarum*. J Antimicrob Chemother. 33(6): 1127-1135.

Zhang, G., Campbell, E. A., Minakhin, L., Richter, C., Severinov, K. and Darst, S. A. (1999). Crystal structure of *Thermus aquaticus* core RNA polymerase at 3.3 A resolution. Cell. 98(6): 811-824.

Zhao, L., Beyer, N. J., Borisova, S. A. and Liu, H. W. (2003). Beta-glucosylation as a part of self-resistance mechanism in methymycin/pikromycin producing strain *Streptomyces venezuelae*. Biochemistry. 42(50): 14794-14804.

APPENDICES

APPENDIX 1: Collection of RIF-resistant Actinomycetes

Isolate/Strain*	Alternate Name†	Strain Collection	Geographic Source	RIF Inactivating
WAC5041	AA4	WAC	Farm soil, Nigeria	+
WAC5122	AD39a	WAC	Garden soil, Burlington, ON	+
WAC5055	CO6	WAC	Orchard soil, Ancaster, ON	+
WAC5059	CP12	WAC	Orchard soil, Ancaster, ON	+
WAC4782	CP33	WAC	Orchard soil, Ancaster, ON	+
WAC4839	PP02	WAC	Park soil, Hamilton, ON	+
WAC4699	PP03	WAC	Park soil, Hamilton, ON	+
WAC4951	PP07	WAC	Park soil, Hamilton, ON	+
WAC4952	PP10	WAC	Park soil, Hamilton, ON	+
WAC4702	PP11	WAC	Park soil, Hamilton, ON	+
WAC4953	PP12	WAC	Park soil, Hamilton, ON	+
WAC4703	PP15	WAC	Park soil, Hamilton, ON	+
WAC4791	PP17a	WAC	Park soil, Hamilton, ON	+
WAC4841	PP19	WAC	Park soil, Hamilton, ON	+
WAC4844	PP24	WAC	Park soil, Hamilton, ON	+
WAC5090	PP33	WAC	Park soil, Hamilton, ON	+
WAC5242	PV2	WAC	Vineyard soils Winona, ON	+
WAC4747	PV20b	WAC	Vineyard soils Winona, ON	+
WAC5038	WMB03	WAC	Watermain, Brampton, ON	+
WAC5188	WMB29	WAC	Watermain, Brampton, ON	+
WAC1438		WAC	Soil, Winnipeg, MB	+
S. sviceus ATCC 29083		BIAC		+
S. griseoflavus Tu4000		BIAC		-
S. viridochromogenes		BIAC		-
S. lividans TK24		BIAC		-
WAC4895	CO07	WAC	Orchard soil, Ancaster, ON	-
WAC4820	CP05	WAC	Orchard soil, Ancaster, ON	-
WAC5010	CP19	WAC	Orchard soil, Ancaster, ON	-

* See TABLE 2-3 for selected 16S rDNA determinations.

† According to D'Costa, V.M. *et al*. 2006. 311(5759):374-377.

APPENDIX 1: Collection of RIF-resistant Actinomycetes Continued

Isolate/Strain*	Alternate Name†	Strain Collection	Geographic Source	RIF Inactivating
WAC5060	CP23	WAC	Orchard soil, Ancaster, ON	-
WAC4833	CU06	WAC	Soil, Cuba	-
WAC4667	CU08a	WAC	Soil, Cuba	-
WAC4668	CU09	WAC	Soil, Cuba	-
WAC5511	CU16	WAC	Soil, Cuba	-
WAC4676	CU17	WAC	Soil, Cuba	-
WAC5017	CU19	WAC	Soil, Cuba	-
WAC4680	CU27	WAC	Soil, Cuba	-
WAC4681	CU31	WAC	Soil, Cuba	-
WAC5065	CU32	WAC	Soil, Cuba	-
WAC4686	CU45a	WAC	Soil, Cuba	-
WAC4913	CU45b	WAC	Soil, Cuba	-
WAC5020	CU46	WAC	Soil, Cuba	-
WAC4661	JA18a	WAC	Soil, Jamaica	-
WAC5078	KAR07	WAC	Garden Soil, Karachi, Pakistan	-
WAC5079	KAR22	WAC	Garden Soil, Karachi, Pakistan	-
WAC4746	NB11	WAC	Soil, NB	-
WAC4842	PP21	WAC	Park soil, Hamilton, ON	-
WAC4854	PP80	WAC	Park soil, Hamilton, ON	-
WAC4764	PV19	WAC	Vineyard soil, Winona, ON	-
WAC4860	PV46	WAC	Vineyard soil, Winona, ON	-
WAC4988	WAC01	WAC	Farm soil, San Francisco, U.S.A.	-
WAC4991	WAT04	WAC	Farm soil, San Francisco, U.S.A.	-
WAC4993	WAT08	WAC	Farm soil, San Francisco, U.S.A.	-
S. coelicolor		WAC		-
S. toyocaensis		WAC		-

* See TABLE 2-3 for selected 16S rDNA determinations.

† According to D'Costa, V.M. *et al*. 2006. 311(5759):374-377.

APPENDIX 2: List of Oligonucleotide Primers

Primer Name	Direction	Sequence (5'→3')*
Bsub_RifR-A	Forward	CGTTTCCCAGCTTGTTCGGTCTCC
Bsub_RifR-B	Forward	TGAATTAACGTACAAGCGTCGTCTGTC
Bsub_RifR-C	Reverse	GACAGACGACGCTTGTACGTTAATTCA
Bsub_RifR-D2	Reverse	GCGGTCATCAAGATTGCGAAGCG
BsubRifR-SeqF	Forward	GGTTTAAGCCGTATGGAGCGTGTG
BsubRifR-SeqR	Reverse	ATTCTGCCCGTTACCTTCCCTGTT
F27	Forward	AGAGTTTGATC(A/C)TGGCTCAG
R14392	Reverse	TACGG(C/T)TACCTTGTTACGACTT
SRPOF1	Forward	TCGACCACTTCGGCAACCGC
SRPOR1	Reverse	TCGATCGGGCACATGCGGCC
BOXAIR	-	CTACGGCAAGGCGACGCTGACG
rgtPartF	Forward	ATGCATGAATTCCGAGGCGGCCGAGGGTTGT
rgtPartR	Reverse	ATGCATAAGCTTCCGCGAGCGAGGACCACACG
rgtF-pIJK	Forward	ATCGATCATATGCGCATGCTGCTGACCAC
rgtR-pIJK	Reverse	ATGCATGGATCCCCGACGGGGGCTGGACTC
rgtF	Forward	ATCGATCATATGCGCATGCTGCTGACCAC
rgtR	Reverse	ATGCATAAGCTTCCGACGGGGGCTGGACTC
rph-Ss-F	Forward	ATGGATCATATGAACAACGTGACCGAGCGGTACGTG
rph-Ss-R	Reverse	ATGGATAAGCTTTCAGGACAGGATCTCGATGTACCCGTCC
rph-Ss-part-F	Forward	ATGGATGAATTCCCTCCTGGTGTCCGGGCTGGTG
rph-Ss-part-R	Reverse	ATGGATAAGCTTGACGCCCGCCAGGAACTCG
Rph-Ss-SUMO-F	Forward	ATGCCACCTGCATGCAGGTATGAACAACGTGACCGAGCGGTACGTG
Rph4747-F	Forward	ATGCATCATATGAGCGGGCGTCTGGTCGTGCAT
Rph4747-R	Reverse	ATGCATAAGCTTTCAGGACAGAAGCTCGATATAGCCCTCCGTC
Rph4747-part-F	Forward	ATGCATGAATTCGGGCGTCCGGCATCCTGTT
Rph4747-part-R	Reverse	ATGCATAAGCTTGAGCAGCTCCAGCCCCATCTCC
Hel4747-part-F	Forward	ATGGATGAATTCAGACGACGGCCGACCTCAC
Hel4747-part-R	Reverse	ATGGATAAGCTTGGCGTCGATGAGTTGTCCAC
Rph-Bc-F	Forward	ATGCATGGTACCATGAGTTCTTTCGTTCTCGATTTTCAGG
Rph-Bc-R	Reverse	ATGCATCTCGAGCTACAACACTTCAATATATCCTTCTGTTCCATG
Rph-Lm-F	Forward	ATGCATGGTACCATGAAACCATATGTACTCAAGTTTCAAGAAATACGG
Rph-Lm-R	Reverse	ATGCATCTCGAGTTAATCAAGAATCTCAATATAGCCTTCTGTCCCA
Rph-Bc-SDM-F	Forward	GAAGTCGGCGGGCTTATGACGGCCGGAGCAGTGATTGCACGTGAG
Rph-Bc-SDM-R	Reverse	CTCACGTGCAATCACTGCTCCGGCCGTCATAAGCCCGCCGACTTC
Rph4747q-F	Forward	GAGCCGTGCCACTCTCCTGG
Rph4747q-R	Reverse	CATCTCCGAGGTCACGTTGT
16Sq-F	Forward	CAGCTCGTGTCGTGAGATGT
16Sq-R	Reverse	AAGGGGCATGATGACTTGAC
P4747-F	Forward	ATGCATGAATTCGCGTCTGGGAGCGGTTCAC
P4747/neo-R	Reverse	CGTGCAATCCATCTTGTTCAATCATCGCGCCACCTCCGGC
P4747/neo-F	Forward	GCCGGAGGTGGCGCGCTGATTGAACAAGATGGATTGCACG
Neo-R	Reverse	ATGCATGGATTCTCAGAAGAACTCGTCAAGAAGGCG
P4747-D-F	Forward	ATGCATGCATGCATGCATGCCCGGTGGGATATACGTTGAGAAGG
P4747-D-R	Reverse	GCATGCATGCATGCATGCATGGTGAGGGCGCAGAATCGTC
AHBA-F	Forward	AGAGGATCCTTCGAGCR(A/G)(G/C)GAGTTCGC
AHBA-R	Reverse	GCAGGATCCGGA(A/C)CAT(G/C)GCCATGTAG

* Underlined sequences indicate restriction sites used for cloning.

APPENDIX 3: ^{1}H and ^{13}C Chemical Shifts of RIF-glucose

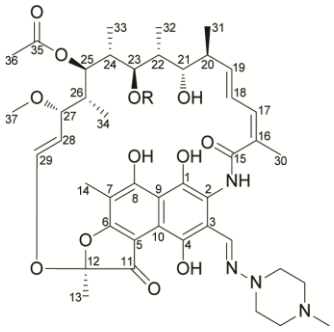

Structure	R
Rifampin (RIF)	H
Rifampin-glucose (RIF-G)	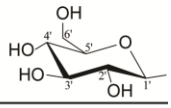

Position	RIF-G		RIF	
	δ_C, type	**δ_H (*J*, Hz)**	**δ_C, type**	**δ_H (*J*, Hz)**
17	141.7, CH	6.10 d (12.1)	132.1, CH	6.24 d (10.7)
18	126.6, CH	7.24 m[a]	127.9, CH	7.11 dd (10.9; 4.8)
19	139.0, CH	5.90 dd (15.5; 6.1)	137.5, CH	5.91 dd (13.0; 8.3)
20	39.9, CH	2.10 m	38.0, CH	2.19 sex (7.4)
21	71.2, CH	3.72 m	72.0, CH	3.76 d (8.1)
22	35.5, CH	1.63 m	33.0, CH	1.59 m
23	**86.7**, CH	**3.33 m**	**76.1**, CH	**2.83 s**
24	29.3, CH	1.23 m	37.6, CH	1.33 m
25	74.1, CH	5.07 m	73.6, CH	5.07 d (10.9)
26	40.3, CH	0.97 m	39.9, CH	1.03 m
27	76.4, CH	3.23 m	76.5, CH	3.23 d (8.8)
28	118.5, CH	5.05 dd (10.0; 6.0)	117.7, CH	4.93 dd (12.5; 8.0)
29	142.2, CH	6.10	142.7, CH	6.19 d (15.4)
30	20.8, CH_3	1.87 s	20.7, CH_3	1.90 s
31	17.6, CH_3	0.82 d (6.5)	17.8, CH_3	0.84 d (7.0)
32	12.6, CH_3	0.89 d (7.1)	11.4, CH_3	0.89 d (7.0)
33	9.9, CH_3	0.51 brs	8.7, CH_3	0.43 d (6.8)
34	8.9, CH_3	0.06 brs	9.0, CH_3	-0.26 d (6.8)
36	20.9, CH_3	1.90 s	20.4, CH_3	1.97 s
37	55.7, CH_3	2.89 s	55.7, CH_3	2.89 s
13	21.5, CH_3	1.60 s	21.9, CH_3	1.63 s
14	7.6, CH_3	1.87 s	7.6, CH_3	1.90 s
Pip-N-CH_3	42.1, CH_3	2.84 brs	42.1, CH_3	2.80 s
1’	103.0, CH	4.19 d (7.7)		
2’	73.8, CH	2.85 m		
3’	76.6, CH	3.07 m		
4’	70.1, CH	2.97 m		
5’	76.8, CH	3.02 m		
6’	63.1, CH_2	3.38 m		

[a] Spin coupling interaction was detected in the COSY spectrum, however coupling constant could not be resolved owing to broad line width. s, singlet; d, doublet; dd, doublet of doublets; sex, sextet; m, multiplet; brs, broad singlet.

APPENDIX 4: ^{1}H and ^{13}C Chemical Shifts of RIF-phosphate

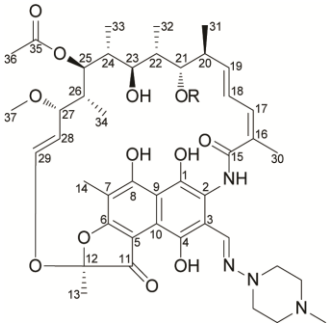

Structure	R
Rifampin (RIF)	H
Rifampin-phosphate (RIF-P)	PO_3H_2

Position	RIF-P		RIF	
	δ_C, type	**δ_H (*J*, Hz)**	**δ_C, type**	**δ_H (*J*, Hz)**
17	131.9, CH	6.24 d (10.5)	131.9, CH	6.24 d (10.7)
18	129.7, CH	7.10 m	127.7, CH	7.10 dd (10.9; 4.8)
19	135.9, CH	5.76 dd (15.0; 8.4)	138.1, CH	5.90 dd (13.0; 8.3)
20	40.7, CH	2.25 sex (7.0)	38.4, CH	2.19 sex (7.4)
21	**79.0, CH**	**4.36 ddd (9.3; 4.8; 4.4)**	**72.3, CH**	**3.76 d (8.1)**
22	36.1, CH	1.66 m	32.8, CH	1.58 m
23	74.9, CH	2.80 s	76.1, CH	2.81 s
24	37.5, CH	1.38 q (7.8)	38.1, CH	1.32 m
25	73.1, CH	4.93 d (10.6)	73.3, CH	5.07 d (10.9)
26	40.4, CH	0.88 m	39.9, CH	1.02 m
27	76.5, CH	3.22 d (8.8)	76.4, CH	3.22 d (8.8)
28	117.9, CH	4.99 dd (12.5; 8.0)	117.7, CH	4.93 dd (12.5; 8.0)
29	143.1, CH	6.18 d (12.7)	131.9, CH	6.20 d (15.4)
30	20.2, CH_3	1.92 s	20.5, CH_3	1.90 s
31	18.9, CH_3	0.99 d (7.0)	17.8, CH_3	0.83 d (7.0)
32	14.3, CH_3	0.83 d (7.0)	11.3, CH_3	0.89 d (7.0)
33	8.8, CH_3	0.27 d (6.8)	8.6, CH_3	0.43 d (6.8)
34	8.8, CH_3	-0.07 brs	8.8, CH_3	-0.26 d (6.8)
36	20.7, CH_3	1.98 s	20.6, CH_3	1.96 s
37	55.6, CH_3	2.89 s	55.6, CH_3	2.89 s
13	21.8, CH_3	1.63 s	22.0, CH_3	1.62 s
14	7.4, CH_3	1.91 s	7.4, CH_3	1.90 s
Pip-N-CH_3	41.9, CH_3	2.83 s	42.0, CH_3	2.80 s

[a]Spin coupling interaction was detected in the COSY spectrum, however coupling constant could not be resolved owing to broad line width. s, singlet; d, doublet; dd, doublet of doublets; ddd, doublet of doublets of doublets; q, quartet; sex, sextet; m, multiplet; brs, broad singlet

APPENDIX 5: List of AHBA Synthase-positive Actinomycete Isolates

Isolate/Strain	Alternate Name[†]	Geographic Source	16S rRNA Gene Relatedness
WAC5038	WMB03	Watermain, Brampton, ON	*Streptomyces hygroscopicus*
WAC5060	CP23	Orchard soil, Ancaster, ON	ND[1]
WAC5122	AD39a	Garden soil, Burlington, ON	*Streptomyces castaneus*
WAC6321		Soil, Nigeria	ND
WAC6323		Soil, Nigeria	ND
WAC6356		Soil, Nigeria	ND
WAC6361		Soil, Nigeria	ND
WAC6362		Soil, Nigeria	ND
WAC6369		Soil, Nigeria	*Actinomadura rifamycini*
WAC6756		Soil, Nigeria	ND
WAC6759		Soil, Nigeria	ND
WAC6767		Soil, Nigeria	*Actinomadura rifamycini*
WAC6771		Soil, Nigeria	*Actinomadura* sp. YIM 75700
WAC6781		Soil, France	*Streptomyces atriruber*
WAC7278		Soil, Nigeria	ND
WAC7295		Soil, Nigeria	*Amycolatopsis vancoresmynica*

[†] According to D'Costa, V.M. *et al*. 2006. 311(5759):374-377.
[1] Not determined.